JPRS-CST-88-011
22 JUNE 1988

224058

FOREIGN BROADCAST INFORMATION SERVICE

# JPRS Report

# Science & Technology

## China



REPRODUCED BY
U.S. DEPARTMENT OF COMMERCE
National Technical Information Service
SPRINGFIELD, VA. 22161

JPRS-CST-88-011
22 JUNE 1988

# SCIENCE & TECHNOLOGY

# CHINA

## CONTENTS



ERRATUM: In JPRS-CST-88-009 of 3 May 1988 in article DESIGN OF NUCLEAR HEAT, POWER CO-GENERATION PLANT DETAILED, on page 36, para. 1, line 4, make "billion" read "million."

COMPUTERS



EARTH SCIENCES



FACTORY AUTOMATION, ROBOTICS



LASERS, SENSORS, OPTICS

TELECOMMUNICATIONS R&D



/12223

## BRIEFS

INTERNATIONAL SATELLITE LAUNCH AGREEMENT--Hong Kong (Xinhua), 24 Feb--China International Trust & Investment Company, England's Great Eastern Telegraph Office Ltd., and Hong Kong's He Ji Telecommunications Ltd. will form a joint venture to employ China's Long March 3 early next year as a space launch vehicle for a communications satellite. This satellite will provide domestic communications service for China and other Asian countries. The satellite will be the United States' WESTAR 6, which has 24 transponders and can provide public and private telephone service, data communications, TV broadcasting, and telemetry. A control and monitoring facility will be set up in Hong Kong. Total cost for the launch will be US$120 million, to be evenly born by the three parties. [Summary] [Shanghai JIEFANG RIBAO in Chinese 25 Feb 88 p 1]

KEY STATE LABORATORIES TO BE BUILT--Dalian (Xinhua), 7 Apr--Key joint national laboratories for scientists involved in "three-beam material modification" high-tech research will be built at Dalian's College of Science & Engineering and at Shanghai's Fudan University. The new joint laboratories, on the basis of China's needs for developing high technology and improving traditional industry, will utilize ion beams, electron beams, and photon beams for paramodulation of the characteristics of materials; for preparation of high-bond-strength, high-quality coatings; and for preparation of surface alloys. This kind of advanced surface engineering is on the international high-tech frontier of the eighties; it is the direction of priority development in basic research. [Text] [Beijing GUANGMING RIBAO in Chinese 8 Apr 88 p 1]

SINO-CANADIAN TELECOMMUNICATIONS COOPERATION--Canada's Northern Telecommunications Ltd. and China's Tong Guang Electronics Company recently formed a joint venture: an agreement for transfer of appropriate technology and for provision of goods was formally signed in Beijing a few days ago. This joint venture will produce integrated services digital networks (ISDNs) and digital telephone sets, and market these products throughout China. Total investment for this joint venture, based in Shenzhen, is over US$13 million; registered capital is US$5.6 million. The signing of this agreement will promote the development of China's information technology and further the campaign for domestic production. [Summary] [Beijing RENMIN RIBAO [PEOPLE'S DAILY] (Overseas Edition) in Chinese 18 Apr 88 p 1]

/9738
CSO: 40080108

# Prospects for Nation's Space Technology Reviewed

40080105 Beijing XIANDAIHUA [MODERNIZATION] in Chinese No 1, 23 Jan 88 pp 12-13

[Article by Min Guirong [7036 2710 2837], President of the Academy of Space Technology]

[Text] Space technology not only is a rapidly growing new technology, it is also an indicator of a nation's military and economic strength. Over the past 20 years, China's aerospace industry closely followed a self-reliant policy in developing a practical and urgently needed aerospace system. Under this policy, China's aerospace industry has achieved an internationally recognized status, and has also begun to produce economic and social benefits. Today, China has established a complete aerospace system of diversified and coordinated disciplines, and has developed a team of highly qualified aerospace specialists. It is safe to say that China's aerospace industry has a promising future with great potential for growth.

On 24 April 1970, China launched its first artificial satellite into orbit; it was a landmark of China's entry into space and also marked the beginning of China's aerospace industry. The development of China's aerospace industry can be divided into the following stages:

The Era of the 70's. The era of the 70's was a stage of construction and exploration of China's aerospace technology. During this stage, China developed a number of scientific experimental satellites and launch vehicles (a total of 8 low-orbit satellites were successfully launched), established a variety of laboratories, bases and supporting facilities, and initiated various programs to explore the universe and space technology.

The Era of the 80's. It is estimated that during the 80's, China will launch approximately 20 satellites of various types, which include low-orbit retrievable satellites, geosynchronous communications satellites, and medium-orbit (solar synchronous) weather satellites; some of these satellites are already in service。 During this stage, China is engaged in the research and development of various technology satellites, and has completed the transfer from the experimental phase to the application phase。

The Era of the 90's. The 90's is expected to be an era of large-scale application of aerospace technology. During that period, China's satellites will provide a wide range of services for China's economic development and scientific research; they include: remote sensing, communications, broadcasting, earth resource exploration, oceanic and meteorological research, navigation and positioning, data collection, and conducting material and biological experiments under micro-gravity conditions in space. The number of satellites to be launched in the 90's is expected to be significantly higher than in the 80's, but more importantly, the satellite performance (in terms of design life and capacity) will be much improved; many of these satellites will reach the advanced standards of similar satellites built by other countries.

Therefore, the era of the 90's will be a period when the aerospace industry makes significant contributions to China's economic development and national construction.

Today, human production activities have expanded into space; consequently, both the United States and the Soviet Union are building permanent space stations to facilitate the development and utilization of space resources, and to carry out production activities in space under micro-gravity conditions. Building permanent space station is an inevitable stage in the history of aerospace development; therefore, looking toward the future, China's aerospace activities will also begin to enter this stage once the targets of the 90's are reached. It is predicted that by early next century, China will begin building a permanent space station and an advanced space transportation system (including a space shuttle). I believe that the State will take the appropriate steps in this regard. When the conditions are ripe, the State will appropriate the necessary funds and human resources to support this program.

Over the past 20 years, the development of China's aerospace industry has followed a policy of self-reliance; this policy will continue in the future. However, when conditions permit, we should also actively pursue international cooperation.

From the objective point of view, the development of aerospace technology should ideally be carried out in an environment of international cooperation. If the individual countries can coordinate their development efforts, rapid progress can be achieved with smaller investments, and greater economic and social benefits can be derived. However, total cooperation in the area of aerospace technology may only be an idealistic wish.

It should be noted that the development of aerospace technology not only involves economic resources and scientific technologies, it also has political and military implications. To enhance their political and military status, the United States and the Soviet Union will undoubtedly engage in a fierce competition. Also, in the last decade of this century, Europe and Japan will significantly increase theirinvestments in this area in order to catch up with the two superpowers. These competitions will undoubtedly cast a shadow in international cooperation.

On the other hand, limited cooperation in certain areas will benefit all the participating countries; therefore, we should actively explore the possibility of cooperating with other countries in certain technical areas.

For example, we have cooperated with France in conducting micro-gravity experiments using retrievable satellites; this year, we have signed an agreement with West Germany to conduct micro-gravity and other application experim-nts onboard China's retrievable satellite. These cooperative efforts will undoubtedly produce valuable useful experimental results, and should be encouraged to create a better environment for international cooperation.

In order to accelerate the development of China's aerospace industry, our aerospace policy should also be modified accordingly.

First, we should abandon the concept that aerospace technology only has political value and does not contribute to economic development. Aerospace is a high-payoff enterprise (the ratio between investment and payoff is 1:14); therefore, we should closely coordinate the development of aerospace technology and China's economic construction in order to take full advantage of the benefits derived from aerospace technology.

Second, self-reliance in aerospace development should still be our long-term policy. Some people have suggested importing or purchasing satellite systems from abroad, but I believe this approach is impractical. Of course, in some areas we should actively pursue international exchange and cooperation.

Third, the State should increase its investment in the aerospace industry, and encourage all aerospace-related organizations to pool their resources in the development of aerospace technology; it should also organize a team of experts to establish China's long-term strategy in aerospace development. This work should be initiated as soon as possible, and should receive strong support from various participating organizations.

Fourth, because of the wide range of activities involved in aerospace technology (research, production, application etc.), the State should establish an authoritative organization (Space Commission) to provide unified leadership and management for the aerospace industry.

3012/9604

## PREMIXED FLAME AND HOMOGENEOUS ISOTROPIC TURBULENT DISTORTION

40090074a Beijing ZHONGGUO KEXUE [SCIENTIA SINICA] in Chinese, Series A No 1, (Jan) 88 pp 35-45

[Article by Xie Xiangchun [6200 6272 2504] (Beijing Institute of Mechanics, Chinese Academy of Sciences). Received 5 Jan 87, revised 15 Jun 87]

[Abstract] A new concept of scale of length to characterize chemical-reaction-layer thickness is introduced in order to arrive at a new formula for speed of propagation of turbulent flames. Next, the relationship between flame layer thickness and incremental changes in tau--the ratio of the quantity of heat released to the initial enthalpy--is derived. In addition, a new speed-compression correlation method is proposed to clarify the mechanism of greatly increased turbulent energy within a turbulent premixed flame layer. Finally, a conclusion on the relevance of this theory to homogeneous isotropic turbulent distortion is reached.

/12232

# RECOVERY OF INTACT VIRUS FROM POLIO cDNA IN MAMMALIAN CELLS

40081044 Beijing BEIJING YIKE DAXUE XUEBAO [JOURNAL OF BEIJING MEDICAL UNIVERSITY] in Chinese Vol 19 No 5, Oct 87 pp 289-291

[Article by Feng Shuyi [7458 2885 8381], Zhang Yingmei [1728 3379 1188], and Ren Ruibao [0117 3843 1405], Microbiology Teaching and Research Department, and Zhang Naiheng [1728 6621 5683], and Zhang Changying [1728 2490 3379], Biochemistry Teaching and Research Department: "A Study on the Recovery of Intact Virus From Polio cDNA in Mammalian Cells." This research topic received financial assistance from the state natural sciences fund.]

[Text] Abstract: An HB 101 strain of E. coli was used to amplify a plasmid containing a whole sequence of poliovirus Sabin 1 cDNA, and different methods were used to extract the polio cDNA (Sabin 1) plasmid. African green monkey kidney (AGMK) kidney cells and 2 BS cells were transfected with the purified DNA. Results showed the polio cDNA that had been extracted using the modified cesium chloride methods to have maintained their nucleotide sequence completely, indicating successful transfection of the cells. Results from an evaluation of biological properties and antigenicity show the virus to be identical with the polio Sabin 1 virus strain.

Advances in genetic engineering technology in recent years have raised the level of allogenic gene transcription and translation, enabling some genes to become fully expressed in prokaryotic cells. However, reports are very rare about the expression in mammalian cells of full length sequences of cDNA. Omata et al.[1] have been successful in using cDNA to transfect mammalian cells, but Semler[2] reported plasmids containing polio cDNA as being unstable; moreover, since types of cells differ, the successful transfection rate also varied. This research work is not only of importance to molecular biology, but also holds important value for virology[1] in being able to use a method that preserves polio cDNA as a repository for poliovirus seed virus and to prevent mutation. There have been no reports in China about work in this regard. The present article explores the extraction of cDNA, methods for transfection to mammalian cells, and the biological properties of recovered virus.

Materials and Methods

1. Materials and Reagents:

The polio cDNA (Sabin 1) plasmid (PVS (1) IC-0(T) and the AGMK cells were kindly donated by Dr Nomoto of Tokyo University. The 2 BS cells and the anti-poliovirus Sabin 1 serum were kindly donated by the Beijing Biological Products Research Institute.

Chemical reagents such as endonuclease are reagents produced in China.

2. cDNA Transformed HB 101 Bacteria:

A Petri dish of LB agar containing ampicillin (75 μg/ml) was selected for use in cloning following the Bernard Perbal method[3], and after culturing for 48 hours at 37°C, a small gray germ colony was inoculated into an LB agar liquid culture containing ampicillin (50 μg/ml) at 37°C, which was vibrated while culturing to multiply the bacteria. The germs were then injected into a Petri dish of LB agar containing tetracyclene and to a Petri dish of LB agar containing chloromycetin and cultured for 48 hours at 37°C. The germs found to be sensitive to the two antibiotics were selected as seed germs.

3. Extraction and Purification of Plasmids Containing Polio cDNA:

We extracted plasmids using the Maniatis alkali method.[4] An alternate method used was the modified cesium chloride method for extracting and purifying cDNA plasmids. First 10 ml of growth logarithmic period seed germ solution was inoculated into 400 ml of LB culturing solution and cultured at 37°C for from 6 to 8 hours while being vibrated; then chloromycetin was added and the mixture was cultured at 37°C overnight. The virus precipitate was collected after centrifuging at 3,500 rpm at 4°C for 15 minutes. Then the precipitate was washed in TSB (10 m of MTris·HCl at a pH of 8.0, and 0.014 MNaCl) after which the precipitate was centrifuged. Next the precipitate was dissolved in 10 ml of TESB (25 percent sucrose, 50 mm of Tris·HCl at a pH of 8.0, and 1 mm of EDTA). To this was added 60 μl of RNase A (10 μg/μl) and 1 ml of lysozyme (40 mg/ml), and then the mixture was placed in an ice bath for 5 minutes. Next was added 4 ml of 0.5 m EDTA, and it was placed in an ice bath for 30 minutes. Then 16 ml of a dissolving mixture (0.1 percent Triton X-100, 50 mm Tris·HCl at a pH of 8.0, and 62.5 mm of EDTA) was added, and it was placed in an ice bath for 15 minutes after which it was centrifuged at 17,000 rpm for 60 minutes. To the supernate was added $\frac{1}{10}$ $(\frac{w}{w})$ PEG 6000, after which $\frac{1}{10}$ $(\frac{v}{w})$ 5 MNaCl was mixed in and the mixture was allowed to stand overnight in a 4°C refrigerator. The mixture was then centrifuged for 10 minutes at 10,000 rpm, and 3.5 ml of TE (10 mm Tris·HCl at a pH of 7.5, plus 1 mm of EDTA) was added to the precipitate as well as 3.745 g of CsCl, and 0.25 ml of ethidium bromide (5 mg/ml). This was then centrifuged for 5 minutes at 2,000 rpm. The supernate was placed in a super centrifuging vial and topped off with liquid paraffin. It was centrifuged at 40,000 rpm for 24 hours at 15°C (using a Beckman Ti 40 rotor), and the DNA strain

extracted using the needle method under a long wave ultra-violet light. Water saturated n-butyl alcohol was used for three extractions. Cold anhydrous ethyl alcohol was used to precipitate the nucleic acid overnight at -20°C. The precipitate was resuspended in TE, and then phenol, chloroform, and isoamyl alcohol were used to make one extraction, and ethyl ether was used to make three extractions. Anhydrous ethyl alcohol was used to precipitate the nucleic acid overnight at -20°C. Then 70 percent ethyl alcohol was used to wash the precipitate three times, and it was stored at -20°C.

4. DNA Endonuclease Breakdown Assay:

We used Chinese produced EcoRI, BamHI, PstI, and HindIII endonuclease, and DNA that was digested and purified by conventional methods in our laboratory. We used agarose electrophoresis to check molecular weight and the number of segments.

5. Polio cDNA Transfection Assay:

We used a single layer of 70 percent grown AGMK cells from which nutrient solution had been removed, and which had been washed twice in DMEM. After removing the DMEM, 1 ml of DMEM was added and the cells were placed in a warm box at 37°C for 30 minutes. Next a DNA calcium phosphate precipitate solution was prepared to which was added 4 µg of polio cDNA (Sabin 1) plasmid DNA, 10 µg of salmon sperm DNA in 400 µl of water. To this was added 100 µl of 5 x HeBs (3.2 g NaCl, 0.148 g KCl, 0.05 g $Na_2HPO_4$, $2H_2O$ 0.4 g dextrose, and 2 g HEPES to which was added 80 ml of NaOH to adjust the pH to 7.05). The mixture was thoroughly mixed. To it was then added 25 µl of 2.5 m $CaCl_2$. This was mixed and allowed to stand at room temperature for 25 minutes. After a minute amount of precipitate became visible, the aforementioned AGMK cells were added, and it was placed in a 37°C 5 percent $CO_2$ warm box for 5 hours. It was then washed four times with a non-serum MEM. After the MEM was removed, 5 ml of MEM containing 5 percent ox serum was added, and it was placed in a 33°C warm box. The CPE was observed daily.

The 2 BS cell transfection method was the same as described above.

6. Blank Spot Reduction Assay:

Both 200 pfu of Sabin 1 virus and regenerated virus were separately neutralized with sheep anti-poliovirus Sabin 1 serum (1:160), and the number of blank spots reduced by the serum neutralization were calculated.

Results

1. Purified Polio cDNA Plasmid Zymogram:

Agarose electrophoresis was used to measure the molecular weight of the DNA that had been extracted using the alkali method and the cesium chloride method. The molecular weight was approximately 13 kb, which was identical with the original standard PVS(I)IC-O(T)DNA. Results after digestion using

endonuclease EcoRI, BamHI, HindIII, and PstI were as follows: Following enzyme cutting using EcoRI, segments were 7.5 kb and 5.1 kb; following cutting with BamHI enzyme, segments were 6.0 kb, 2.6 kb, 2.5 kb, and 1.8 kb. Following cutting with HindIII enzyme, segments were 9.3 kb, 1.4 kb, 1.1 kb, 0.6 kb, and 0.5 kb; and following cutting with the PstI endonuclease, segments were 6.4 kb, 2.5 kb, 2.3 kb, 1.1 kb, and 0.43 kb. The number of segments and their molecular weights following digestion of the DNA were consistent with the standard plasmid zymograms, showing that the plasmid DNA we extracted contained full length nucleotide sequences of polio cDNA.

2. The regenerated virus obtained following the transfection of animal cells with the extracted and purified DNA were as follows:

We used the DNA extracted by the alkali method to transfect AGMK cells and 2 BS cells, which showed no cell affection during 7 days of observation. After blind breeding of another generation and observing them for 7 days, no affection appeared in either kind of cells. The DNA obtained from the modified cesium chloride method was used to transfect AGMK cells, 5 days after which cell affection appeared as shown in Plate 2 [not reproduced]. Following breeding of a successive generation, the virus titer reached $10^6$ pfu/ml. Three days following transfection, the 2 BS cells showed cell affection as shown in Plate 4 [not reproduced]. Following breeding of a successive generation, the virus titer reached $10^6$ pfu/ml. The form of cell affection was the same as the form of cell affection from the polio virus Sabin 1.

3. Evaluation of the Biological Properties of the Regenerated Viruses:

a. Comparison of Blank Spot Size:

The regenerated virus and the poliovirus Sabin I virus were each inoculated into a single layer of AGMK cells. After covering with agar, they were cultured at 30°C for 3 days. Observation of blank spots was as shown in Plate 5 [not reproduced]. The size and shape of blank spots for both viruses was the same.

b. Effect on Virus Growth of $NaHCO_3$ Concentrations:

Table 1 shows a generally identical reliance on acid sodium carbonate for growth by both the regenerated virus and the poliovirus Sabin 1 virus, showing similar biological properties for the two viruses.

Table 1. Effects of $NaHCO_3$ Concentration on Virus Growth

| Virus | $\log_{10}$pfu/ml of virus growth at different $HaHCO_3$ concentrations | |
|---|---|---|
| | 0.225% | 0.03% |
| Regenerated virus | 7.65 | <3.0 |
| Poliovirus Sabin Type 1 | 7.04 | <3.0 |

c. Effect on Virus Growth of Different Temperatures:

The results shown in Table 2 show both viruses as having identical sensitivity to temperature.

Table 2. Effects of Different Temperatures on Virus Growth

| Virus | Titer of virus growth at different temperatures $log_{10}$pfu/ml | | | Log value difference |
|---|---|---|---|---|
| | 33°C | 36°C | 39.5°C | 36/39.5 |
| Regenerated virus | 6.98 | 7.30 | <0.30 | >7.00 |
| Poliovirus Sabin Type 1 | 7.06 | 7.06 | <0.30 | >6.76 |

d. Comparison of Antigenicity of the Regenerated Virus and the Poliovirus Sabin 1:

The similarity between blank spots for the two kinds of virus neutralized by the same serum demonstrates a similar antigenicity for the two kinds of viruses.

Discussion

It is known from extant reports that success in the transfection of DNA in eukaryocytes is closely related to the topology of DNA.[5] Polio cDNA transcription of virus RNA is also dependent on the sequence and structure of cDNA being intact. Our analysis of the molecular weight and zymograms of DNA extracted using the modified cesium chloride method and the alkali method shows the properties of both kinds of DNA to be generally similar. However, for the DNA extracted by the former method, a substantial amount of the superhelical structure was successfully transfected. The DNA extracted by the alkali method may have been damaged by the acid and alkali processing, and this may have been a factor in the failure of transfection.

Semler reported that the plasmid containing polio cDNA was unstable when amplified in E. coli, and that the transfection rate varied with different kinds of mammalian cells. We were successful in transfecting both AGMK cells and 2 BS cells and in the regeneration of viruses. Results of the assay showed the method used for preserving the polio cDNA can prevent mutation of the virus seed in the natural world, and that polio cDNA may be used to regenerate virus when virus seeds are needed.

The biological properties of the regenerated virus and the Sabin 1 virus were compared. Results of the assay show these properties to be the same for both viruses.

It is currently known that the assembly and maturation of poliovirus goes through a complex molecular biological reaction process.[6] Success in this research shows that polio cDNA in mammalian cells can express all the

components of virus plasmids, and that the assembled live virus plasmids hold important significance in molecular biology. It also holds substantial value in the work of preparing vaccines.

## REFERENCES


1. Kohara, M., et al.: An infectious cDNA clone of the poliovirus Sabin strain could be used as a stable repository and inoculum for the oral poliovirus vaccine. Virology 1986; 151:21.

2. Semler, B., et al.: Production of infectious poliovirus from cloned cDNA is dramatically increased by SV 40 transcription and replication signals. Nucl Acids Res 1984; 12:5123.

3. Perbal, B., et al.: A Practical Guide to Molecular Cloning. New York: John Wiley & Sons 1984: 268-269.

4. Maniatis, T., et al.: Molecular Cloning. New York Cold Spring Harbor Laboratory 1982: 88-89.

5. Weintraub, H., et al.: Expression of Transfected DNA Depends on DNA Topology. Cell 1986; 46:115.

6. Arnold, E., et al.: Implications of the Picornavirus Capsid Structure for Polyprotein Processing. Proc Natl Acad Sci USA 1987; 84:21.


9432/6091

Pulsed Nd:YAG Laser Irradiation Injury Threshold of Retinas

40101008 Beijing CHINESE MEDICAL JOURNAL in English Vol 100 No 11, Nov 87 pp 855-858

[Text] Five eyeballs of Chinese patients scheduled to exenteration were used to determine the retinal injury threshold for irradiation with pulsed Nd:YAG laser at 150 μs. The injury threshold $ED_{50}$ was 1.55 mJ, with a confidence limit of 1.30-1.86 mJ. When the laser energy approximated the value causing injury to the retina, the power intensity of the laser reaching the cornea was $P=429W/cm^2$.

Experiments on rabbits and rhesus monkeys showed that the retinal injury thresholds of 150 us pulsed Nd:YAG laser were 0.885 mJ and 0.259 mJ respectively. The ratios of retinal injury thresholds for grey rabbits, rhesus monkeys and yellow people were 1.0:3.4:6.0. Obviously, the human eye is more tolerant to laser at 1.06 μm wave length than rabbit and monkey eyes.

Pulsed Nd:YAG laser is widely used in ophthalmic clinics. Since the injury threshold of the human retina plays an important role in determining the standard value of measurements of safety protection and prevention and in clinical laser use, researchers[1-4] have done many animal experiments. In our study, we used living patient eyeballs scheduled for exenteration to arrive at the threshold of laser cause injury to the retina.

Material and Methods

The output of the selected pulsed Nd:YAG laser was monomode by the mode locking technic. The tolerance of energy output variation was set at below 5 percent. The laser expanding beam was directed to the eyes by a slip-lamp and Hruby lens.

Real-time monitoring apparatus was used to measure the laser beam energy by using a beam splitting lens on the slit-lamp. THe laser beam passing through this lens was split into two parts, one illuminating the eye, the other the energy-meter indicator, which recorded the energy value of each illumination. The laser energy entering the eye was then calculated by spectroscopic proportion value. To keep the spectroscopic proportion value stable, the compensation method of polarization was used to decrease the variation of laser energy caused by changes in reflected light and that transmitted through the lends, ensuring the measurement accuracy.

The retinal injury threshold was measured by the amount of laser power penetration the cornea. The formula of Calculation is: /\p=/\t . /\A./\t denotes the time of laser irradiation, which is controlled by the rotating place of a step by step motor. In our experiment, the time was 150 μs./\A denotes the area of the cornea irradiated by the laser. This area was measured videophotographically and calculated by amplification ratio.

Five living Chinese eyes with orbital malignant tumors scheduled for orbital contents exenteration were used. They had normal corneas, lenses, vitreous bodies, and fundi. Before exenteration, the eyes were irradiated by pulsed Nd:YAG laser for 150 μs following pupil dilation with 1 percent atropine and 10 percent neosynephrine. One hour and 24 hours after laser irradiation, each retina was separately examined by direct ophthalmoscopy. Injury reaction was recorded as positive if a pigmented spot and a tinycoagulation spot and/or small bleeding spot were observed in the irradiated area.

The energy value of irradiation ($ED_{50}$), which causes retinal injury at 50 percent ratio, was calculated by weighting linear regression. This value represents the threshold of retinal injury.

The used eyes were enucleated after orbital exenteration, and the pathological change in the irradiated retina were examined by light microscope.

Calculations: $\bar{x} = \Sigma nwx/\Sigma nw = 8.61/224.8 = 0.038\ 3$

$$\bar{y} = \Sigma nwy/\Sigma nw = 1\ 051.31/224.8 = 4.677$$

$$b = \frac{\Sigma nw(x-\bar{x})(y-\bar{y})}{\Sigma nw(x-x)^2} = \frac{\Sigma nwxy-(\Sigma nwx)(\Sigma nwy)/\Sigma nw}{\Sigma nwx^2-(\Sigma nwx)^2/\Sigma nw}$$

$$= \frac{48{\cdot}52-8.61x1\ 051.3/224.8}{4.21-8.61^2/224.8} = 2.12$$

Linear regression: $\hat{Y} = y + b(x-\bar{x}) = 4.677 + 2.12(x-0.383)$

if $\hat{Y} = 5.000$

$$m = x/\hat{Y} = 5.000 = x + \frac{5-\bar{y}}{6} = 0.1907$$

$$E_{ED50} = \text{antilo}_3\ \text{nm} = 1.5513\text{mJ}$$

Results

A total of 426 laser pulse irradiations were applied to the 5 living eyes. The retinal injury changes were observed before and 1 hour after irradiation.

The lowest irradiated laser energy value used was 0.38 mJ and the highest 1.70 mJ.

$E_{ED50}$ is the energy of 150 μs Nd:YAG laser entering the eye and causing retinal injury at the ratio of 50 percent; this is the retinal injury threshold Sm is the standard error of m.

$$Sm^2=\frac{1}{b^2}\left[\frac{1}{\Sigma nw}+\frac{(m-x)^2}{\Sigma nw(x-x)^2}\right]=\frac{1}{b^2}\times 1.04\times 10^{-2}$$

Sm=0.04 95 percent confidence limit of $E_{ED50}$ $\log^{-1}(m+1.96Sm)$ $\log^{-1}(m-1.96SM)$ ⇒ ⇒1.86 mJ → 1.30mJ

From the calculation, the human retinal injury threshold of pulsed 150 μs Nd:YAG laser irradiation is 1.55 mJ (1.30-1.86mJ). When the laser beam enters the eye, the corneal light spot area is $\triangle A=2.41$ mm². Therefore, when the laser energy approaches the value of injury, the power intensity of the irradiated laser is P=429 w/cm².

In our study, the eyeballs, in which morphological changes of typical retinal injury were observed on ophthalmoscopic examination, were examined microscopically. The injury to the retina with a laser energy of 2.17 mJ is shown in Fig 1. In the injured portion, the inner limited membrane was broken with severe damage to the neurofiber layer, inflamed cell infiltration (lymphocytes), edema and breakage of neurofiber cells. Slight effects on the inner nuclear layer were observed in some areas.

The eyeballs without retinal morphological changes caused by laser energy irradiation (0.91 mJ) below the threshold of injury were also examined microscopically (Fig 2). Some evidence of injury was also present. The inner limiting membrane adhered to the neurofiber layer and was contracted and depressed; there were bubbles, protein exudation and decreased cells in the depressed inner nuclear layer. The outer nuclear layer and outer limiting membrane were normal.

Figure 1. Injured retina after Nd:YAG laser irradiation (2.17 mJ).
Figure 2. Injured retina after Nd:YAG laser irradiation (0.91 mJ).

Discussion

The injury threshold of laser irradiation varies with the type of laser used and the injurious effects are closely related to the spectral t ansil-lumination characteristics and eye tissue absorption. Even with the same laser, the effect varies with continuous or pulsed waves. The injury

threshold of the same laser varies with the animal species tested. This means that the injury threshold varies not only with the tissue structure, but also with the degree of laser tolerance. In our study the human retinal injury threshold of a 150 us pulsed Nd:YAG laser was 1.55 mJ and that of the rhesus monkey and grey rabbit was 0.885 mJ and 0.259 mJ respectively.[5] The ratio of retinal injury threshold in grey rabbit rhesus monkeys and yellow people was 1.0:3.4:6.0. This shows that the tolerance to laser at 1.06 μs is higher in human eyes than in rabbit and money eyes. Because of the difficulty in obtaining injury values of human living eyes caused by different types of lasers, animal eyes were used for the observation. The ratios obtained are of reference value for human eyes.

As to the energy values below the threshold of Nd:YAG laser irradiation, injurious effects on the retina was not seen, despite some changes were evident on pathological examination. It is suggested that minimal injury reaction cannot be detected ophthalmoscopically, and that the laser energy values obtained cannot be considered to be absolutely safe.

Acknowledgements:

We are grateful to Professor Kuo Bing-kuan of Shanghai Medical University for his advice in preparing this paper.

REFERENCE

1. Bonner RF, et al. Threshold for retinal damage associated with the use of high-power neodymium-TAG lasers in the vitreous. Am J Ophthalmol 1983; 96:163.

2. Ham WT, et al. Ocular hazards from picosecond pulses of Nd:YAG laser radiation. Science 1974; 185:362.

3. Goldman AI, et al. Ocular damage thresholds and mechanisms for ultrashort pulses of both visible and infrared laser radiation in rhesus monkey. Exp Eye Res 1977; 24:45.

4. Xu Jiemin, et al. Retinal injury threshold by CW $Nd^{3+}$: YAG laser light. Zhongguo Jiguang (Chinese Journal of Lasers), 1985; 10: 612.

5. Chu Renyuan, et al. Retinal injury threshold of rabbits and monkeys irradiated by CW or pulsed YAG laser beams. Zhongguo Jiguang (Chinese Journal of Lasers), 1985; 10: 634.

/12232

Viral Hepatitis and HLA

40091050a Beijing ZHONGHUA NEIKE ZAZHI [CHINESE JOURNAL OF INTERNAL MEDICINE] in Chinese Vol 26 No 11, Nov 87 pp 646-648, 677

[Article by Wang Chin-huan, Si Chong-wen, Xi Hong-li, et al. Department of Infectious Diseases, the First Hospital, Beijing Medical University

[Abstract] HLA were typed in 103 patients with chronic viral hepatitis in order to study that whether the immune-genetic factors play an important role in the pathogenesis of chronic viral hepatitis, especially viral hepatitis B. Sixty-seven patients with chronic active hepatitis and 36 patients with chronic persistent hepatitis were included, most of them were serum HBsAg positive. Eighty-nine healthy people were also detected as controls. Using microlymphocytotoxic technique, 8 HLA locus A and 16 HLA locus B antigens were detected. The specificity of each HLA antigen was defined by more than three HLA antisera and 70 antisera were used for HLA typing.

Result: Antigen frequencies of HLA-A, B were no significant difference between patients with chronic viral hepatitis and normal controls. The result was consistent with some other reports and suggested that the immune-genetic factors seemed to be not involved in the pathogenesis of chronic viral hepatitis B. However further study is needed to research the association of chronic viral hepatitis with other HLA antigens such as HLA-DR locus antugens.

/12232

# Post-Transfusion Hepatitis B Virus (HBV) Infection and Effect of Prevention with Hepatitis B Immunoglobin (HBIG)

40091050b Beijing ZHONGHUA NEIKE ZAZHI [CHINESE JOURNAL OF INTERNAL MEDICINE] in Chinese Vol 26 No 11, Nov 87 pp 649-650, 677-678

[Article by Zhong Xiao-feng, The General Hospital of Nanjing Military Area; Wang Shu-hua, Blood infusion Institute, Chinese Academy of Medical Sciences, Wang Wei-ye, Department of Infectious Disease, Changhai hospital, The Second Military Medical University]

[Abstract] From 1984 to 1986, we examined 196 bottles of bottle-contained donor blood, 22 bottles were positive with 1 or more than 1 HBV marks, making up 11.22 percent of the above-mentioned blood of them were injected with HBIG before or after transfusion. The remaining 91 not receiving HBIG served as control. The results of comparing two groups were as follows: Patients of the HBIG group received 13 bottles of HBV positive blood, 6 of them became positive for HBV after transfusion (6.25 percent). Patients of the control group received 9 bottles of HBV positive blood; 17 of them were positive for HBV (18.65 percent) later, 3 of the 17 had clinical diagnosis of hepatitis. The difference between the two groups is of great statistic significance. It is shown that HBIG has the effect of preventing and alleviating post-transfusion HBV infection.

/12232

# Radioimmunoassay For Procollagen Type III Peptide and Its Diagnostic Value For Liver Fibrosis

40091045A Beijing ZHONGHUA YIXUE JIANYAN ZAZHI [CHINESE JOURNAL OF MEDICAL LABORATORY TECHNOLOGY] in Chinese Vol 10 No 6, Nov 87 pp 313-316

[Article by Mei Changlin [2734 7022 2621], Kong Xiantao [1313 2009 3447], Zhang Guozhi [1728 0948 3112], Li Shi [2621 4258], and Xie Yinghua [2503 5478], Long March Hospital, Second Military Medical University]

[Abstract] This article reports the preparation from purified procollagen type III peptide (PIIIP) of fetal bovine skin origin of its specific antiserum to construct a blood serum PIIIP radioimmunoassay method. The blood serum PIIIP content from 50 health blood donors, from 40 patients suffering from acute hepatitis, from 29 patients suffering from chronic persisting hepatitis (CPH), from 33 patients suffering from chronic active hepatitis (CAH), from 31 patients suffering from decompensated cirrhosis, and from 13 patients suffering from nonhepatic ailments was respectively 7.7±1.6, 22.2±11.2, 15±5.7, 23.4±10.3, 15.2±5.2, and 9.0±4.8 ng/ml($\bar{X}$±SD). It was markedly higher in the hepatic group than in the normal group and the nonhepatic group $P<0.01$); it was markedly higher for the acute hepatitis and CAH than for the CPH and the cirrhosis group. There was no correlation between the blood serum PIIP content of patients suffering from hepatic diseases and conventional liver function test results; however, there was an extraordinarily marked correlation between the number of fibrous cells in hepatic disease pathogenic tissue and fibrosis ($r=0.746$, $P<0.01$). There was no correlation to intralobular necrosis. Sensitivity in the diagnosis of liver fibrosis was superior to that for monoamine oxidase (MOA), glucosaminidase (NAG), proline (Pro), and hydroxyproline (FHYP). The foregoing results suggest that determination of blood serum PIIIP content may reliably reflect the extent and activeness of liver fibrosis, and may be a useful indicator in the early diagnosis of liver fibrosis.

This four page article sets forth critical information in tabular form, and eight of the 10 references cited are in English.

9432/9738

## Study of the Detection of an E System by the RIA Method Using Monoclonal HBe

40091045B Beijing ZHONGHUA YIXUE JIANYAN ZAZHI [CHINESE JOURNAL OF MEDICAL LABORATORY TECHNOLOGY] in Chinese Vol 10 No 6, Nov 87 pp 340-342

[Article by Zhang Zheng [1728 2973], Li Xinfu [2621 2450 1381], Sun Yan [1327 3508], and Tao Qimin [7118 0366 2404], Hepatopathy Institute, Beijing Medical University]

[Abstract] Experiments have demonstrated the use of monoclonal anti-HBe to make a RIA kit for the detection of HBeAG and anti-HBe to be a specific, sensitive, and duplicatable method. In the detection of HBeAg, only when immunoactive monoclonal antibodies are properly matched is it possible to derive satisfactory results. In keeping with China's circumstances, use of coated polyclonal anti-HBe to mark monocolonal anti-HBe (b) also produces fine results. Anti-HBe kit research shows selection of a neutralizing HBeAG of a certain quality to be crucial. This article discusses principles to be used in making the selection.

Inasmuch as the detection of an e system when observing the development of chronic hepatitis holds major importance for both prognosis and prevention, because the presence of such a system suggests an integration of HBV-DNA with host liver cells rather than a dissipation of viruses, detection of the system is of crucial importance. However, since it is difficult to purify HBeAG and since it is difficult to find anti-HBe of a high titer in human blood plasma, detection of the e system is greatly restricted. This work consequently built on the advanced method worked out by M. Imai in 1982, using monoclonal antibodies to build RIA kits for use in the detection process. The article explains the methodology and the results.

9432/9738

# A Study of the Serotypes of Pathogenic Cryptococcus Neoformans Strains Isolated in China

40091045C Beijing ZHONGHUA YIXUE JIANYAN ZAZHI [CHINESE JOURNAL OF MEDICAL LABORATORY TECHNOLOGY] in Chinese Vol 10 No 6, Nov 87 pp 350-352

[Article by Li Zhuqing [2621 4554 7230], Shao Jingzheng [6730 4842], Liao Wanqing [1674 8001 3237], and Li Shuqin [2621 3219 3830], Department of Dermatology, Long March Hospital, Shanghai Second Military Medical University; and Sun Xiantao [1313 2009 3447], and Xie Yinghua [6200 2503 5478], Immunology Laboratory, Long March Hospital, Shanghai Second Military Medical University]

[Abstract] Cryptococcus neoformans is the pathogen for cryptococcus meningitis. This article has applied standard serotype strains, and has used a combination of biochemical identification culturing and serological verification in the first fairly systematic study undertaken in China of the serotypes of pathogenic Cryptococcus neoformans strains. Typing shows the most outstanding feature of Chinese serotypes of pathogenic Cryptococcus neoformans strains to be a lack of type C. Their geographic distribution is characterized as follows: (1) Type A is in the majority; (2) type D is rare; (3) types AD and U (for unknown) are evident; (4) there is a certain percentage of type B, but type C is missing.

The bromothymol-caravarine-glycine (BCG) method designed by K.J. Kwon-Chung, and the glycine-cycloheximide-phenol red (GCP) method designed by I.F. Salkin were used as cultures for biochemical identification because of their convenience in differentiating A or D and B or C serological strains.

The article displays in tabular form the number of strains and the percentage found in blood serum types A, D, A and D, B, C, and U, the geographic distribution within China of Cryptococcus neoformans strains found in the various blood types, and the grographic distribution among China, Japan, Thailand, Vietnam, Kampuchea, and Nepal of serotypes of pathogenic Cryptococcus neoformans. The data for Japan and the southeast Asian countries is taken from work done previously outside of China by J. Ikeda and K.J. Kwon-Chung.

9432/9738

ENHANCEMENT OF FC RECEPTOR EXPRESSION

40081056a Beijing KEXUE TONGBAO in Chinese Vol 32 No 24, Dec 87 pp 1892-1894

[Article by Li Xingqiang [2621 5281 1730], Zhang Zongliang [1728 1350 2733] and Yao Zhen [1202 6855 3778], Shanghai Cytobiology Institute, Chinese Academy of Sciences: "In Vitro Immunomodulation of Suppressor Macrophages From Mouse Abdominal Cavities To Enhance FC Receptor Expression." This project received financial assistance from the State Natural Science Fund.]

[Text] Macrophages are able to mediate all sorts of immune effects such as the destruction of microbes and virus granules, the elimination of immunocomplexes, and the killing or injuring of tumor cells. These actions may be enhanced by the interaction of specific Fc receptors on the surface of antibodies and macrophage membranes.[1, 2] Research carried out in recent years has shown that FC receptor participation in immunoresponse regulation, such as antigen delivery, T cell activation and reproduction, as well sa antibody production play an important role.[3] However, the expression of FC receptors on the surface of macrophage membranes is by no means constant. Evidence shows the expression of macrophage Fc receptors to be related to macrophage differentiation and maturation, [4] and that some factors that promote macrophage differentiation, such as interferon gamma (IFN-gamma), also markedly enhance Fc receptor expression.[5] Consequently, Fc receptors are also an important indicator of the macrophage membrane surface.

Work done during the past several years in our laboratory has shown that use of high dosages of cell lipopolysacchraides (LPS) to treat sodium thioglycollate-induced mouse abdominal cavity suppressor macrophages has enabled the macrophages to maintain their cytostatic effect against tumors, and has also markedly reduced their suppression of T and B lymphocyte and NK cell activity. We have terms this phenomenon "immunomodulation."[6]] Further work found that changes in immunomodulated suppressor macrophage function accompanied a marked enhancement of the secretion of activated molecules such as interleukin-1 (Il-1).[7] However, we remain uncertain as to whether any changes occurred in the surface characteristics of macrophages following immunomodulation. It has already been established that production of IL-1 may be related to IFN-gamma, [8] and that the latter may be able, in turn, to enhance the expression of the Fc receptors.[5] We are very interested in studying suppressor macrophage Fc receptor expression following

immunomodulation, and presume that sodium thioglycollate-induced suppressor macrophage following LPS immunomodulation enhances Fc receptor expression. Even though study of Fc receptors os currently being done more and more deeply,[9,10] there have as yet been no reports from either inside or outside China about changes in the expression of Fc receptors when suppressor macrophages that have been immunomodulated change into helper macrophages (as far as certain functions of T and B lymphocytes and of NK cells are concerned). In order to verify this hypothesis, we used a combination of iodine marked mouse IgG and microphage assays to study Fc receptor expression before and after immunomodulation of mouse abdominal cavity suppressor microphages. Results are reported below.

## 1. Materials and Methods

A protein A-sepharose 4 B affinity chromatography column was used to isolate the mouse serum IgG.[11] Immune double diffusion and polyacrylamide gel electrophoresis identification showed no mingling of any other type of immunoglobulin. The IgG was iodized via the chloramine T method, and following iodization, the specific activity was approximately 2.5 $\mu C_i$/mg.[12] A suspension containing different amounts of $^{125}$I-IgG and 1 x $10^6$ mouse abdominal cavity suppressor macrophages or immunomodulated suppressor microphages (see reference 6 for specifics about the sodium thioglycollate-induction and the LPS immunomodulation method) was incubated at 24 degrees C for 1 hours. The reaction solution containing 0.5 percent ox blood serum albumin and 0.2 percent $NaN_3$ was centrifuged at approximately 4 degrees C and washed three times with Hanks' solution. The microphage precipitate was counted in a gamma counter to determine the radiation intensity of microphage bonding. Excess IgG was added to the control tube at the same time to determine the radiation intensity of non-specific bonding.

## 2. Results and Discussion

Results of the four times repeated experiment showed the cpm value as being markedly higher for the LPS immunomodulated suppressor microphage bonding to $^{125}$I-IgG than for the sodium thioglycollate-induced, non-LPS processed suppressor microphages (figures 1, $p < 0.05$). The Scatchard graphing method was used to analyze data from the iodine marked IgG and Fc receptor bonding experiments, two parallel straight lines being obtained (Figure 2). This shows: (1) a marked increase in the number of Fc receptors for the immunomodulated suppressor microphages; and (2) no change in the affinity of the Fc receptors and the IgG (Table 1). This means that the increase in immunomodulated microphage bonding to $^{125}$I-IgG results from an increase in the number of Fc receptors rather than from an increase in affinity between the Fc Receptors and the IgG.

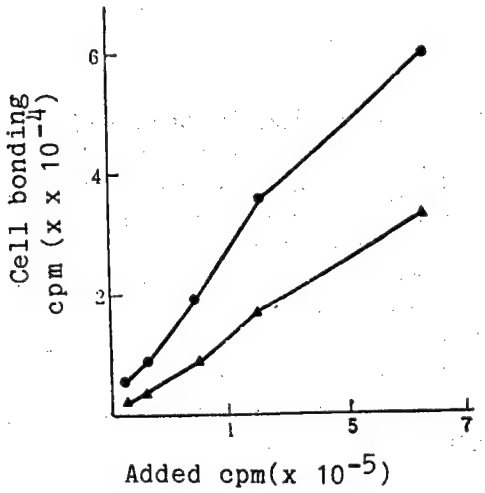


Figure 1. macrophage and $^{125}$I-IgG Bonding

▲—▲ sodium thioglycollate-induced suppressor macrophages;
●—●: LPS immunomodulated suppressor macrophages.

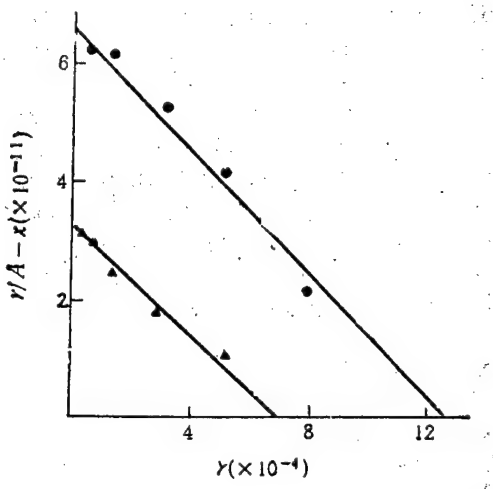


Figure 2. Scatchard Graphing Method Analysis of Assay Data on Macrophage and $^{125}$I-IgG Bonding

Y/A - x = nK = rK, r = number of bonding sites, A = $^{125}$I-IgG moar concentration, x = cell bonding $^{125}$I-IgG moar concentration, and n = number of receptors per cell. Legend is the same as for Figure 1.

Table 1. Microphage IgG Fc Receptor Affinity Coefficient and Number of Receptors*

| Cells** | Affinity Coefficient $K(M^{-1})$ | No. of Receptors per Cell |
|---|---|---|
| Sodium thioglycollate-induced suppressor macrophages | $5.0 \times 10^6$ ($p>0.05$) | $0.65 \times 10^5$ ($p<0.05$) |
| LPS immunomodulated suppressor microphages | $5.2 \times 10^6$ | $1.26 \times 10^5$ |

*Affinity coefficient K and number of receptors per cell (n) have been derived from the Scatchard graphing method (results of the experiments repeated four times).

**See reference 6 for the method used to obtain these two kinds of cells.

Simultaneous with determining the expression of Fc receptors, we also observed the cytostatic effect of microphages against tumors and in the suppression of lymphocyte transformation. Results showed that in addition to increasing Fc receptor expression, immunomodulated suppressor microphages not only maintained a marked cytostatic effect against tumors, but also markedly reduced the suppression of T and B lymphocyte transformation, as well as accelerated the reaction of lymphocytes on the reproduction of the sources of cell division [fenlieyuan 0433 5933 0626] (Results from reverification of source 6. Data omitted.)

This work showed an enhancement of rat abdominal cavity microphage Fc receptor expression following LPS immunomodulation. This step showed the effect on suppressor microphages of immunomodulation to be widespread and diverse. Nevertheless, numerous questions remain unanswered, such as to what IgG subclass of receptors the Fc receptors enhanced in this experimental system belong, whether the Fc receptor mediation function undergoes changes at the same time; what is the inherent correlation between Fc receptor enhancement and the loss of certain suppressor functions of immunomodulated suppressor microphages; and whether pertinent lymphokines take part in regulating Fc receptor expression. It is anticipated that the answers to these questions will greatly help explain the mechanism of LPS immunomodulation.

Gratitude: The author is grateful to Comrades Liu Guoliang [0491 0948 5328] and Sun Lanying [1327 5695 5391] for their energetic technical assistance.

References

1. Unkeless, J.C., et al., Avd. Immunol., 31(1981), 247.

2. Adams, D.O. and Hamilton, T.A., Ann. Rev. Immunol., 2(1984), 283.

3. Chang, T.W., Immunol. Today, 6(1985), 245.

4. Lotem, J. and Sachs, L.J., Cell. Physiol., 92(1977), 97.

5. Trinchieri, G. and Perussia, B., Immunol. Today, 6(1985), 131.

6. Zhang Zongliang et al., SHIYAN SHENGWU XUEBAO [JOURNAL OF EXPERIMENTAL BIOLOGY], 17(1984), 435.

7. Dong Qianggang [5516 1730 0474], and Zhang Zongliang, SHIYAN SHENGWU XUEBAO [JOURNAL OF EXPERIMENTAL BIOLOGY], 18(1985), 503.

8. Philip, R. and Epstein, L.B., Nature, 323(1986), 86.

9. Anderson, C.L. and Looney, R.J., Immunol. Today, 7(1986), 264.

10. Lewis, V.A., et al., Nature, 324(1986), 372.

11. Ey, P.L. et al., Immunochemistry, 15(1978), 429.

12. Greenwood, F.G. et al., Biochem. J., 89(1963), 114.

09432/06662

MONOCLONAL ANTIBODIES AGAINST MALARIA DEVELOPED FROM HYBRIDOMA CELL LINE

40081056b Beijing ZONGHUA YIXUE ZAZHI [NATIONAL MEDICAL JOURNAL OF CHINA] in Chinese Vol 67 No 12, Dec 87 p 675

[Article by Li Jiliang [2621 4764 5328], Chao Sui [1560 4482], Ouyang Minghui [2962 7122 2494 6540], and Li Yingjie [2621 5391 2638], Malaria Immunity Laboratory, First Military Medical University: "Establishment of a Heterologous Hybridoma Cell Line That Secretes Idiotype Monoclonal Antibodies Against Malaria"]

[Text] In order to study the immunodiagnosis and immunoprophylaxis role of monoclonal antibodies against malaria, we successfully established a unique hybridoma cell line from the crossing of rat and mouse cells that secretes idiotypical determinants of hongneiqi [red blood cell phase 5767 0355 2601] $IgG_2b$ sub-class monoclonal antibodies against Plasmodium falciparum. The Protein A-Sepharose CL-4 B affinity chromatography method was used on the ascitic fluid induced from the rat x mouse hybridoma cell line 94D1 that secreted hongneiqi sub-class monoclonal antibodies against Plasmodium falciparum. The purified IgG that was obtained was used in the subcutaneous immunization of pure strain Wistar rats at many points, Freund's complete adjuvant being added the first time, and Freund's incomplete adjuvant being added the second time, each rat receiving 0.75 mg each time. Three days following enhancement of immunity, homologous cell bonding with SP 2/0 tumor cells from mice was done. The H and T dosages in the hypoxanthine, aminopterin, pyrimidine nucleoside selective medium solutions were double the usual amounts. Strict checking and screening using the direct ELISA method and five clonings were done, a heterologous hybridoma cell strain (4 IRF 5) that showed consistent growth, that secreted antibodies continuouslym and that was able to withstand the freezing and revivification process without difficulty was derived. So far, culturing of successive generations in vitro has been going on for 6 months with a stability that approximates that of the hybridoma cells being obtained from a cross between a mouse and a mouse. Specific identification was made for the second monoclonal antibody obtained from the 4IRF5 using the indirect ELISA method, i.e., a comparison of the reactivity of the following eight first monoclonal antibodies, including the six strains of Plasmodium falciparum hongneiqi monoclonal antibodies: 21E3, 92D4 ($IgG_2b$), 93A3 ($IgG_1$), 94C3 ($IgG_1$), and 94D1 ($IgG_2b$), as well as one line of Plasmodium inui hongneiqi antibody 32A12 ($IgG_1$), and one line of dengue fever Type III virus antibody 215 D3 ($IgG_2b$). SP 2/0 IgG served as a control.

Results showed that the 4IRF5 second monoclonal antibody reacted only with the 94D1, a negative reaction occurring with all the other coated antigens. This demonstrated that the 4IRF5 had good anti 94D1 monoclonal antibody idiotypic determinant specificity. The specific anti-idiotypic antibody titer of the supernate from culturing of the 4IRF5 was 1:1,280. No ascitic fluid could be evoked from the bodies of BALB/C mice by using conventional methods.

The successful preparation of second monoclonal antibodies against malaria antibody idiotype determinants has laid a foundation for further study of the immunoregulatory role of malaria anti-idiotype antibodies.

(Draft received on 2 July 1987)

09432/06662

# Kala-Azar Infected Serum Circulating Antigens and Their Characteristics Detected by Monoclonal Antibody

40101011a Beijing CHINESE MEDICAL JOURNAL in English Vol 101 No 1, Jan 88 pp 1-6

[Article by Hu Xiaosu [5170 1321 4790], et al., Department of Parasitology, West China University of Medical Sciences, Chengdu. Project supported by the Science Fund of the Chinese Academy of Sciences.]

[Excerpts] Leishmania donovani antigens were successfully identified in the sera of kala-azar patients by monoclonal antibody (McAb). The serum antigens were absorbed onto nitrocellulose paper, then bound to high titer McAb-C2 against L. donovani and detected by ELISA (McAb-AST). Of 51 serum samples tested, 48 were McAb-AST positive, while sera from 367 controls (normal individuals from kala-azar endemic or non-endemic areas and patients with other infectious or parasitic diseases) were all negative. The difference between positive and negative results (ELISA color reaction expressed in ISA) was distinct and the positive degree (+-+++) decreased with the increase of serum dilution. Follow-up study of 8 kala-azar cases pre- and post-specific therapy demonstrated that McAb-AST results correlated well with their clinical symptoms and L. donovani amastigote findings. The circulating antigens in sera of kala-azar patients were found to be glycoproteins by PAS stain and trypsin digestion. They separated into 4 bands (Rf 0.35, 0.25, 0.20 and 0.06) by PAGE. By SDS-PAGE, they migrated as 3 bands (MW 96, 52 and 30 KD). Their isoelectric point (pI) as determined by IEF was between pH 8.71-9.16 and showed 7 bands. These findings indicate that the circulating antigens were a group of glycoproteins with different molecular weights and pIs.

Immunodiagnosis of parasitic diseases by detecting specific antibodies against the pathogens has been used for a long time. The method is usually very sensitive, but its specificity is sometimes unsatisfactory due to commonly encountered cross-reactions. This limits its application in some cases. The detection of circulating antigens could serve as a very specific diagnostic test.

We analyzed a total of 418 sera samples by McAb-AST, a method combining the high specificity of monoclonal antibody and high sensitivity of ELISA. The McAb-AST designed by the authors has been improved over the original as the results yield a quantitative value represented by the integral of surface

area (ISA) instead of a qualitative result only. It is demonstrated that there are circulating antigens in the sera of kala-azar patients which can be absorbed onto nitrocellulose paper and detected by McAb-AST.

Of the 51 kala-azar cases tested in our laboratory, 48 were McAb-AST positive (94.1 percent). Among them the sera of Cases 1 and 2 remained McAb-AST positive when diluted up to 1:16 (equal to 0.125 µl serum per test). Cases 3 and 7 were diagnosed clinically due to typical kala-azar symptoms and good response to antimony treatment, although no L. donovani amastigotes were found in their bone marrow smears. Their sera, nevertheless, were McAb-AST positive, indicating that the test is very sensitive to kala-azar circulating antigens. The control sera tested were all negative by McAb-AST, demonstrating the method's high specificity. When some of the positive and negative sera were tested repeatedly by McAb-AST, the results were consistent. The clinical course of 8 kala-azar patients was followed up by McAb-AST, the results correlated well with their clinical symptoms and L. donovani amastigotes bone marrow smear findings. As drug resistant kala-azar cases are increasing in number, a sensitive method to monitor their treatment is of practical significance. Our observations suggest that McAb-AST is ideal for this purpose. Some additional advantages of McAb-AST are its painlessness (as compared with pathogen detection through bone marrow biopsy) and simplicity. For each test, only 2 µl of serum is required and a large number of samples may be tested simultaneously on a single nitrocellulose sheet, ensuring consistent test results at low cost. Since negative McAb-AST results are light yellow while positive results are enlarged dark brown spots, they are easily differentiated by the naked eye. This facilitates field application.

Preliminary characterization of L. donovani circulating antigens in patient sera recognized by McAb C-2 showed that they are a group of glycoproteins with molecular weights between 30-96 KD and pIs between pH 8.71-9.16. They share an identical common-epitope recognized by McAb C-2. McAb against Leishmania spp. reported by other authors had similar characteristics, binding to a group of antigens from the protozoa instead of a single antigen molecule. Since the circulating antigens are in circulating blood and fluctuate with the patient's parasite load, they must be secreted directly by the amastigotes within macrophages. Whether they can induce protective immunity when used as immunogens in animal models remains unclear. Related research is currently under way in our laboratory.

/6091

# Characterization of VP1 as Immunodominant Antigen of Enterovirus Type 70 and Antigenic Analysis of Virus Strains by Monoclonal Antibodies

40101011b Beijing CHINESE MEDICAL JOURNAL in English Vol 101 No 1, Jan 88 pp 20-24

[Article by Liu Yang [0491 7122], et al., Department of Microbiology and Immunology, Institute of Basic Medical Science, Chinese Academy of Medical Sciences, Beijing]

[Text] The neutralizing antigens of enterovirus type 70(E70) are characterized immunochemically. It was found that all of the 7 neutralizing McAbs tested could combine with both naturally-occurring top components (NTC) and virions in immunodot test, five of them could combine with VP1 in the immunoblot system, and patient sera and antibodies from immune and hyperimmune animals could only combine with VP1. Furthermore, 10 McAbs (including the mentioned 7) were used to analyse the antigenic differences of 8 E70 strains isolated in China in 1985 and the prototype virus J670/71. The results indicate that the 10 McAbs can neutralize all 9 viruses almost equally. The data indicate that VP1 is immunodominant and stable enough to keep neutralizing antigenicity during treatment in the immunoblot system.

Enterovirus type 70(E70), one of the etiological agents of acute hemorrhagic conjunctivitis (AHC), was recognized as a type of enterovirus in 1973.[1] Later on, it was found to be composed of a single stranded RNA with a molecular weight (MW) of $2.5 \times 10^6$ daltons[2] and four structural proteins: VP1, VP2, VP3, VP4, with MWs 35,000, 28,000, 27,000 and 9,000.[3] However, little attention has been paid to the nature of its neutralizing antigen. Using the McAbs previously reported[4] and polyclonal antibodies from convalescent patient sera and animal antisera, E70 neutralizing antigens were characterized immunochemically.

## Material and Methods

Viruses. E70(J670/71) was given us by Dr. J.L. Melinck and was put through three passages in both LLCMK2 and Vero cells in our laboratory. Eight E70 strains were isolated in Beijing in 1985, as previously described. Poliovirus type II, MEF-1 (PII) and its polyclonal reference antiserum were also used.[5]

Antibodies. 10 hybridomas secreting McAbs to E70 were established by fusion of myeloma SP2/0 with spleen cells from mice immunized with E70 (J670/71) infected LLCMK2 supernatant.

Some McAbs properties are listed in Table 1. Convalescent sera from 2 AHC patients both with neutralization titers of 256, 2 mouse immune ascites fluid specimens with neutralization titer 128, and hamster hyperimmune serum with neutralization titer of 1,024 were also used.

Table 1. Some Properties of 11 Monoclonal Antibodies* to E70

| McAbs | Neutralization titers of ascites fluid** | Ig classes or subclasses*** | Sensitivity† (Lg $TCID_{50}$/ml) |
|---|---|---|---|
| N11 | 1024 | N.D.†† | N.D. |
| N13 | 1024 | IgG3 | 5.2 |
| N16 | 1024 | IgM | N.D. |
| N17 | 2048 | IgG1 | 4.6 |
| N19 | 32 | IgG2b | 5.2 |
| N21 | >8192 | IgM | N.D. |
| N22 | 256 | IgG2a | 6.1 |
| N24 | 512 | IgG3 | 5.2 |
| N34 | 2048 | IgG3 | 5.2 |
| N61 | >8192 | IgM | 5.8 |
| N159 | 64 | IgM | N.D. |

*Monoclonal antibodies were obtained by screening with neutralization test.
**The reciprocals of the highest dilution of McAbs that could neutralize 100 $TCID_{50}$ of enterovirus type 70(J670/71).
***As determined by double immunodiffusion.
†The minimal amount of virions as expressed in Lg $TCID_{50}$/ml detectable by immunodot test.
††Not done.

Purification of E70. E70 was purified essentially in the same way as the other enteroviruses.[6] Briefly, the virus-infected cell supernatants were concentrated 200-fold with polyethylene glycol, MW 6,000. The concentrates were then ultracentrifuged through 15-45 percent sucrose gradient medium. By the end of ultracentrifugation, the medium was fractionated from top to bottom with 200 µl to each fraction. The fraction distribution of viral antigens was determined by their reaction with E70 McAb N13 in the immunodot test. Reactive peaks 1 and 2 were collected and stored at -20 C.

Immunochemical methods. SDS-PAGE (polyacrylamide gel electrophoresis in the presence of SDS) and enzyme-linked immunotransblot (EITB)[5] and immunodot test[7] were done as described. Microneutralization test was essentially the same as reported by Rosenbaunm.[8]

Mice E70 antigen immunization in peaks 1 and 2. Male mice of 20-30g were immunized intravenously 3 times with 0.1 ml of fractionated peak 1 or 2 at intervals of one and two weeks. One week after the last immunization, blood was collected and sera prepared.

Results

Characterization of E70 peaks 1 and 2 prepared by sucrosegradient ultracentrifugation. After centrifugation, E70 antigens were distributed in two peaks, 1 and 2. Further tests indicated that peak 1 is about 3,500-fold less infectious than peak 2. The peaks are consistent with those found in other enteroviruses and are named the same way,[9] i.e., peak 1, naturally-occurring top components (NTC) and peak 2, virions. Both NTC and virions were used to immunize mice to test the immunogenicity. The results are shown in Table 2. It is seen that both NTC and virions are quite competent in inducing antibodies capable of combining specifically with the virions. However, the antibodies induced have different properties, those induced by NTC have higher titers in combining with virions but are less competent in neutralizing E70 (I/N ratio 1:8), while those induced by virions are competent in both combining with and neutralizing E70 (I/N ratio 1:2).

Table 2. Immunogenicity of E70 NTC and Virions as Determined by the Properties of the Antibodies They Induced in Balb/C Mice*

| Mice No. | Immunogens | Antisera titers** | | |
|---|---|---|---|---|
| | | Immunodot*** | Neutralization | I/N† |
| 1 | NTC | 1280 | 160 | 8 |
| 2 | NTC | 1280 | 160 | 8 |
| 3 | Virions | 2560 | 1280 | 2 |
| 4 | Virions | 2560 | 1280 | 2 |
| 5 | Virions | 2560 | 1280 | 2 |

*Balb/C mice immunized by either NTC or virions intravenously 3 times.
**Reciprocals of the last dilution to give the positive results.
***E70 virions as antigens. The sera reacted with the cellular antigens of controls with a titer of less than 40.
†The ratios of the titers of immunodot test to those of neutralization test.

McAbs reactivity with E70 NTC and virions. 7 neutralizing McAbs to E70 were tested for their ability to combine with NTC and virions in the immunodot system. As shown in Fig. 1 [photo not reproduced], all 7 McAbs combine specifically with both NTC and virions, but not with the cellular antigen controls prepared by procedures corresponding either to NTC or virions.

To exclude the possibility that the McAbs reaction with NTC was caused by trace virion contamination of NTC, the McAbs sensitivity in detecting virions was determined by serial dilutions of virions. The results showed that the sensitivity of different McAbs varied from 4.6 to 6.2 Lg $TCID_{50}$/ml (Table 1), much higher than the infections NTC titer (3.8 Lg $TCID_{50}$/ml). McAbs cannot detect trace virions present in NTC.

Reactivity of 7 neutralizing McAbs with E70 structural proteins. Identification of E70 structural proteins by immunoblot test. The position of E70 structural proteins in our EITB system were determined by comparison with those of poliovirus type II MEF-1. A rabbit anti-PII serum was known to combine with VP1 and VP2 of PII in EITB.[5] Fig. 2 [photo not reproduced] indicates that McAb N13 can combine with E70 VP1 in the immunoblot system.

McAbs reactivity with E70 structural proteins. Fig. 3 [photo not reproduced] shows that of the 7 McAbs tested, 5 (N13, N17, N19, N22, N34) combine with E70 VP1, while McAbs N24 and N61 fail to do so.

Polyclonal antisera reactivity with E70 structural proteins. Fig. 4 [photo not reproduced] shows, quite surprisingly, that the 2 patient convalescent sera, mouse immune ascites fluid and hamster hyperimmune serum to E70 could only combine with E70 VP1 but not with the other structural proteins.

Characterization of the antigenic differences of wild strains and prototype virus J670/71. 10 McAbs (all but N19 listed in Table 1) were tested for ability to neutralize 8 wild E70 strains isolated in Beijing in 1985 and prototype virus J670/71. The results show that the McAbs can neutralize 9 viruses with titers all above 64.

Discussion

The antigenic characteristics of human enteroviruses, including the NTC, virions and structural proteins have been investigated. In polioviruses, it was generally accepted that the neutralizing antigens are highly dependent on the quaternary structure of the virions, thus neither C antigens nor individual proteins induce the production of neutralizing antibodies, nor can they combine with them.[10-12] Most efforts to locate the neutralizing antigenic determinants on the structural proteins have been unsuccessful.[13,14] However, the situation is different with other enteroviruses. Beatrice et al.[15] found that the VP2 of Coxsackie virus B3 is as competent as its virions in inducing neutralizing antibodies to homotypic virus. In Echovirus type 12, it was shown that NTC was antigenically very similar to its virions.[16] As far as we know, no reports concerning the antigenic properties of E70 are available.

Our data shows that, although both the NTC and virion are almost equally competent in inducing antibodies capable of combining with virions, and both are capable of inducing neutralizing antibodies to homotypic virus, NTC induced antibodies are much less active neutralizers, the actual mechanism of which remains unknown. Our previous work suggested that poliovirus NTC prepared in the same way could not induce neutralizing antibody at all. These results suggest that the NTC and virions of E70 are immunologically distinguishable but are more inter-related than those of poliovirus.

Of 7 neutralizing McAbs, 5 were able to combine in immunoblot test with VP1 while the other 2 failed to combine with any structural proteins. All 7 McAbs could combine with E70 NTC and virions in the immunodot test. This strongly suggests that E70 neutralizing antigens are less dependent on the

quaternary structure of virions, the primary structure, and/or the conformation of individual structural proteins may be more important.

Surprisingly, AHC patient convalescent sera, polyclonal mouse immune ascites fluid and hamster hyperimmune serum can only combine with E70 VP1. This differs with the results of other authors using other enteroviruses, suggesting that E70 VP1 is highly immunodominant.

When 10 neutralizing McAbs were used to characterize the antigenic differences of 9 viral strains, it was found that the 8 strains of E70 isolated during an epidemic in 1985 in Beijing were antigenically closely related to each other and to J670/71 isolated in 1971 in Japan, suggesting that there has been no dramatic antigenic variation in E70 during the past 15 years. This result contrasts with that of polioviruses where the antigenic differences between viruses from different areas and times can be easily detected by neutralizing McAbs, but agrees with Anderson et al.'s results that two neutralizing McAbs tested could neutralize 9 wild viruses isolated during 1971 to 1981 from different places all over the world.[17-19] The stability and immunodominance of VP1 as E70 neutralizing antigen suggests the possibility of using VP1 as an effective vaccine for acute hemorrhagic conjunctivitis caused by E70.

Recently, Hogle et al.[20] succeeded in deciphering the atomic structure of poliovirus and were able to locate the neutralizing antigenic sites in four distinct clusters. Further study of the fine antigenic structure of E70 and comparison with that of poliovirus will be valuable for understanding the nature of viral antigen quaternary structure dependence.

## REFERENCES


1. Mrikovie, R.R., et al., Enterovirus type 70: the etiologic agent of pandemic acute hemorrhagic conjunctivitis. Bull WHO 1973; 49:341.

2. Yamazaki, S., et al., Purification and biophysical properties of acute hemorrhagic conjunctivitis virus. J Virol 1974; 14:1357.

3. Esposito, J.M., et al., Enterovirus type 70 virion and intracellular proteins. J Virol 1976; 18:1160.

4. Mu Guifan, et al., Establishment of Hybridoma Cell Lines Secreting Monoclonal Antibodies Against Enterovirus 70. Chinese Journal of Ophthalmology, 1987; 23 (3):131.

5. Liu Yang, et al., Study on Common Antigens of Human Enterovirus. Graduate Dissertation, Xiehe Medical University in China, 1985.

6. Liu Yang, et al., A Highly Stable and Conserved Neutralizing Antigenic Determinant Poliovirus. Chinese Journal of Microbiology and Immunology, 1985; 5 (4):229.

7. Liu Yang, et al., Preliminary Study of McAb Immuno-Spot Test on Poliovirus Typings. Chinese Journal of Immunology, 1986; 2 (3):173.

8. Rosenbaunm, M.J., et al., A simplified method for virus tissue culture procedures in microtitration plate. Proc Soc Exp Biol Med 1963; 113:224.

9. Gu Gangzhou, et al., Study on Common Antigens of Enterovirus 7. 1987; not published.

10. Rubert, R.P., et al., On the morphogenesis of picornavirus. Comprehensive virology. Vol. 6, New York: Plenum, 1977:131-213.

11. Heloen, R.H., et al., Comparison of the antibodies elicited by the individual structural proteins of foot and mouth disease virus and poliovirus. J Gen Virol 1979; 45:761.

12. Derinick, R., Antigenic structure of poliovirus. Devel Biol Stand 1981; 47:319.

13. Thorpe, R., et al., Immunochemical studies of poliovirus: Identification of immunoreactive virus capsid polypeptides. J Gen Virol 1983; 63:487.

14. Ferguson, M., et al., Neutralization epitopes on poliovirus type III particles: an analysis using monoclonal antibodies. J Gen Virol 1984; 65:197.

15. Beatrice, S.T., et al., Induction of neutralizing antibodies by the Coxsackie virus B3 virion polypeptide, VP2. Virology 1980; 104:426.

16. Halperen, S., et al., Evidence for uncoupled synthesis of viral RNA capsid. Virology 1964; 24:36.

17. Mertens, T.H., et al., Cross-antigenicity among enterovirus as revealed by immunoblot technique. Virology 1983; 129:431.

18. Gu Fangzhou, et al., Antigenic Analysis of 100 Strains Poliovirus I by McAb. Chinese Journal of Preventive Medicine, 1985; 19 (5):265.

19. Anderson, L.J., et al., Detection of enterovirus 70 with monoclonal antibodies. J Clin Microbiol 1984; 20:405.

20. Hogle, J.M., et al., Three-dimensional structure of poliovirus at 2.9 A resolution. Science 1985; 229.1355.

/6091

# Studies on Antigenic Variation of Types I and III Poliovirus Using Neutralizing Monoclonal Antibody

40101011c Beijing CHINESE MEDICAL JOURNAL in English Vol 101 No 1, Jan 88 pp 32-36

[Article by Guo Ren [6753 0088], et al., Institute of Medical Biology, Chinese Academy of Medical Sciences, Kunming]

[Text] Cross-neutralizing assays were done on 85 strains of poliovirus type I with 5 groups of monoclonal antibodies. According to the antigenic differences, these 85 type I strains were classified into 10 subgroups. There were remarkable differences in the antigenicity among the 10 subgroups, of which P1-2 (27.06 percent) and P1-5 (40 percent) are dominant and have been found to be epidemic in China in recent years. These two subgroups were antigenically different from the Sabin-1 strain, but shared common antigenic epitopes with the Mahoney strain and the Brunhilde strain according to their responses to group C monoclonal antibodies. Similarly, 91 strains of type III poliovirus were classified into 6 subgroups with other 5 groups of monoclonal antibodies. The results showed that the strain P3/Yunnan/2/84 which was isolated from cases of poliomyelitis in Yunnan Province of China in 1984 and the strain P3/Finland/23127/84 which was isolated in Finland in 1984 were both antigenically different from the Sabin-3 strain and the reference virulent strain.

There are 3 stable serotypes in poliovirus antigenicity. In recent years, some obvious antigenic variations in intratypic strains have been found by using specific monoclonal antibodies at different laboratories. Some differences in antigenicity of common strains (Leon 12alb or Saukett) and strains isolated from poliomyelitis cases occurring in Finland in 1984 were noted.[8,9] Our preliminary studies on antigenic variation of polioviruses types I and III were performed with neutralizing monoclonal antibodies in our laboratory. The results of our study are reported in this paper.

## Poliovirus Type I

Viruses. Eighty-five strains of type 1 poliovirus were chosen for analysis. These strains included 75 strains isolated from stools of patients in different areas of 9 provinces in China; 6 strains donated by Dr. Schild and Dr. Ferguson isolated in different countries and supplied by several laboratories; 4 reference strains stored in our laboratory (Table 1).

Table 1. Virus Strains of Poliovirus Type I Used in the Analysis of Antigenic Variations

| Source of viruses | Number of strains | Source of strains | |
|---|---|---|---|
| | | Patients | Contacts and healthy children |
| Fujian | 10 | 7 | 3 |
| Jiangxi | 3 | 3 | 0 |
| Jiangsu | 4 | 4 | 0 |
| Guangdong | 10 | 8 | 2 |
| Yunnan | 16 | 2 | 14 |
| Henan | 12 | 12 | 0 |
| Shanxi | 4 | 4 | 0 |
| Shandong | 7 | 7 | 0 |
| Shanghai | 9 | 9 | 0 |
| WHO | 6 | | |
| Reference strains* | 4 | | |
| Total | 85 | 56 | 19 |

*The 4 reference strains from our laboratory are: Sabin I (LSc, 2ab), Zhong $I_9$, Mahoney and Brunhilde.

Monoclonal antibodies (Table 2). Type 1 Sabin vaccine strain (LSc 2ab) and Brunhilde strain (a type 1 reference "wild" strain) were chosen as antigens to immunize Balb/c mice. After fusing, screening and cloning, 32 hybridoma cell lines secreting specific monoclonal antibodies against type 1 poliovirus were established in our laboratory. Cross-neutralizing assays were used to determine the neutralizing capacities of 32 monoclonal antibodies with 4 reference strains of type 1 poliovirus respectively. These assays divided 32 monoclonal antibodies into 6 groups. Because group F antibodies failed to recognize the antigenic differences of the representative strains, this group was not used in the test. Five antibodies chosen from another five groups were used in antigenic analysis.

Antigenic analysis of the viruses. Using 5 groups of monoclonal antibodies (A-E), cross-neutralizing assays were done on 85 strains of poliovirus type I. The results in Table 3 indicate that in the light of antigenic differences, these 85 type 1 strains were classified into 10 subgroups. There were marked disparities in the antigenic characteristics of the 10 subgroups. The constituent proportion of every subgroup showed that P1-2 (27.06 percent) and P1-5 (40.0 percent) were dominant and these two subgroup strains have caused epidemics in China during recent years. There are obvious antigenic variations between the two subgroup strains and the Sabin strain. But the two subgroup strains, Mahoney and Brunhilde, share common antigenic epitope as they all respond to group C monoclonal antibodies. The reaction pattern of subgroup P1-2 to 5 groups of monoclonal antibodies was very similar to that of the Mahoney strain (subgroup P1-3), so subgroup P1-2 may derive from the Mahoney strain. There were notable differences in the antigenicity of subgroup P1-5 and other strains. As subgroup P1-5 was dominant in the recent epidemic, it ought to merit our attention.

Table 2. Grouping of Monoclonal Antibodies Against Poliovirus Type I

| Groups of antibodies | Neutralizing capacities of representative strains* | | | | Number of McAb | Name of McAb |
|---|---|---|---|---|---|---|
| | Sabin I | Zhong I9 | Mahoney | Brunhilde | | |
| A | + | - | - | - | 3 | 1S-3, 1S-5, 1S-10 |
| B | - | - | - | + | 13 | 1B-1, 1B-2, 1B-3, 1B-4, 1B-5, 1B-6, 1B-9, 1B-11, 1B-12, 1B-13, 1B-16, 1B-17, 1B-19 |
| C | - | + | + | + | 3 | 1B-7, 1B-8, 1B-15 |
| D | + | + | + | - | 5 | 1S-2, 1S-4, 1S-6, 1S-8, 1S-14 |
| E | + | - | + | - | 4 | 1S-7, 1S-11, 1S-12, 1S-13 |
| F | + | + | + | + | 1 | 1S-9 |
| Unclassed | | | | | 3 | 1B-10, 1B-14, 1B-15 |

*Neutralized with 100 $TCD_{50}$ virus; when the neutralization titer is >1:20, it is recorded as +; when <1:20, it is -.

Table 3. Antigenic Analysis of 85 Strains of Type I Poliovirus With 5 Groups of Specific McAb

| Grouping of strains of type I poliovirus according to antigenic variation | Antigenic characteristics* | No. of virus strains | % | Representative virus strain of group |
|---|---|---|---|---|
| P1-1 | A+B-C-D+E+ | 3 | 3.53 | Sabin-1 (LSc-2ab) |
| P1-2 | A-B-C+D+E- | 23 | 27.06 | Zhong I9, 8/P1/Henan/82 |
| P1-3 | A-B-C+D+E+ | 13 | 15.28 | Mahoney |
| P1-4 | A-B+C+D-E- | 5 | 5.88 | Brunhilde |
| P1-5 | A-B-C+D-E- | 34 | 40.00 | 149/P1/Yunnan/81 |
| P1-6 | A-B-C-D+E+ | 1 | 1.18 | 477/P1/Fujian/82 |
| P1-7 | A-B-C-D-E+ | 1 | 1.18 | 13/P1/Henan/82 |
| P1-8 | A-B-C+D-E+ | 3 | 3.53 | A/P1/WHO |
| P1-9 | A+B-C+D-E+ | 1 | 1.18 | D/P1/WHO |
| P1-10 | A+B-C+D+E+ | 1 | 1.18 | F/P1/WHO |

*See Table 2.

Subgroups P1-8, P1-9 and P1-10 were isolated in different countries and varied in antigenic characteristics. The results show that the antigenic shift and variation of polioviruses are marked.

Poliovirus Type III

Viruses. Ninety-one strains of poliovirus type III were chosen for analysis. These strains included 81 strains isolated from patients in different parts of 11 provinces throughout China; 2 strains donated by Dr. Schild and Dr. Ferguson isolated from patients infected with poliovirus type III in Finland in 1984; 5 strains or vaccine strains also proviced by Dr. Schild and Dr. Ferguson isolated from patients in different countries; and 3 reference strains (Leon 12a1b, Zhong $III_2$ and Saukett) stored in our laboratory (Table 4).

Table 4. Virus Strains of Poliovirus Type III Used in Our Studies

| Source of virus strains | Number of strains | History | Provider |
|---|---|---|---|
| China | 81 | Poliomyelitis | 11 sanitary and anti-epidemic stations |
| Finland | 2 | Poliomyelitis | Dr. Schild and Dr. Ferguson |
| WHO | 2 | Poliomyelitis | ibid. |
| | 2 | Vaccine related | ibid. |
| | 1 | Leon $12a_1b$ | ibid. |
| Reference | 1 | Leon $12a_1b$ | IMB, CAMS* |
| | 1 | Zhong $III_2$ | ibid. |
| | 1 | Saukett | ibid. |

*IMB, CAMS: Institute of Medical Biology, Chinese Academy of Medical Sciences, Kunming.

Monoclonal antibodies. Eight McAb to poliovirus type III were used in the analysis. McAb 3Saul was prepared by immunizing with Saukett strain, McAb 3S1, 3S12, BW54-4 and 3S9 were all prepared by immunizing with Leon 12a1b strain. McAb (NIB472, 204 and 842) were supplied by Dr. Schild and Dr. Ferguson. McAb NIB842 was prepared by immunizing with P3/Finland/23127/84 strain which was epidemic in Finland during 1984. The cross-neutralizing assays were used to determine the neutralizing capacities of 8 monoclonal antibodies with 4 representative type III strains (Leon 12a1b, Zhong III2, Saukett and P3/Finland/23127/84). These assays divided the 8 McAb into 5 groups (A-E). Five antibodies chosen from the five groups were used in the antigenic analysis (Table 5).

Antigenic analysis of the viruses. Using 5 groups of monoclonal antibodies (A-E), cross-neutralizing assays were done on 91 strains of poliovirus type III. The results in Table 6 reveal that according to antigenic differences, the 91 strains of type III were classified into 6 subgroups (P3-1 to P3-6). Sabin 3 vaccine strain (Leon 12a1b) was a representative virus of subgroup P3-1 and was neutralized by McAb B, C and D prepared by immunizing with the

Table 5. Monoclonal Antibodies to Polioviruses Type III Used in the Studies

| Anti-bodies | McAb name | Source | Neutralizing response to representative strains* Leon 12a1b | Zhong III2 | Saukett | P3/Finland/23127/84 | McAb grouping | Immunizing virus |
|---|---|---|---|---|---|---|---|---|
| McAb | 3Sau-1 | IMB, CAMS** | - | - | + | - | A | Saukett |
| | 3S-1 | ibid. | + | - | - | - | B | Leon 12a1b |
| | 3S-12 | ibid. | + | + | - | - | C | Leon 12a1b |
| | BW54-4 | Pasteur Inst. | + | + | - | - | C | Leon 12a1b |
| | 3S-9 | IMB, CAMS | + | + | + | - | D | Leon 12a1b |
| | NIB472 | NIBSC*** | + | + | + | - | D | |
| | NIB204 | ibid. | + | + | + | - | D | |
| | NIB842 | ibid. | - | - | - | + | E | P3/Finland/23127/84 |
| PcAb | | IMB, CAMS | + | + | + | + | | Saukett |

*See Table 2. **See Table 4. ***NIBSC: National Institute for Biological Standards and Control, London.



Table 6. Antigenic Analysis of 91 Strains of Type III Poliovirus With Specific McAb

| Grouping of strains type III poliovirus according to antigenic variation | Antigenic characteristics recognized by McAb | Immune sera (PcAb) | Number of virus strains | % | Representative virus strain in group |
|---|---|---|---|---|---|
| P3-1 | A-B+C+D+E- | + | 20 | 21.9 | Leon 12a1b |
| P3-2 | A-B-C+D+E- | + | 7 | 7.6 | Zhong III2 |
| P3-3 | A-B-C-D+E- | + | 50 | 54.9 | 374/Japan/57<br>Henan/13/80<br>Yunnan/7/84<br>Finland/02575/84 |
| P3-4 | A-B-C-D-E+ | + | 1 | 1.1 | Finland/23127/84 |
| P3-5 | A-B-C-D-E- | + | 1 | 1.1 | Yunnan/2/84 |
| P3-6 | A+B-C-D+E- | + | 12 | 13.2 | Saukett |

same strain. Zhong $III_2$ was a representative virus of subgroup P3-2, which was an attenuated type III vaccine strain selected by us,[10] its antigenic characteristics were similar to those of Leon 12alb. P3-3 has been one of the main epidemic type III strains causing poliomyelitis here, it was first found in Japan in 1957 and later appeared in China. The isolated strain (P3/Finland/02575/84) which was epidemic in Finland during 1984 also belonged to subgroup P3-3 according to its antigenicity. Yet the antigenicity of P3/Finland/23127/84 strain was entirely different from the other mentioned strains including P3/Finland/02575/84 strain isolated during the same period. Of the 81 test strains isolated in China, none shared common antigenicity with the P3/Finland/23127/84 strain (Table 6). This suggests that the strain may be a new virus derived from other strains of type III poliovirus, and this should be noted. Interestingly enough, it was found that P3/Yunnan/2/84 strain was identified as a type III poliovirus by being neutralized with sheep antiserum specific to type III poliovirus. But P3/Yunnan/2/84 strain could not be neutralized by any of the 5 groups of monoclonal antibodies used in our laboratory. This strain is close to, yet different from, the P3/Finland/23127/84 strain in antigenicity. The P3/Yunnan/2/84 strain was isolated from poliomyelitis cases caused by a local epidemic in Yunnan Province during 1984. This strain is under further study in our laboratory.

Discussion and Suggestions

Using neutralizing monoclonal antibodies, it is proved that there are obvious antigenic variations in intratypic strains. The specific patterns governing antigenic shifts and changes, the relation between antigenic variation and multiplication of attenuated vaccine strains in human intestines and evolutionary pressure caused by population antibody levels should be further studied.

Our results show that in some strains antigenic variation is more obvious in types I and III poliovirus, such as subgroup P1-5 of type I, and P3/Finland/23127/84 strain and P3/Yunnan/2/84 strain of type III. These strains may cause poliomyelitis epidemics outbreak. Therefore, the preventive efficacy of inactivated poliovirus vaccine and live attenuated poliovaccine in human populations free of infection by these three viruses should be further clarified.

In our preliminary studies, it was found that not a single strain of the 81 type III poliovirus strains isolated in different parts of China could be identified with P3/Finland/23127/84 strain. But it was found that P3/Finland/02575/84 strain shared common antigenicity with most of the strains isolated in China.

If feasible, we suggest that international collaborative studies on the problems cited be organized and financed by WHO so a world wide program for poliomyelitis control can be carried out.

## REFERENCES


1. Guo, R., et al., Antigenic analysis of poliovirus type I with neutralizing monoclonal antibodies. Kexue Tongbao 1985; 3:273.

2. Gu, F.Z., et al., Application of ELISA for screening McAb against type III polioviruses and its antigenic analysis. Acta Acad Med Sin 1985; 7:359.

3. Minor, P.O., et al., Genetic and antigenic variation in type III polioviruses, characterization of strain by McAbs and T1 oligonucleotide mapping. J Gen Virol 1982; 61:167.

4. Ferguson, M., et al., Neutralizing epitopes on poliovirus type III particles: An analysis using McAb. J Gen Virol 1984; 65:197.

5. Crainic, R., et al., Antigenic variation of virus neutralization epitopes. Inf Immunol 1983; 41:1217.

6. Crainic, R., et al., Antigenic variation of poliovirus studied by means of monoclonal antibodies. Rev Inf Dis 1984; 6 (Suppl 2):535.

7. Diamond, D.C., et al., Antigenic variation and resistance to neutralization in poliovirus type I. Science 1985; 229:1090.

8. Leinikki, et al., Paralytic poliomyelitis in Finland. Lancet 1985; 31:507.

9. CDSC Report. Outbreak of poliomyelitis in Finland. Br Med J 1985; 291:41.

10. Guo, R., et al., Studies on new attenuated strains of type III live poliomyelitis vaccine I: Development of a new type III attenuated poliovirus. Chin Med J 1980; 93:583.


/6091

Clinical Evaluation of HBV DNA Reverse Spot Hybridization

40091051a Shanghai ZHONGHUA CHUANRANBING ZAZHI [CHINESE JOURNAL OF INFECTIOUS DISEASES] in Chinese Vol 6 No 1, Feb 88 pp 7-10

[Article by Chen Yangqing, et al., Shanghai Cancer Institute, etc.]

[Abstract] The assay of HBV DNA reverse spot hybridization has been more simplified by using the filter with crude pBR322-HBV DNA spot, which was prepared by NaOH/SDS method. As a market of HBV infection, the serum of hepatitis patients from several hospitals in Shanghai were assayed. Three hundred eighty-three samples f hepatitis patients with HBV immunoserological markers and HBV DNA sot assay were analysed by double blind test. It indicated that all the 63 cases of HBsAg(+)/HBeAg(+)/HBV DNA(+) and 23 out of the 28 cases of HBsAg(+)/HBeAg(-)/HBV DNA(+) showed positive reaction; 28 cases of non-HBV hepatitis including 11 HAV and 6 NANB patients were negative. It is proved that this assay is a sensitive dependable marker for identifying the infectious status of HBV carriers.

Key words: Crude pB322-HBV DNA HBV reverse hybridization assay HBV hybridization and immunoserological markers

/12232

## Immunohistochemical Assay for HbsAg and HbcAg in HBV and HAV Double Infection by Monoclonal Antibody and ABC Method

40091051b Shanghai ZHONGHUA CHUANRANBING ZAZHI [CHINESE JOURNAL OF INFECTIOUS DISEASES] in Chinese Vol 6 No 1, Feb 88 pp 11-13, 26

[Article by Zhu Chunwu, et al., Dept of Pathology, the 302 Hospital, PLA]

[Abstract] The immunohistochemical assays for HBsAg and HBcAg in liver sections of 30 cases with serum anti-HAV IgM positive acute hepatitis were performed. Twenty-one cases (70.0 percent) of HAV and HBV double infection were detected. Five cases of coinfection were histopathologically diagnosed as acute hepatitis, of which 3 showed serum HBV markers negative by HBcAg positive in liver section. Sixteen cases of superinfection were histopathologically diagnosed as CAH in 7, CPH in 5, ACH in 2 and involution changes in 2 cases. Three of there were HBsAg or HBcAg positive in liver sections in acute phase of HAV infection, but serum HBV markers were negative. The results showed that the expression of HBV markers might be inhibited when double infection occurred. The immunohistochemical assay for HBsAg and HBcAg could increase the rate of eliciting the double infection.

Key words: Hepatitis A hepatitis B coinfection superinfection

/12232

Study on Relationship Between HBV DNA and e System in Hepatitis B Patients

40091051c Shanghai ZHONGHUA CHUANRANBING ZAZHI [CHINESE JOURNAL OF INFECTIOUS DISEASES] in Chinese Vol 6 No 1, Feb 88 pp 14-17

[Article by Min Xian, et al., Dept of Infectious Diseases, the First Affiliated Hospital, Nanjing Medical College]

[Abstract] We have assessed the presence of HBV DNA in serum samples from 172 patients with HBsAg-positive hepatitis B by hybridization test with cloned HBV DNA probe. It was found that the positive rates of serum HBV DNA were 90.10 percent, 28.13 percent and 23.52 percent in HBeAg positive, anti-HBe positive and e system negative patients respectively. The results indicate that there is a close correlation between serum HBV DNA and e system. The serum HBV DNA is more sensitive than e system in reflecting the replication of HBV. On the other hand, the data showed that the model of both positive HBV DNA and HBeAg was often seen in HBsAg carrier, acute hepatitis and CPH, while the model of both positive HBV DNA and anti-HBe often seen in cirrhosis and CAH. It seems that there are some relationships between the aforementioned different models and various degrees of severity of hepatitis.

Key words: Hepatitis B HBV DNA spot hybridization test

/12232

Study on the Cellular Immunoregulatory Effect of $a_2$-Macroglobulin on Chronic Active Hepatitis

40091051d Shanghai ZHONGHUA CHUANRANBING ZAZHI [CHINESE JOURNAL OF INFECTIOUS DISEASES] in Chinese Vol 6 No 1, Feb 88 pp 18-22

[Article by Wang Hongyang et al., Changzheng Hospital, Shanghai]

[Abstract] The purpose of this paper is to explore the immunoregulatory effect of $a_2$-macroglobulin ($a_2$M) on cellular immunity and the association of $a_2$M purified from human plasma was capable to suppress the proliferative response of lymphocytes to several different lectins (the effect noted was dose-dependent). T lymphocytes were found to have surface-bound $a_2$M by the direct immunofluorescent technique. The serum levels $a_2$M were found elevated in 8 of the 30 CAH patients (26.7 percent). The proliferative response (in vitro) of lymphocytes in patients with CAH was markedly increased or even restored to normal by the addition of anti-human $a_2$M, which suggest that the function of cellular immunity of patients with CAH is closely related to $a_2$M.

Key words: Association of $a_2$-M with CAH immunoregulatory effect of $a_2$-M suppressing effect of $a_2$-M on cellular immunity

/12232

Study of the Metabolic Kinetics of Amino Acids in Fulminating Hepatitis

40091051e Shanghai ZHONGHUA CHUANRANBING ZAZHI [CHINESE JOURNAL OF INFECTIOUS DISEASES] in Chinese Vol 6 No 1, Feb 88 pp 23-26

[Article by Zhou Xiaqiu, et al., Ruijing Hospital, Shanghai Second Medical University]

[Abstracts] The mechanism of various amino acids imbalance in fulminating hepatitis was studied with a stable isotope tracer method for observing simultaneously the metabolic kinetics of several amino acids. $^{15}$N-L-Ala, (2, 3aB $^{2}$H)-L-Leu and (2, 3-aB $^{2}$H)-L-Phe were selected as representatives of non-essential, branched chain and aromatic acids. A single injection of 40mg $^{15}$N-Ala, 20mg $^{2}$H-Leu and 20mg $^{2}$H-Phe was given to each human subject. Blood samples were taken just before and at different times (up to 60 min) after the injection. The total free amino acids were isolated form the plasma with a small Dowex 50 X 8 eolumn and converted to trifluoresceetyl derivatives. Their abundance was then analyzed with a GC-MS labeled amino acids. Thus a two pool model was designed and applied for compartmental analysis. Significant changes were found in the kinetic parameters of Phe and Leu in patients with fulminant hepatitis. The half-life of Phe was longer and the pool size was larger than normal subjects, while the half-life and pool size of Leu changed in the opposite direction. No significant change was found in Ala.

Key words: Stable isotope Fulminant hepatitis kinetic parameters plasmatic pool cellular pool

/12232

One Step Incubation ELISA for the Detection of HBsAg

40091051f Shanghai ZHONGHUA CHUANRANBING ZAZHI [CHINESE JOURNAL OF INFECTIOUS DISEASES] in Chinese Vol 6 No 1, Feb 88 pp 31-33

[Article by Yao Jilu, et al., Dept of Infectious Diseases, Sun Yat-Sen University of Medical Sciences]

[Abstract] A new technique for the detection of HBsAg by one step incubation ELISA was developed. Two strains of monoclonal hybridoma cell (D2H5 and H3F5) were selected for the production of monoclonal anti-HBs, and the antibodies were used respectively for conjugation with peroxidase or for coating the solid phase in this ELISA system. Procedure of the technique is described. The sensitivity level of this ELISA system was up to 1 to 3 ng HBsAg/ml with P/N ratio 2.1 to 5.0. 32 HBsAg negative samples were tested by this ELISA system repeatedly, no false positive result was found. 269 HBsAg carrier sera were detected parallelly by both RIA and this ELISA system by different technicians, and the results were all found positive. One thousand samples from the population in Guangzhou area were determined by RIA and this ELISA system by two groups of technicians, the results were highly comparative. The authors hold that this assay is considered as a technique of high sensitivity, simplicity and specificity.

Key words: HBsAg McAb ELISA

/12232

# The Single-Cell Protein Productivity of Rhodopseudomonas Sphaeroides S Growing on Rice Slurry Effluent

40091048 Beijing ZHONGGUO HUANJING KEXUE [CHINA ENVIRONMENTAL SCIENCE] in Chinese Vol 8 No 1, Feb 88 pp 50-54

[Article by Gu Zuyi, Department of Environmental Sciences, East China Normal University, Shanghai; passages in slantlines published in italics]

[Abstract] The growth characteristics, protein productivity and protein content of /Rhodopseudomonas sphaeroides/ S were studied in chemostat cultures of facultative anaerobic-light (S-I, DO$\approx$0 mg $l^{-1}$, lamplight), facultative aerobic-light (S-II, $0 < DO < 5$ mg $l^{-1}$, lamplight) and aerobic-dark (S-III, DO$\approx$5 mg $l^{-1}$, dark) conditions on rice slurry effluent. The growth of /Rp. sphaeroides/ S observed in S-I and II was superior to that in S-III. The values of protein productivity determined in S-I and II were 1.5 to 2 times of that in S-III. It was found that maximum value of protein productivity calculated was 0.0227 g-protein $g^{-1}$ $h^{-1}$, i.e. 0.545 kg-protein $kg^{-1}$ $day^{-1}$; in experiment S-I at dilution rate of 0.04-0.06 $h^{-1}$. It may be concluded that facultative anaerobic-light or facultative aerobic-light might be excellent for the protein productivity by /Rp. sphaeroides/ S.

This experiment indicated that cells of /Rp. sphaeroides/ S growing on rice slurry effluent under facultative anaerobic-light, facultative aerobic-light and aerobic-dark conditions had protein contents of 74.97, 50.1 and 62.45 percent respectively. The value of protein content obtained under facultative anaerobic-light condition is remarkably higher than those of yeast cells, egg and soybean and other photosynthetic bacteria.

It is then possible to product single-cell protein by /Rp. sphaeroides/ S from rice slurry effluent. Its productivity is quite large.

/09599

## Cryogenic Preservation of Erythrocytes Using Dimethylsulfoxide (DMSO)

40091046 Beijing JIEFANGJUN YIXUE ZAZHI [MEDICAL JOURNAL OF CHINESE PEOPLE'S LIBERATION ARMY] in Chinese Vol 13 No 1, Feb 88 pp 9-11

[Article by Liu Jinghan and Han Yufeng, Transfusion Department, General Hospital of PLA]

[Abstract] Erythrocytes were frozen with DMSO of different concentrations (not over 20 percent) as a cryoprotective agent in freezers of different temperatures.

The rate of temperature drop was not controlled. Of the erythrocytes actually frozen, the average recovery rate after thawing was 91.3 percent (range 87.5 ~ 95 percent). The average survival rate of erythrocytes stored at -20 degrees C, -30 degrees C, or -80 degrees C for up to 8 months was 90.9 percent (range 88.2 ~94.5). As compared with glycerol, which is in common use internationally, DMSO seems to be a better cryoprotective agent.

/09599

## Establishment of Four Monoclonal Antibodies to a Poorly Differentiated Gastric Cancer Cell Line MKN-46-9 and Immunohistochemical Study on Their Corresponding Antigens

40091046 Beijing JIEFANGJUN YIXUE ZAZHI [MEDICAL JOURNAL OF CHINESE PEOPLE'S LIBERATION ARMY] in Chinese Vol 13 No 1, Feb 88 pp 12-15

[Article by Fan Daiming, et al., Digestive Laboratory, Xijing Hospital, Fourth Military Medical College, Xi an]

[Abstract] Four murine monoclonal antibodies, MG5, MG7, MG9, and MG11, are produced by Balb/c mice immunized with a poorly differentiated gastric cancer cell line MKN-46-9. They can react immunohistochemically with cancers of gastric, colonic, esophageal or pulmonary origin as well as epithelium of fetal colonic mucosa, but not with normal tissues and cancers of liver, pancreas, eye, skin, and ovary. The staining intensity and the number of the stained cancer cells using MG7 and MG9 are markedly higher in gastric cancers than in cancers of other organs. This suggests that antigens recognized by MG7 and MG9 mainly exist in the tissues of gastric cancers. The antigens may be new tumor associated embryonic antigens not related to CEA, because CEA treatment of MG5, MG7, MG9, and MG11 did not affect their immunohistochemical reactivity on the tested tissue specimens of the afore mentioned cancers.

/09599

# Radiogenotoxicological Effect of Fission Fragment $^{147}Pm$ on BALB/C Mice

40091047 Beijing ZHONGHUA FANGSHE YIXUE YU FANGHU ZAZHI [CHINESE JOURNAL OF RADIOLOGICAL MEDICINE AND PROTECTION] in Chinese Vol 8 No 1, Feb 88 pp 8-11, 69

[Article by Zheng Siying, Zhu Shoupeng, Luo Zhongyu, et al., Faculty of Radiological Medicine, Suzhou Medical College, Suzhou]

[Abstract] The purpose of the present study is to ascertain the radiogenotoxicological effect, such as chromosome aberration, sister chromatid exchange and micronucleus formation in bone marrow cells induced by fission fragment $^{147}Pm$. Forty-two male BALB/C strain mice were used. Results indicated that the chromosome aberration rates elevated along with increasing doses of $^{147}Pm$. It showed a linear relationship between dose and effect: $Y = -4.403 + 1.435 \text{ Ln } X$. Five aberrations in one cell could be induced. This phenomenon might be partly due to nonuniform irradiation of bone marrow cells by local deposition of $^{147}Pm$. Chromatid type of chromosome aberrations could also be observed. Chromatid breakages were predominant, accompanied by a few chromosome fragments and translocations. The micronucleus rates also elevated with the increase of contamination dose of $^{147}Pm$.

/09599

## Study on Introgression of Useful Genes From Hordeum Bulbosum to Common Wheat

40091052a Beijing YICHUAN XUEBAO [ACTA GENETICA SINICA] in Chinese Vol 15 No 1, Feb 88 pp 1-8

[Article by Wang Liquan, Zhu Hanru, Rong Junkang, Liang Zhuqing, Zheng Yiren, Department of Agronomy, Zhejiang Agricultural University, Hangzhou and Guan Qiliang, Department of Biology, Hangzhou University]

[Abstract] Some $F_1$ intergeneric hybrids between wheat variety Chinese Spring (2n=6x=42) and Hordeum bulbosum USSR (2n=4x=28) were obtained by dripping GA3 to the wheat stigmas 2.02 percent in seed setting. It was found that the hybrids were self-sterile, while in backcross with fertility of backcrossing was 0.59 percent. The morphological characters of $F_1$ and $BC_1F_1$ manifested an apparent hybrid vigor. Both the spike shape and structure of $BC_1F_1$ were similar to those of $F_1$. The length and awn type of their spike were like that of the male parent, but the polyanthous of its spikelets like the female one. However, the flag leaves of $BC_1F_1$ were evidently longer in size than those of $F_1$ and their parents. There were 24-30 chromosomes in many pollen mother cells of $F_1$ at metaphase I, and there were 45-49 chromosomes (20-21 pairing bivalents and 3-7 univalents) in most pollen mother cells of $BC_1F_1$ at diakinesis. When $BC_1F_1$ some number of $BC_1F_2$ at diakinesis or metaphase I was 48--56 (some of them was 24-28 pairing bivalents). The hybrids plants of $BC_1F_3$ segregated distinctly into four types in morphological characters and chromosomes number, but all of them were aneuploid, including monosomic addition lines (21II + 1I) and double monosomic addition lines (21II + 1I + 1I). The hybrid progenies segregated continuously in later years. In 1985-1986, 6 alien disomic addition lines, alien octoploid and several euploid hybrids to T. aestivum-H. bulbosum were produced. Two addition lines had protein content of 22.3 percent and 20.37 percent (the female parent progenies were as resistant to wheat yellow mosac virus disease (WYMV) as their male parent after a 2-year test. It might be proved that resistant gene (WYMV) of H.bulbosum had been transferred to common wheat for the first time.

Key words: Hordeum bulbosum, Monosomic 5B of Chinese Spring, Intergeneric hybrids, Alien disomic addition lines, Euploid hybrids, Alien octoploid.

/12232

# Variation of Somaclonal Male Sterile Lines of Indica Rice by Cell Culture*

40091052b Beijing YICHUAN XUEBAO [ACTA GENETICA SINICA] in Chinese Vol 15 No 1, Feb 88 pp 9-14

[Article by Ling Dinghou, Ma Zhenrong, Chen Wunying, Chen Meifang, South China Institute of Botany, Academia Sinica, Gangzhou]

[Abstract] Nature seeds and young panicle of IR8 and IR54 were regenerated. Under the culture of MS medium added with 6 percent sucrose, some hormones and other supplements. Among the regenerated plants one male-sterile plant, which was a fertile and sterile chimaera in IR54, was found in each variety. Among the somaclonal lines of $R_2$ generation in IR24 and IR54, each line of the two varieties was found to be segregated in fertility. Two types of pollen failed to develop, pollen free (without pollen) and pollen abortive, could be identified. IR24 was a semi-storer for ms-plants of pollen-free type derived from the second generation of IR54 somaclones. The segregation ratio of fertile: sterile gave a complete fit to the formula 15/16:1/16,showing that the male-sterile could be produced by hybridization, or mutagenesis, sometimes could be found in nature by spontaneous mutation. Recently the cytoplasmic male sterile of tobacco was produced by protoplast fusion. But it was first reported that male sterile was found in regenerated plants and their offsprings from somatic cell culture.

Key words: Male sterile, Tissue culture, Somaclonal variation, Indica rice

---

*Project supported by the national Nature Science Fund of China.

/12232

Mutation, Transfer and Location of Symbiotic Genes of Rhizobium Leguminosarum Biovar Phaseoli By Insertion of Tn5-MOb

40091052c Beijing YICHUAN XUEBAO [ACTA GENETICA SINICA] in Chinese Vol 15 No 1, Feb 88 pp 25-33

[Article by C.L. Wang, Department of Soil and Agrochemistry, Huazhong Agricultural University, Wuhan, Hubei, PRC; P.R. Hirsch, Dept. of Soil Microbiology, Rothamsted Experimental station, Harpenden, Herts, AL5 2JQ UK]

[Abstract] Effective transfer of indigenous plasmids from R. leguminosarum biovar phaseoli strain RCR3622 was accomplished by transposon Tn5-Mob accompanied by the mobilizing plasmid RP4-4 Transfer of two of the four plasmids of RCR3622 into R. leguminosarum biovar vicene B151 occurred at frequence of $10^{-3}$. One of them, Psym3622 (Ca. 285 kb) was proved to be the symbiotic plasmid. It carries both nod and mel genes spanned in a region about 70 kb. Introduction of nod genes into the nodulation defective strain R. leguminosarum biovar viceae B151 and R. leguminosarum biovar phaseoli JI8400 caused the mutants being able to nodulate Phaseolus vulgaris cv. "Jamapa." Nodules formed by B151 transconjugants were non-effective, while those formed by JI8400 transconjugants were fully effective.

Key words: Transposon Tn5, Mobilizing transfer, Symbiotic plasmid, Nodulation

/12232

# Study on Homology Between Two Kinds of Human Thymidine Kinase Gene by Southern Blot Analysis*

40091052d Beijing YICHUAN XUEBAO [ACTA GENETICA SINICA] in Chinese Vol 15 No 1, Feb 88 pp 61-67

[Article by Zhao Shouyuan, Cai Wucheng, Wang Wenhua, Zhang Jue, Institute of Genetics, Fudan University, Shanghai]

[Abstract] In this paper, we described the investigation of the possible homology between human cytosolic thymidine kinase (TK-C) gene (mapped to chromosome 17) and mitochondrial thymidine kinase (TK-M) gene (mapped to chromosome 16). Three Alu repetitive sequence-free fragments were isolated form human TK-C gene and then subcloned into plasmid pBR322. These recombinant plasmids were designated as pRR0.92 ($Ap^r$ $Tc^r$), pXR15, ($Ap^r$ $Tc^s$) and pHK1.25 ($Ap^r$ $Tc^s$). Results of Southern blot hybridization showed that DNAs isolated from mouse cell lines Ltk, CD-1, A9 and BALB/c cannot be hybridized to $^{32}P$-labelled, nick translated pXR1.5 and pHK1.25,but Chinese hamster cell line E36 DNA showed a 23 kb fragments after BamHI digestion and then probing with pXR1.5. It suggested that there maybe more homology between human beings and Chinese hamster in TK-C gene than that between human beings and mouse. Under less stringent condition, DNA samples of human cells, and mouse-human hybrid cell lines $16^-17^+$ (on human chromosome 17 only), $16^+17^-$ (on human chromosome 16 only) and $16^-17^-$ (having no human chromosomes 16 and 17) were digested with HindIII and hybrized to the pHK1.25. Prominent bands were shown in the lanes of human DNA and $16^-17^+$ DNA, but nothing can be seen in the lane of $16^-17^-$ DNA. However, we can detect a faint band with a molecule size of about 7.5 kb in the lane of $16^+17^-$ DNA. Thus, we inferred that there may be some homology existing between human TK-C gene and TK-M gene, and TK-C gene HindIII/KpnI 1.25 kb fragment may be helpful for further investigation of TK-M gene.

Key words: Human cytosolic thymidine kinase (TK-C) gene, Human mitochondrial thymidine kinase (TK-M) gene, DNA hybridization, Homology

---

*Project supported by the Science Fund of Chinese Academy of Sciences.

/12232

# STUDIES OF EXTRACTION BEHAVIOR OF SOLUBLE NEUTRON POISON GADOLINIUM WITH TBP, ITS SOLUBILITY IN NITRIC ACID SOLUTION

40090086a Beijing HE HUAXUE YU FANGSHE HUAXUE [JOURNAL OF NUCLEAR AND RADIOCHEMISTRY] in Chinese Vol 10 No 1, Feb 88 pp 1-7

[English abstract of article by Yu Enjiang [0060 1869 3068], et al., of the Institute of Atomic Energy, Beijing]

[Text] Gadolinium has been proposed for use as neutron poison for the control of criticality during spent nuclear fuel dissolution, feed preparation and solvent extraction. The distribution ratio of gadolinium ($D_{Gd}$) in the system TBP-nitrate, concentration profiles of Gd in the countercurrent extraction process with TBP and the solubility of gadolinium nitrate in aqueous solution are presented. The effects of the concentration of nitric acid, sodium nitrate, uranyl nitrate and gadolinium nitrate, temperature and irradiation of TBP-kerosene on $D_{Gd}$ are investigated.

A maximum and minimum of $D_{Gd}$ vs nitric acid concentration curves at about 3 mol/l and 7 mol/l nitric acid are observed, respectively. $D_{Gd}$ increases with the increase in concentration of sodium nitrate in the aqueous phase. The maximum and minimum for $D_{Gd}$ are not found in the sodium nitrate solution. Uranium concentration in the equilibrated organic phase influences $D_{Gd}$ significantly. The change in $D_{Gd}$ is not appreciable when the gadolinium concentration in the aqueous phase increases to 13 g/l. No difference can be seen between the $D_{Gd}$ with solvent irradiated by $^{60}Co$ to a level of $3.6 \times 10^5$ Gy and the $D_{Gd}$ with a solvent not irradiated. Cascade countercurrent extraction tests have been carried out and decontamination factors from Gd of $10^4$-$10^5$ have been obtained.

The effects of such factors as the concentration of nitric acid and uranium and the temperature on the solubility of gadolinium nitrate in the aqueous solution have been investigated. The results show that the value of solubility of gadolinium nitrate in the aqueous solution decreases with the increase in concentration of nitric acid and uranyl nitrate.

9717

KINETIC STUDIES OF EXTRACTION OF U(VI) FROM PHOSPHORIC ACID MEDIUM WITH HDEHP

40090086b Beijing HE HUAXUE YU FANGSHE HUAXUE [JOURNAL OF NUCLEAR AND RADIO-CHEMISTRY] in Chinese Vol 10 No 1, Feb 88 pp 25-29

[English abstract of article by You Jianzhang [1429 1696 4545], et al., of the Nuclear Science Department, Fudan University, Shanghai]

[Text] The kinetics involving the extraction of U(VI) from phosphoric acid solution with di-(2-ethyl)phosphate (HDEHP) in cyclohexane has been investigated using the Lewis cell technique. The extraction rate has been determined as a function of the stirring speed and temperature. It is shown that the extraction rate of U(VI) may be diffusion controlled at the concentration of 4-6 mol/l $H_3PO_4$ aqueous solution, and it may be interfacial chemical reaction controlled at the concentration of 0.5 mol/l $H_3PO_4$ aqueous solution. For the diffusion controlled system, the extraction rate expression is found to be of the pseudo-first order in the concentration of U(VI) and of the 3/2 order in the concentration of HDEHP, respectively, while the rate of extraction is nearly independent of temperature.

9717

## TRITIUM LABELING OF TETRAMETHYLPYRAZINE BY MICROWAVE DISCHARGE ACTIVATION OF TRITIUM GAS

40090086c Beijing HE HUAXUE YU FANGSHE HUAXUE [JOURNAL OF NUCLEAR AND RADIOCHEMISTRY] in Chinese Vol 10 No 1, Feb 88 pp 42-46

[English abstract of article by Ding Shaofeng [0002 4801 7685], et al., of the Department of Chemistry, Beijing Normal University; Shen Decun [3088 1795 1317], et al., of the Institute of Atomic Energy, Beijing]

[Text] Tetramethylpyrazine is labeled with tritium by microwave discharge activation (MDA) of tritium gas. The labeled sample is hydrogenated in the presence of a 0.5 percent Pd catalyst on alumina-silica support, and the labeled sample is partially hydrogenated to form tetramethyldihydropyrazine.

Theoretical calculations (CNDO/2) show that the π-bond electron polarizability (superdelocalizability) of the Pd-pyrazine ring is greater than that of the Pt-pyrazine ring, the Rh-pyrazine ring or the pyrazine ring.

9717

NEW DEVELOPMENTS IN CHEMICAL INDUSTRY, RESEARCH

Quasicrystallography

40080082 Beijing HUAXUE TONGBAO [CHEMISTRY] in Chinese No 12, (Dec) 87 pp 12-13

[Article by Zeng Jingmin* [2582 2417 3046], Department of Chemistry, Beijing Normal College: "Quasicrystallography--A New Type of Crystallography"]

[Excerpt] The famous Chinese crystallographer and mineralogist Professor Peng Zhizhong [1756 1807 1813] recently proposed the novel "Icosahedron Principle" and "Principle of the Golden Mean". Based on these principles, Peng also deduced the "particle fractional dimension structure model".[11] The icoshedron principle states that when atoms of similar size form dodecal ligands, the icosahedral coordination is in terms of energy the most favorable. The principle of the golden mean states that the atomic arrangement in the quasicrystals obeys the rule of the golden mean. These two principles apply to systems made up of a small number of atoms and to certain biological systems. Based on these two principles, the simplest quasicrystal model may be deduced by using the Fibonacci series. Since this model is characterized by its fractional dimensional structure, it is known as the particle fractional dimension structural model of the quasicrystal. The $MnAl_{12}$ icosahedron in this model is not coprismatic; this represents a major difference from previous beliefs of the nature of quasicrystals. This model has now been verified in three areas. First, the deduced pattern of electron diffraction agreed completely with the actually measured electron diffraction pattern, and is the inverse of the electron diffraction pattern computed by D. Levine and P. J. Steinhardt. Second, the atomic vector diagram predicted by the model agreed completely with the spectral experimental results.** Finally, the model can interpret all the details of the high-resolution diagram of Al-Mn quasicrystals photographed by Hiraga in Japan. Obviously this model is a breakthrough in the understanding of the material world. It is basically a quantitative computational tool for the structure of quasicrystals and is very important for both the theoretical analysis and experimental measurement of quasicrystal structures.

* Present address: Institute of the History of Natural Science, Chinese Academy of Sciences

**From a presentation by Professor Peng Zhizhong

The model is of course only the simplest form of the quasicrystal structure and there are many other structural forms yet to be investigated. The current challenge to the experimentalists is the preparation of larger, purer, and better quasicrystalline specimens. For the theorists, the challenge is to establish a unified geometric theoretical system that is valid for both regular crystals and also quasicrystals. Such a theoretical endeavor is expected to be completed before long.

Since we have always been taught to believe that crystals have precise translational periodicity, this premise must now be re-examined. The theory of solids is basically a theory of crystals. For example, the solution of the single-electron Schrodinger equation in the calculation of the energy bands begins with the periodicity of the potential energy and the Bloch function. The energy-band theory evidently needs revision and augmentation. One may have to re-examine the chemical theories of crystal growth, crystal structure, solid reaction, metals and alloys and such chemical data as the atomic radius, ion radius, and lattice energy. Since the study of quasicrystals involves the transition from random particles to ordered particles, it is particularly important to the theories of chemical reaction dynamics and catalysis.

In any case, the quasicrystal is a brand new state of matter. The science of quasicrystals may be called quasicrystallography. The subject of study of quasicrystallography is the long-range ordered structure in systems of a small number of particles, whereas the subject of classical crystallography is lattice structures of large numbers of particles. The classical theory of crystallography may not apply to quasicrystals, but it soon will become part of a unified crystallography.

## REFERENCES


1. I. Peterson, "Breaking the Rules in Crystallography," SCIENCE NEWS, 128(7), 102 (1985).

2. Tang Youqi [0782 2589 4388], "Crystalline Chemistry," Higher Education Publishing House, 1957. Ch 14.

3. "History of the Development of Chemistry," Science Publishing House, 343-350 (1980).

4. D. Shechtman, et al, "Metallic Phase With Long-Range Orientational Order and No-Translational Symmetry," Phys. Rev. Lett., 53(20), 1951 (1984).

5. D. Levine and P. J. Steinhardt, "Quasicrystals: A New Class of Ordered Structures," Phys. Rev. Lett., 53(20), 2477 (1984).

6. American Science News, 21, 3 (1985). Originally published in SCIENCE NEWS, 127(3), January 19, 1985.

7. Guo Kexin [6753 0668 0207], "Fivefold Symmetry and Quasicrystals," Wuli (Physics), 14(8), 449 (1985).

8. L. Pauling, "The Nature of Chemical Bonds," translated by Lu Jiaxi [4151 0857 6932], et al, Science and Technology Publishing House, Shanghai, 360, 364 (1966).

9. T. L. Mackay, NATURE 315(6021), 636 (1985).

10. J. Maddox, "Towards Fivefold Symmetry?," NATURE, 313(24), 263 (1985).

11. Peng Zhizhong, "The Structural Principles and Particle Fractional Dimension Structural Model," DIQIU KEXUE (EARTH SCIENCE), 10(4), 159 (1985).

12. I. Peterson, "The Fivefold Way for Crystals," SCIENCE NEWS, 127(12), 12 (1985).

13. P. A. Heiney, "Quasicrystallography--The Famous Icosahedron Symmetry," translated by Wu Ziqin [0702 5261 0530], WULI (PHYSICS) 14(10, 639 (1985).

14. A. L. Mackay, et al, "Some Answers but More Questions," NATURE, 316(6023), 17 (1985).

15. G. H. W. Milben [phonetic], "X-Ray Crystallography," translated by Wang Shoudao [3769 1343 6670], Higher Education Publishing House, 170 (1983).

## Healthy Growth in Chemical Industry

40080082 Beijing RENMIN RIBAO [PEOPLE'S DAILY] (Overseas Edition) in Chinese 5 Feb 88 p 1

[Article by Jiang Shaogao [3068 4801 7559] and Peng Jialing [1756 0857 7117]: "Healthy Growth in Chemical Industry Has Begun"]

[Text] Minister of Chemical Industry Qin Zhongda [4440 0112 6671] said today that in 1987 the Chinese chemical industry has reversed the two-year trend of increased production but decreased efficiency, and has begun a healthy growth. Total output value in 1987 was 59.32 billion yuan, an increase of 13.8 percent over 1986. The tax income in 1987 was 10.85 billion yuan, 26.4 percent more than that in 1986, and the contract payment of tax was 7.8 billion yuan, 13.4 percent higher than the 1986 figure. The number of businesses in the industry that suffered a loss in 1987 decreased by 806 from the previous year and the loss decreased by 640 million yuan. The small chemical fertilizer industry that suffered a loss of 300 million yuan in 1986 did much better in 1987 and had a net profit of about 1 billion yuan.

What caused such a large turn-around in one year? Although there are a number of reasons, the basic reason is that the industry adopted contract management, accelerated technological improvement and scientific management. According to statistics of 32 provinces, regions, direct-jurisdiction municipalities, and project cities, 65.8 percent of the people-owned enterprises and 80 percent of the medium- and large-scale enterprises in the chemical industry have implemented contract management. Contract management stimulated technological improvement of the enterprises and accelerated the pace for converting research

results into productivity. In 1987 there were 163 research results applied to production, representing an increase of 87 percent in technology transfer, 300 new products were developed last year, including 80 items never produced before, and 20 technologies reached international standard in 1987.

Through technological improvement and better management, good results have been achieved in energy conservation and quality improvement. The energy consumption per unit of production has decreased. Industry-wide energy savings last year amounted to 500,000 tons of standard coal and energy consumption per 10,000-yuan production was reduced by 2.5 percent. In 1987 the quality of 83.3 percent of the major chemical products was maintained or improved and 12 products received national quality awards; 80 products were classified as Ministry-Quality Products.

## Chemical Ministry's Strategy for Year 2000

40080082 Beijing RENMIN RIBAO [PEOPLE'S DAILY] (Overseas Edition) in Chinese 15 Feb 88 p 3

[Article by Peng Jialing [1756 0857 7117]: "Ministry of Chemical Industry Proposed Strategy for Year 2000"]

[Text] In a nationwide bureau and office chiefs meeting currently being held by the Ministry of Chemical Industry, strategies for the year 2000 in the chemical industry are stated to be: actively develop agricultural chemical products, basic chemical engineering materials and synthetic materials, and strive to open new areas in precision chemical engineering products.

There have been rapid developments in the chemical industry in China in recent years. Total output value has reached fifth place in the world and the output of certain major products has ranked among the top in the world. The production of synthetic ammonia, sulfuric acide, pure alkali, and chemical fertilizer has reached second or third place in the world, and the percentage of high-grade and precision chemical engineering products has increased. However, as the national economy has grown, there have been full-scale shortages in chemical products. Supply and demand problems exist in agricultural chemicals such as fertilizer, pesticides, and plastic films, and in basic chemical materials and synthetic materials. The production structure has problems: traditional low-grade products and high energy consumption products still make up the bulk of the products and many chemical products are not produced according to internationally accepted standards.

In an interview with this reporter, Deputy Minister Wang Min [3769 3787] pointed out that the most effective means for achieving the goals of the year 2000 is to raise the technological level of the chemical industry. The chemical industry is a technology-intensive enterprise, and China must not lag behind in high-technology development. Research and experimental exploration must be conducted for chemicals needed in new structural materials, functional materials, microelectronics technology, and information sciences, and in biochemical technology and the new generation of coal chemistry.

Wang Min pointed out that, in order to reach these goals, research results must be transformed into productivity. Today there is still a gap between China's chemical industrial research and its production. The enterprises should be encouraged to absorb and adopt new technologies. Large enterprises with more resources should establish their own intermediate test and development facilities to conduct research in new technology and develop new products.

9698/9274

JAPAN MONTHLY REVIEWS STATUS OF CHINA'S COMPUTER INDUSTRY

43063021 Tokyo DENSHI KOGYO GEPPO in Japanese Feb 88, pp 68-70

[Text] 1. Strategy of Seventh 5-Year Plan and Objectives

The general mission of China's computer industry during the Seventh 5-Year Plan (1986-1990) is to emphasize use and application aspects, to stimulate expansion, and to give first priority to development of personal computers with a wide range of uses and accompanying software.

The objectives are to make computer production total 6 billion yuan (¥240 billion at 1 yuan = ¥40) by 1990, and to realize a certain volume of exports along with reaching a 40 percent domestic-manufacture computer self-sufficiency rate for medium and large computers and 60 percent for small computers. It is also an objective to attain the technology and quality levels which existed abroad from the end of the 1970s to the early 1980s. It is said that the average annual growth rate of Chinese computer production will be about 30 percent during the next 5 years.

2. Scale of Computer Industry

According to a September 1986 survey by China's Ministry of Electronics Industry, there were 465 companies (total number of employees: 85,000) engaged in the computer industry nationwide as of the end of 1985. A detailed survey was conducted on 430 of these companies.

Among the 430 companies, 181 are in the computer manufacturing industry, 216 are in the software and information processing service industry, and 33 are research centers. These are 42.09 percent, 50.23 percent, and 7.67 percent of the whole, respectively.

The production total for the computer industry was about 2 billion PRC yuan (¥80 billion at 1 yuan = ¥40) at the end of 1985, with domestic demand at 3 billion yuan. Consequently, there was a difference of 1.1 billion yuan for importers of computers. Computers held a 7.3 percent share of total production in the electronics industry at the end of 1985.

3. Status of Computer Installation

The history of computer development and use in China is old. It began about 30 years ago. However, it was also influenced by the cultural revolution

along the way and it was about 1978 that full-scale installation and use of computers began. As seen in the following table, there were 7,479 general use computers/mini computers and 190,000 PC (called microcomputers in China) as of the end of 1986.

Estimates are that general use/minis will reach 13,000 and PC's 600,000 in 1990.

Table 1. Changes in Number of Computers Installed (1981-1986)

| Year | 1981 | 1982 | 1983 | 1984 | 1985 | 1986 |
|---|---|---|---|---|---|---|
| General/mini | 3,200 | 3,819 | 4,454 | 5,407 | 6,838 | 7,479 |
| PC | 10,892 | 18,000 | 30,000 | 75,800 | 130,000 | 190,000 |

4. Strategy for Expansion of Computer Industry

(1) Market Strategy

First, to promote development and expansion of the domestic market in response to nationwide needs.

Participation in international market.

(2) Strategy in Technology Area

--Development of 4th generation computer.

For this purpose, design of VLSI and development of CAD, CAT, CAM, advanced production technology, systems engineering, and new computer architecture.

--Establishment of quality assurance system.

--Contact with international standardization agencies concerning computers and information processing

--Development of PCs and super mini computers, machines compatible with foreign machines, Chinese text processing, domestic production, Chinese version of OS, and development of 32-bit work station.

--Joint ventures with foreign countries in general purpose machine field.

--Development of special terminals for banks and businesses.

--Development of LAN, DB, telecommunications.

--Linkage of computer technology and IC technology, ASIC, gate arrays, development standard protocols.

--Linkage of computers and communication.

--Strengthening of research on computer system software, utility software, and application software.

(3) Strategy in Industry Area

--Expansion of computer industry to conform to economic scale.

--Expansion of information service industry.

--Networking of computer installation, training, and maintenance.

--Wider dissemination of application projects.

--Strengthening of computer pre-and afterservice.

--Expansion of computer lease industry.

--Establishment of commercial computer center.

--Exhibitions of new computer products, displays at trade fairs.

(4) Strategy to Develop Human Resources

--Strengthening training of computer application technicians.

--Training of mid-level and senior technicians and managers.

--Training of personnel abroad.

--Dissemination of basic computer knowledge to primary and middle schools.

--Dissemination of basic computer knowledge to executives.

5. Basic Policies for Development of Computer Industry

Based on the above strategies, the basic policies employed for development and expansion of the computer industry are 1) appropriate and adequate policies for the use and application of computers, or, in other words, no problems in the development and sale of computers; 2) limited protection policy, policy to do ourselves what we can do; 3) preferential policy, e.g., a 15 percent return on sales prices to manufacturer for computer development, to be allotted for capital for the next development.

6. Major Projects Currently Being Conducted

Currently in China a reorganization is being conducted in government, government agencies, research centers, and companies. That related to computers is as follows:

(1) Grouping of research departments

The current research centers related to computer development were set up in three groups.

Zhangcheng Computer Group Company, Beijing

Zhangjiang Computer Group Company, Shanghai

Zhangbai Computer Group Company, Shenyang

(2) Conduction of joint research between research centers and universities

This is called NIC (North Beijing High-tech Development "NIC" Complex). It is formed from seven companies, universities, and research centers in Beijing: the Chinese Academy of Sciences, Beijing University, Qinghua University, Beijing Information Engineering Institute, Huabei Computer Technology Research Center, China Computer Technology Service Company, and China Software Technology Company. In the Seventh 5-Year Plan, the following eight joint centers will be established within NIC:

1. Computer Product Quality Investigation Center

2. Information Processing Standardization Center

3. PCB, VLSI Design Center

4. Software Engineering Laboratory

5. Production Technology Center

6. Computer System Application Development Center

7. Systems Engineering Center

8. Computer Software Training Center

(3) Establishment of CAD Centers in Huabei, Huanan.

(4) Establishment of Software Development Centers in Huabei, Huanan Districts.

(5) Establishment of Beijing IC Design Center.

(6) Establishment of Microcomputer Plant in Economic Zone (Shenquan)

7. Establishment of Computer-related Groups

The following groups and companies related to computers will be established act under the guidance of the Ministry of Electronics Industry in China.

China Computer Users Group

China Software Industry Group

China Computer Industry Group

China Computer Technology Sales Company

China Computer Software Technology Company

China Computer Systems Engineering Company

China Machine Room Facilities Engineering Company

12256\12232

MILITARY COMMUNICATIONS , GRAPHICS SYSTEMS

## Naval Network Terminal System

40080091a Beijing JISUANJI SHIJIE [CHINA COMPUTERWORLD] in Chinese 3 Feb 88 p 2

[Article: "Navy Office of Automation Develops a Network Terminal Automatic Start-Stop System"]

[Text] In order to fully exploit the advantages of computer communications networks and to improve office efficiency, the Office of Naval Automation recently developed the "Zh1 Network Terminal Start-Stop System" for the Naval Branch System of the All-Forces Military Information Processing System. This system has undergone a period of testing, which has proven it to be reliable in performance, convenient to operate, and very useful. The Communications Department under the Naval Commander recently arranged for relevant specialists to technically evaluate this system in Beijing, which received unanimous high praise from the experts.

The automatic start-stop device in this system is composed of asynchronous communications controllers, decoders, start-stop controllers, relays, clock generators, power sources, and sound generators. The developers also created packet automatic reception software to go with it. When a terminal is not on, this system can automatically start up a network terminal and receive the packet being sent. This is similar to placing a message in a mailbox. Starting and stopping is accurate, message reception is reliable, the system can respond to various rates of transmission and calling signals, and it also has a very good prompt function.

The experts feel that this system is a new application for computer communication networks within the armed services, that technically it ranks as advanced domestically, and is worth dissemination.

## High-Resolution Graphics System

40080091a Beijing JISUANJI SHIJIE [CHINA COMPUTERWORLD] in Chinese 3 Feb 88 p 2

[Article by Tian Feng [3944 0023]: "A Microcomputer High-Resolution System Grabs Military Price for Advancement"]

[Text] A microcomputer high-resolution graphics system for use in management and command automation recently won a second-place prize for military

scientific and technological progress after its evaluation in Nanjing under the auspices of the General Logistics Department.

This graphics system was developed by the Automation Station of the Nanjing Military Region Logistics Department over the past 2 years, and it is primarily composed of a microcomputer, high-resolution color video controller card, and a large screen projector. It can draw images that are complex and yet life-like. It has more than 40 functions, including the changing of size, color changing, editing, remote control, dynamic auto-tracking, and concurrent handling of multiple files. It not only meets the needs of management and command automation in various areas both within and outside the military, but can be used as well in CAD/CAM for scientific research and production. The experts feel that this graphics system is strong in its scope and in its software functions, that it has a viable interface, is convenient to expand, that the graphics definition is stable, and that the primary technical indicators rank it in the forefront domestically. They said that its successful development has laid an excellent foundation for Chinese automation of management and command. Currently, this achievement is being used by 17 units both in and outside this country.

## Navy's Office Automation Network

40080091a Beijing JISUANJI SHIJIE [CHINA COMPUTERWORLD] in Chinese 10 Feb 88 p 12

[Article: "The Navy Has Completed a Communications Office Automation Network"]

[Text] The Navy Communications Office Automation Network System passed its technical evaluation recently in Beijing. The evaluation was conducted by more than 30 specialists from units at Qinghua University, Beijing University, Beijing School of Engineering, the Ministry of Electronics, the Ministry of Posts and Telecommunications, the Commission on National Defense Science and Engineering, the Headquarters of the General Staff, and the Navy.

This system is a distributed computer network made up of communications sub-networks and resources sub-networks that is both suitable for local communications and also for long-distance communications. The hardware and software for the microcomputer nodes on the communications subnets and the software for the resource-subnet hosts were all designed and developed by the station for command automation of Qinghai University and the Naval Command. This network is a system for both general and specialized work. It can be small or large in scale, and within the network any two points may be either directly linked or linked by use of modems for telecommunications. The communications subnet allows various means of communication. There is much high-level software for this system, and the self-developed file-transfer system, the electronic mail system, and the resources-sharing system can all serve users through either program calls or through keyboard commands. The host communication software is memory resident, which for single machines resolves the problem of reentrant system function calls, for once the network

is entered neither the network environment nor the operating system environment is dispersed. At the same time files are being received, the user may run any desired applications program.

A high degree of difficulty was involved with the design of the Naval Communications Office Automation Network System, and in using international standard protocols in development and construction of a practical network system, the relevant technology ranks at the forefront domestically in terms of developmental technology, by using the internationally newest formal descriptive methods, the cost of development was less and results came about more quickly, all of which has had positive results in improving the level of automation.

12586/12232

## 3.5-INCH 2M/1M DISKETTE DRIVE DEVELOPED

40080093b Beijing JISUANJI SHIJIE [CHINA COMPUTERWORLD] in Chinese 10 Feb 88 p 1

[Article: "3.5-Inch 2M/1M Compatible Disk Drive System Developed"]

[Text] Development of a 3.5-inch 2 megabyte-1 megabyte disk drive meeting advanced world standards was completed this January by the Jiannan Machinery Plant in Hunan, which will soon put it into series production.

The drive is a new type, first developed internationally in 1987, with a maximum storage capacity of 2 megabytes. It can use either ordinary diskettes, on which it can store 1 megabyte of data, or high-density disks, on which it can store 2 megabytes. In addition to its large storage capacity and ability to accommodate a wide range of disks, the drive is small in size and has low power requirements, making it ideally suited for modern microcomputer systems, intelligent devices, and office automation systems. In the latter half of 1987, after developing a 3.5-inch 1-megabyte disk drive and putting it on world markets, the Jiannan Machinery Plant kept track of the world state of the art, acquired relevant foreign information and technical documents and concentrated its efforts on developing this dual-compatibility disk drive.

Expert evaluation and the results of testing by the relevant organizations have indicated that the drive's technical characteristics and quality indices are all up to foreign standards for equipment of this type. Five of its technical characteristics, including its track access time, data transmission rate and memory density, are in line with the world state of the art. The drive is also compatible with signal ports and fully capable of replacing the 5.25-inch disk drives now widely used in China. Its development fills a gap in Chinese-produced magnetic storage devices and marks a further advance of China's computer industry toward the world forefront.

08480/06662

## BEIJING IRON, STEEL INSTITUTE ISSUES DESIGN SOFTWARE PACKAGE

40080093c Beijing JISUANJI SHIJIE [CHINA COMPUTERWORLD] in Chinese 10 Feb 88 p 14

[Article: "Beijing Iron and Steel Institute Produces the MOD Software Package Designed for Process Optimization"]

[Text] The MOD constrained nonlinear mixed discrete-variable design optimization software package, developed with funds from the State Science and Technology Funding Committee, recently passed evaluations in Beijing.

Constrained nonlinear hybrid discrete-variable optimization is a new field with important practical applications in the theory and practice of optimal design. It focuses primarily on optimizing problems involving discrete variables (i.e. variables that can take only a limited number of values) that frequently arise in engineering practice, such as the number of teeth and the characteristics of gears, the dimensions of shaped stock, and large bodies of tabular data. Optimal solution of problems by continuous-variable optimization methods generally is not suited to problems of the above type. Discrete-variable optimization is a research topic in optimal design that urgently requires solution.

Over a period of more than 3 years, the Beijing Iron and Steel Institute completed the MOD software package and made useful theoretical investigations into mixed discrete-variable optimization methods. The MOD software package consists of five routines and programs (MDOD, MDCP, MDRP, MDHP, MDGP) with unified macrostructure, allowing them to be used in combination, thus greatly increasing the success rate and solution reliability. The software is highly modular, with excellent aggregability, portability, and maintainability; it has good man-machine interaction capabilities and an iterative process chart tracking capability. The software is implemented on an IBM PC/XT microcomputer system. It uses little internal storage and has a full range of technical documentation and user instructions, suiting it for widespread adoption.

The MOD package can be used in constrained nonlinear optimation problem involving continuous and/or discrete variables. It has a wide range of applications in engineering design and as support software for CAD [computer-

aided design], as well as extensive application potential in such fields as operations research, management science, computer science, reliability engineering, and automatic control. Some of the modules in the package are already being used for applications, and there are already more than 30 users at Hefei Industrial University. They include optimizing the design characteristics of the extensible boom of the QY125 truck-mounted hydraulic crane, optimised selection of the number of teeth and tooth characteristics of the TDC gear roller series, design of optimum cross-sectional dimensions for the pentagonal large-turning-angle extensible boom of a 20-ton truck-mounted crane, and optimizing the structural characteristics of the M74100A main axle circular-table surface grinding machine. It has produced excellent economic benefits in all of these applications.

The evaluation committee concluded that this ia a pioneering effort in China and a major research achievement with important practical value which is at the international state of the art. Its application will help raise the level of Chinese optimized engineering design, promote technical progress, and produce considerable economic benefits.

08480/06662

# An Approach to Quick Evaluation for Air Pollution by Luminous Bacteria

40091049 Beijing ZHONGGUO HUANJING KEXUE [CHINA ENVIRONMENTAL SCIENCE] in Chinese Vol 8 No 1, Feb 88 pp 59-62

[Article by Wu Zirong, Chang Ping, Pei Xiuying, Jiang Huiyong, Department of Biology, East China Normal University, Shanghai; passage in slantlines published in italics]

[Abstract] In this paper, it is reported that /Photobacterium phosphoreum/ 502 is used as an indicator organism, and several toxic gases such as cigarette smoke, car emission, xylene, ammonia and so on are tested.

The results indicate that the light intensity of the luminous bacteria is apparently inhibited by the toxic gases being measured; with the increase of concentration of toxic gases, the light intensity of the luminous bacteria declines and that the correlation between the ability of light inhibition and bacterioidal ratio is also certain.

Compared with the other ways of bioassay for evaluating air pollution, this method mentioned above is simpler, faster and more sensitive.

/09599

## The Xiamen Marine Enclosed Ecosystem Experiment and Its Application in Marine Environment Studies

40091049 Beijing ZHONGGUO HUANJING KEXUE [CHINA ENVIRONMENTAL SCIENCE] in Chinese Vol 8 No 1, Feb 88 pp 63-67

[Article by Fu Tianbao, Wu Jinping, Hou Shumin, Chen Xiaolin, Chen Qihuan, Zhuang Dongfa, Wu Shengshan, Third Institute of Oceanography, State Oceanic Administration, Xiamen]

[Abstract] Two kinds of Marine Enclosed Ecosystem Experiment (MEEE) facilities were set up in Xiamen Bay, which were a cooperative programme between China and Canada. The aim was to determine the fate of pollutants and their effects on the structure and function of the marine plankton community of Xiamen Bay. The facilities were the modifications of CEPEX, using plastic bags to enclose a part of natural water column. Two experiments were conducted in 1985 and 1986. The pollutants added were the mixture of heavy metals (Cu, Cd, Hg, Pb, and Zn) sediment, oil dispersant and corexit dispersed crude oil. The experiments were generally successful and gave some useful results in understanding the nature and for the marine environmental protection.

/09599

SHANGHAI GOALS IN APPLIED MICROELECTRONICS LISTED

40080093a Beijing JISUANJI SHIJIE [CHINA COMPUTERWORLD] in Chinese 3 Feb 88 p 1

[Article: "Focus Effort on the Ten Breakthrough Areas"]

[Text] In the last 2 years, Shanghai's industrial system has gradually expanded the range of traditional industries reequipped with microelectronics technology, moving to increasingly advanced applications and reaping considerable benefits. Citywide, 928 machine tools and 103 heating furnaces and kilns have been reequipped with microelectronics, microcomputer control has been installed on more than 300 vulcanizing units, and 250 textile dyeing units, and 50 production optimization monitoring systems and 16 electric-power grid control systems have been installed. The direct economic effect has reached 50 million yuan.

To proceed further with the technical modernization of traditional industries in Shanghai, the city's industrial system is scheduled to make major efforts in ten breakthrough areas by 1990:

--use of digital displays and economical, simple numerical control technology to modernize 7,000 machine tools;

--use of microcomputer automatic control systems to modernize 500 industrial boilers, furnaces, and kilns with capacities of 10 tons or more;

--installation of microcomputer automatic control in 800 rubber-vulcanizing units, accounting for more than 90 percent of capacity in the city, and expanding the modernization to the entire industry;

--use of wired and wireless microelectronic control systems to institute power system load control down to the household level;

--reequipment of 500 high-temperature, high-pressure textile dyeing vats with microcomputer control instrumentation, and reequipment of 1,000 shuttle-type looms and institution of essentially complete electronic control;

--reequipment of 30 electroplating production lines with microcomputers or programmable control units;

--use of dispatching and optimization technologies such as pattern recognization, multivariate statistics, linear regression and process simulation, focusing on extending their use to 15 enterprises;

--introduction of microcomputer systems to control five fermentation production lines in order to achieve optimal control;

--use of microcomputers for control of chemical fertilizer production;

--use of microcomputer control for cement-kiln batching and prepelletizing and closed-kiln firing.

08480/06662

Excimer Laser With Double Pre-Ionization

40080088 Beijing WULI [PHYSICS] in Chinese No 12, Dec 87 pp 739-740

[Article by Huang Nantang [7806 0589 1016], Lu Jianyi [7120 1696 0001], and Xu Jiren [1776 4480 0088] of the Institute of Physics, Chinese Academy of Sciences: "Double Pre-Ionization Excimer Laser"]

[Text] Excimer laser is a high efficiency device with a strong output in the ultraviolet. Due to its applications in laser chemistry, VLSI and biology, it has received considerable attention. In China, some devices are gradually being moved out of the laboratory and some still require further improvement. The development of the double pre-ionization excimer laser has a significant impact on improving the performance of these devices. Pre-ionization has a great effect on the performance of an excimer laser. Double pre-ionization by corona discharge and ultraviolet excitation can achieve relatively sufficient pre-ionization which makes the high pressure, large volume discharge in the laser cavity more uniform and stable. This is extremely important for increasing the laser energy output, reducing the energy output instability and improving the overall efficiency. It is also helpful to the development of a device with a high repetition rate.

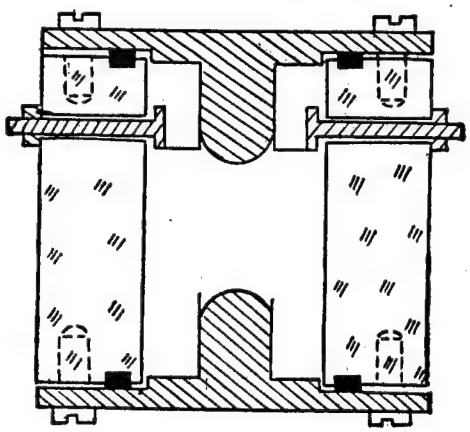

Figure 1

Figure 1 shows the structure of the cavity for the double pre-ionization excimer laser. The electrodes were made of brass and the surface was nickel plated. The gap between electrodes is 2.7 cm. Both electrodes are similar in shape, 46 cm long and 1.2 cm wide with a spherical radius of 6 mm. A 0.1 mm thick copper foil was adhered to both sides of the electrode to create a tip for corona pre-ionization. The tip cannot be higher than the top of the spherical radius, usually 1-2 mm blow it, to prevent the discharge across the electrode and the top of the copper foil. Two arrays of ultraviolet pre-ionization probes are placed on both sides of the cathode approximately 1 mm away from the top of the copper foil. The distance between two probes is 15 mm. The two rows are offset in such a way so that the actual gap is 7.5 mm. There are a total of 55 probes. During discharge, a spark is generated at the tip of the probe and the copper foil. Since the sparks are very close to the discharge zone and are very concentrated, the effect of ultraviolet pre-ionization is very obvious. An energy transfer circuit [1] was used with 14 2200 pF ceramic capacitors connected directly to the electrodes as the emptying capacitance (or peaking capacitance). The energy storing capacity is provided by 7 low inductance 0.01 $\mu$F dielectric capacitors in parallel. They are connected to each probe through 55 small inductors. In the discharge process, when the energy stored in the energy storage capacitors is transferred to the peaking capacitors, sparks are formed at the pre-ionization probes and the tip of the cathode and then triggers the glow discharge between the two electrodes. All leads in the discharge circuit are made of thin large area copper foil. It is compact in structure. All components (including charging power supply, control circuit, gas plumbing, and cavity) are installed in a 400 x 750 x 250 $mm^3$ case.

With different working gases, it is possible to get laser output from XeCl, KrCl, KrF, XeF, ArF, and atomic F. We measured the laser output from XeCl, KrF, and KrCl. At an operating voltage of 30 kV and a pressure of 3.5 atm, the maximum single pulse energy from the XeCl laser is 310 mJ. Figure 2 shows the relation between the output energy and operating voltage of the XeCl, KrF, and KrCl lasers with Ne, He, and Ar as the diluting gas. Figure 3 shows the dependence of the XeCl laser energy output on the pressure of the working medium when the operating voltage is fixed at 30 kV. The energy gauge used was calibrated. Its model number is $N_j$-$J_i$. The wave form of the laser is recorded by a Model SS-6300 wide band oscilloscope with a high density tube. The half height width of the pulse was measured to be 10 ns and the base width 26 ns. At 20 ns, there is a small peak. Its peak is approximately one third of the main peak.

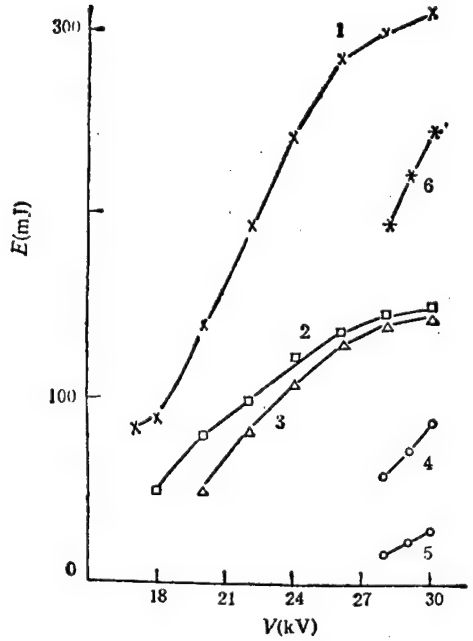


Figure 2. 1. HCl: 6 Torr, Xe: 60 Torr, Ne: 3.5 atm;
2. HCl: 6 Torr, Xe: 60 Torr, He: 2.9 atm;
3. HCl: 6 Torr, Xe: 60 Torr, Ar: 1.5 atm;
4. HCl: 6 Torr, Xe: 60 Torr, Ar: 2.0 atm;
5. HCl: 6 Torr, Kr: 153 Torr, He: 2.6 atm;
6. $F_2$: 9 Torr, Kr: 270 Torr, He: 180 Torr, Ne: 3 atm

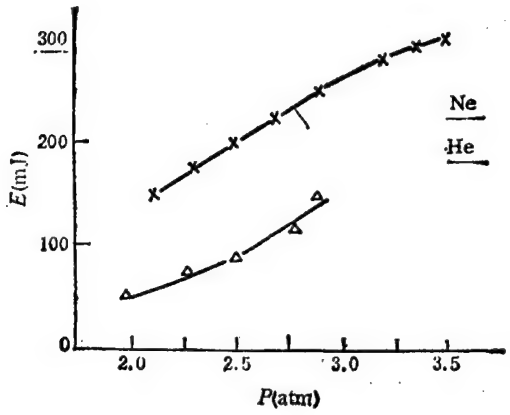


Figure 3. (HCl: 6 Torr; Xe: 60 Torr)

In order to evaluate the effect of the discharge circuit on the performance of the device, two different energy transfer circuits were tested on the device. One was described earlier where pre-ionization sparks are generated by small inductors through the energy storage

capacitor. The other circuit eliminated those small inductors and the pre-ionization sparks are generated by the peaking capacitors. It was experimentally determined, although the circuits are structurally different, the characteristics of the device are identical. This is because the number of pre-ionization probes remained unchanged. Both circuits have the same pre-ionization effect. This indicates that pre-ionization is the key factor determining the performance of the device. The latter circuit requires 55 ceramic capacitors while the former circuit only 14. Therefore, it is simpler to use small inductors to generate ultraviolet pre-ionization.

During the experiment, the thin copper foil used to generate corona pre-ionization was removed to allow the direct discharge between the ionization probes and the cathode. It was observed that both the laser energy output and uniformity of the discharge dropped significantly.

Based on these preliminary experimental results, we have the following discussion.

(1) In a 52 cm long cavity with an activation volume of 42 x 2.7 x 0.4 $cm^3$, a 310 mJ output was obtained from a XeCl laser. For a fast discharge device, the volumetric efficiency is already considerable. However, due to limitation imposed by the high voltage capacitor and pressure resistance of the cavity, the device did not fully demonstrate its energy output capability. From Figures 2 and 3 we can see that the energy output is not saturated.

(2) Generally, the energy of a KrF laser should be much higher than that of a XeCl laser. However, in Figure 2 the energy of KrF is lower. The reason is that KrF requires a higher operating voltage than XeCl. At 30 kV, it is on the linear rise curve. The next reason is the purity of fluorine used is not as high.

(3) The best result was obtained when Ne was used to dilute XeCl. The use of Ar could lower the total pressure. In Figure 2 it shows that the result obtained with Ne dilution is similar to that with Ar dilution. In fact, there is an optimum pressure for each of the three gases [2] under which the laser has the maximum energy output. If 2 atm of Ar is used for dilution, the maximum energy is not necessary lower than that with Ne. However, a higher operating voltage is required. In Figure 2 it shows that the laser begins to oscillate at 28 kV when filled with 2 atm of Ar. With Ne there is an energy output at 18 kV.

(4) The narrow laser pulse may be related to the discharge characteristics. Sufficient pre-ionization can reduce the plasma resistance in the discharge region to narrow the pulse.

(5) The energy storage capacitors and the peaking capacitors are made in China. The energy storage capacitors are electrolytic capacitors soaked with a dielectric medium. The model number is C804. Although it is not wound, there is some inductance. The peaking capacitor is a low cost, high temperature coefficient ceramic capacitor. In the device,

this capacitor can still attain a 5 percent stability for single pulse energy and a 6.8 J/l volumetric energy density. Good pre-ionization can reduce the requirements on components to allow the device to be constructed with Chinese made parts.

## References


1. Zhang Guozhi [1728 0948 3112], Han Quansheng [7281 0356 3932], and Huang Nantang, WULI [PHYSICS], 12-4 (1983).

2. Zheng Chengen [6774 2110 1869], GUANGXUE XUEBAO [JOURNAL OF OPTICS], 3-6 (1985), 525.


12553/09599

# DEVELOPMENT OF LASER S&T IN 1987 CHRONICLED

40080077a Shanghai ZHONGGUO JIGUANG [CHINESE JOURNAL OF LASERS] in Chinese Vol 15 No 2, 20 Feb 88, pp 65-69

[Article by Zhao Meicun [6329 2734 2625], Lei Shizhan [7191 0099 3277], Huang Yongkai [7806 3057 2818] and Wang Runwen [3769 3387 2429]: "A Look at the Development of Laser Science and Technology in China in 1987"]

[Text] Editor's Note: 26 years have passed since the advent of the laser in China. It is now in full bloom. We plan to start a special annual review column from 1987 in order to summarize new discoveries, inventions, and advancement in laser science and technology in a timely manner to promote the development of laser in China. Contributions are welcome from researchers in the laser community to help the editor to reflect the overall progress in laser research in China.

1987 was another year of laser achievements in China. The $10^{12}$ W Shenguang device passed certification a the national level. The CPM ring dye laser which uses a prism in the cavity to compensate for the group velocity scatter has a direct output of a 19 fs wide laser pulse. It surpassed the 27 fs record accomplished at Bell labs in 1985. A high quality non-linear crystal $LiB_3O_5$ was successfully grown to make a 34.2 W frequency doubled AG laser. There are representative results. Laser devices are becoming more practical. It has made progress toward its application in the national economy.

## 1. Laser Devices

### 1.1 "Shenguang" ["Magic Light"] Device Passed National Certification

The Shenguang device was assigned to the Shanghai Institute of Optical Instrument of the Chinese Academy of Sciences with the approval of the Ministry of Nuclear Industry and the Chinese Academy of Sciences. With the cooperation of Institute No 9 of the Ministry of Nuclear Industry, it was completed in 1985. After a year and half in operation, it passed national certification on 27 June 1987.

The Shenguang device is a large multi-disciplinary engineering project. It consists of the laser, target, laser parameter measurement, energy and

environment protection systems and a control center. The laser system consists of two subsystems, including two main oscillators of different pulse width, 10 phosphate rod amplifiers of various specifications, 12 amplifier sheets, 12 space filters with image transfer capabilities and three electro-optical isolators. The optical path to the target is 100 meters. The two paths are synchronized to an accuracy of less than 10 ps. Fifteen techniques or processes were used for the first time in China. For instance, a semiconductor opto-electronic switch is used to improve the signal to noise ratio by 2 -3 orders of magnitude. Adaptive optics is used to improve the optical quality of the laser. A lens array is used to enhance the homogeneity of the incident laser beam on the target surface. The peak power output of the device is $10^{12}$ W and the pulse width is $10^{-9}$ - $10^{-10}$ s. More than 80 percent of the laser energy is concentrated within the 10th order of diffraction (0.3 mrad). This device can be used to initiate nuclear fusion, simulate nuclear explosions and study high-power laser plasma physics. We are also prepared to use it to study the mutual interaction between the high-power laser and the target.

1.2 34.2 W Frequency Doubled YAG Laser

The Precision Instrument Department of Tianjin University and the Institute of Crystal Research of Shandong University successfully developed a high-power frequency doubled YAG laser. The average power output in the green (0.532 μm) is 34.2 W.

The device uses two krypton lamps to pump a 6mm diameter 100mm long Nd:YAG rod. The light focusing cavity is gold plated. A KTP frequency doubler is used. The length in the direction of the light beam is 5.5mm. The center frequency of the fused quartz Q-switch is 40 MHz. It is tunable and the reproducibility in frequency is 1 - 10 kHz. A piece of 1.06 μm high transmission plate and a 0.532 μm high reflection mirror are inserted between the cavity and the frequency doubling crystal to enhance the frequency doubling effect. The laser cavity is 570mm long. When the krypton lamps are continuously pumping at 26 A and the Q-switch is repeating at 9 kHz, an output at 34.2 W in the green is obtained. The pulse width of the laser is 200 ns. The scatter angle of the laser beam is less than 10 mrad. The output power fluctuates less than $\pm$ 2 percent.

1.3 Construction of a Raman Free Electron Laser

A free electron laser based on Raman scattering excitation has been developed by Shanghai Institute of Optical Instruments of Chinese Academy of Sciences. The energy of the laser pulse is 16.8 mJ and the peak power is 0.84 MW. The pulse width is 20 ns and the electron efficiency is 1.4 percent. The wavelength is 8mm (K band).

1.4 Practical High Mean Power XeCl Excimer Laser

A practical 10 W level fast electrically pumped XeCl excimer laser was developed by Anhui Institute of Optical Instruments and Changchun Institute of

Optical Instrument of the Chinese Academy of Sciences. They used techniques such as fast thyratron switching, fast lateral gas circulation, gas purification and lens protection. The laser at Anhui can operate over $10^6$ times with one charge. The maximum repetition rate is 130 Hz and the highest mean power is 20 W.

Shanghai Institute of Optical Instruments of the Chinese Academy of Sciences successfully developed a large area X-ray pre-ionized excimer laser. The cathode of the electron gun is made of graphite. The uniformity of the X-ray has been improved to within 25 percent in an area of 100 $cm^2$. In addition, a corrosion resistant sealed high pressure technique is used. The discharge volume is approximately 0.4 liter. The maximum power output is 29.5 W and the short-term power fluctuation is within 1.4 percent. The shelf life is 100 hours once it is filled.

1.5 $CO_2$ Laser Over 10,000 W in Output Power

After learning the degeneration mechanism of the gas inside a laser, Shanghai Institute of Optical Instruments lengthened the operating time of a 1,000 W flow over $CO_2$ laser to over 30 hours with each fill. The electrical discharge length is 1 m. The multi-mode power output is 1.3 - 1.5 kW and the power fluctuation is less than 1 percent. The conversion efficiency is 15 percent.

The laser institute at Huazhong Institute of Engineering used argon instead of helium as the auxiliary gas to make a helium-free 3 kW electrically excited flow over $CO_2$ laser. In addition, two 5 kW devices of the multiple needle-plate discharge type were placed in series and then energized to obtain a multi-mode laser output at 10.35 kW through a coated gallium arsenide window. This is the highest power CW $CO_2$ laser system in China.

1.6 He-Ne Laser Outputs at Six Wavelengths Simultaneously

The Chinese Academy of Metrology designed a He-Ne laser which simultaneously emits six spectral lines at 612, 629, 633, 635, 640, and 650 nm. The total power is 1 mW. They also used an external cavity discharge tube with a Brewster window to realize a 40 μW He-Ne laser at 543.5 nm. The academy also proposed a new method to continuously tune the frequency of the laser along the optimal S curve to build a 1.52 μm flow over constant frequency Zeeman laser. The tuning range is greater than 170 Hz and the sampling time is 1 ms - 100 s. The frequency stability is between $4 \times 10^{-10}$ to $4 \times 10^{-11}$.

Nanjing Institute of Engineering developed a practical 1.52 μm coherent laser source for optical fiber communication. The single mode power output is 0.4 mW and the beat frequency width is less than 1 MHz. The frequency stability is of the order of $10^{-10}$. The mode does not change after 24 hours of continuous operation at room temperature and its life is of the order of $10^4$ hours. It is already in production.

Nanjing Institute of Engineering developed an 80-MW He-Ne laser at 632.8 nm with a 1-m tube. From a 3-m long He-Ne tube, Zhejiang University obtained a 115 MW laser beam at 632.8 nM in the $TEM_{00}$ mode. The power fluctuation per hour is less than 0.6 percent. The power output for a flow over multi-mode laser has reached 150 mW.

1.7 The 16 μm Parahydrogen Excited Raman Laser System

Changchun Institute of Optical Instruments of the Chinese Academy of Sciences successfully developed a 16 μm parahydrogen excited Raman laser. It is tunable in the operating range of 14 - 17 μm. The energy per pulse is greater than 500 mJ and the pulse width is 30 ns. The energy conversion efficiency is greater than 13 percent. The output wavelength range coincides with the spectral range of $UF_6$ isotopes to promote work in this area.

1.8 New Progress in Semiconductor Lasers

Beijing Institute of Semiconductors of the Chinese Academy of Sciences used a special design to manufacture a uniform phase semiconductor laser diode for measuring distance with precision. The power output is 2 - 10 mW and the modulation rate is 1 - 2 Gb/s. The wavelength is 820 - 860 nm.

The Radio Department of Qinghua University made new progress in the development of practical semiconductor laser devices. A 1.3 μm bonded outer cavity single mode semiconductor laser was developed. The power output is greater than 2 mW and the line width is less than 1 MHz. The angle of divergence is 1 mrad. Its stable operation period is greater than 24 hours.

Shanghai Institute of Optical Instruments developed a continuously tunable medium infrared PbSnSe laser operating in the 14 - 18 μm range. Its single mode tunable range is 3 $cm^{-1}$ and the overall tunable range is 160 $cm^{-1}$. the maximum operating temperature is 48 K.

1.9 Narrow Pulse Laser With 30 pps Repetition Rate

Shanghai Institute of Optical Instruments solved the thermal stability problem of the cavity under mode locking condition and developed a high repetition rate (10, 20, 30 pps), high mode locking probability (100 percent), high stability (fluctuation within 2 percent) narrow pulse 930 - 50 ps) YAG laser. This laser has been used in high precision satellite ranging.

1.10 Pulse YAG Laser With 200 W Average Output Power

Shanghai Institute of Optical Instruments successfully developed a 200 W YAG laser for industrial processing and surgery. This devise is pumped with a long pulse krypton lamp and operates at a high small signal gain to significantly improve the average power and pumping efficiency. The device operates at 1 - 30 Hw at a peak power of 5 kW. The angle of divergence of the beam is approximately 10 mrad.

## II. New Materials

### 2.1 A Series of Phosphate Laser Glasses

Shanghai Institute of Optical Instruments of the Chinese Academy of Sciences developed a series of phosphate laser glasses and successfully placed them in a large sheet laser amplifier in the Shenguang device. The absorbance of phosphate glass is less than 0.15 percent per cm at 1.06 μm. The stress double refraction belongs to type 1. Its optical uniformity is $2 - 4 \times 10^{-6}$. In addition, neodymium doped phosphate glasses of different specifications have been developed for small and medium scale applications, including different lasing cross-section and neodymium concentrations. The diameter ranges from 6 - 10mm and length 70 - 150mm. The repetition rate of the finished device is 30 pps and the efficiency is 1.5 - 2 percent. In part, it can replace YAG.

### 2.2 High Quality Non-Linear Crystal

Fujian Institute of Material Structure developed a new high quality non-linear $LiB_3O_5$ crystal. The crystal is large in size, not deliquescent, optically uniform and has a high threshold for destruction. In use, its frequency doubling efficiency is twice as high as that of KTP. In addition, its matching angle can be adjusted by 1°. It is suited for use in a large, multi-stage laser system or a commercial laser system.

### 2.3 Self-Activated Laser Crystal $NdAl_3(BO_3)_4$

NAB is a high neodymium, low threshold, high gain laser crystal. It is an ideal material for a small solid state laser. Fujian Institute of Material Structure discovered a new flux to grow large optically uniform NAB crystals. The semi-finished crystal is 20x20x45 $mm^3$ in size. When the optical uniformity is 0.3 λ/in, it may be processed into a 3.2mm diameter 23.7mm long laser rod. The power output of such a long pulse laser is 422 mJ, its wavelength is 1.063 μm and its angle of divergence is 2 mrad.

### 2.4 High Quality Nd-YAG Laser Rod

Institute 11 of the Ministry of Electronic Industry developed a high neodymium Nd:YAG rod by doping $Mg^{2+}$ and controlling the atmosphere. The Nd concentration is 1.1 $\pm$ 0.1 atomic percent. There are no scattering particles and color centers in the crystal. The extinction ratio is high, 41 dB on the average. The power of continuous laser produced per unit volume is 71 $W/cm^3$. This product is already available in the market.

### 2.5 New Laser Dyes

Tianjin Institute of Dye Industry developed new laser dyes such as ppo and sulfonated triazinestilbene. The characteristics for ppo are: laser wavelength 370 nm, tunable range 359 - 391 nm, efficiencies 13 percent (pumped with $N_2$ laser) and 7.1 percent (with xenon lamp). The characteristics for

sulfonated triazinestilbene are: laser wavelength 405 nm, tunable range 400 - 480 nm, efficiency 24 percent (with $N_2$ laser) and absorption centered at 340 nm.

## 2.6 Laser Protection Glass

Shanghai Institute of Optical Instruments developed laser protection glasses in ultraviolet (200 - 300 nm) and infrared (600 - 1100 nm). Selective absorption of the additive is used to provide the protection. In the region of protection, transmission is less than 0.5 percent. It is comparable to similar products produced in other countries.

# III. Basic Research

## 3.1 19 fs Narrow Laser Pulse Attained

Chen Guofu [7115 0948 1133] et al (Xi'an Institute of Optical Instruments, Chinese Academy of Sciences) used a CPM ring dye laser with four prism group velocity compensation and seven mirror horizontal nozzle cavity to get a $19 \times 10^{-15}$ s pulse. It is a world record. The laser reflective mirror was coated with a film to cut off yellow and red light. This limits the bandwidth of the pulse while ensuring the narrowness of the pulse to improve the stability of the laser. In addition, the efflux thickness of the absorbent is chosen to be 130 μm. A suitable gain medium concentration was selected to enhance the saturated gain effect to further compress the laser pulse. Their success is considered as the short click made by a laser clock.

## 3.2 Laser Spectrum Atomic Uranium

Shanghai Institute of Optical Instruments produced a high concentration of uranium vapor at a hollow uranium cathode by pulse discharge. Two homemade YAG laser pumped dye lasers were used for triple photon ionization at two wavelengths when the discharge was stopped. The same electrode was used to collect ionization signals to study the triple photon ionization of atomic uranium. A great deal of data was obtained.

Changchun Institute of Applied Chemistry of Chinese Academy of Sciences first established the laser photo-current spectrum technique to determine the displacement spectra of $^{235}U$ and $^{238}U$ and the superfine spectrum of $^{235}U$. These spectra are important in the triple photon process which has practical value in laser isotope separation.

## 3.3 Simple Model for Chain Reaction $F_2/H_2$ Pulse Chemical Laser

Dalian Institute of Chemical Physics perfected a simple model for chemical laser which can simultaneously calculate the time resolution characteristics of 98 spectral lines of HF laser with 7 vibrational energy levels and 14 rotational energy levels. It is very helpful in studying the HF chemical laser. The results can predict the effect of inhibitor, initiator pre-reaction on the $H_2/F_2$ reaction.

3.4 Surface Enhanced Raman Spectroscopy

Beijing Institute of Engineering employed surface coating technology to study surface Raman spectroscopy. This lifts the constraint that only water soluble molecules can be studied. Raman spectra of a large number of water insoluble compounds can be measured and background fluorescent interference is effectively suppressed.

3.5 Observation of Super Raman Scattering of Excited Doublet in Sodium Vapor

The Institute of Optoelectronics at Harbin Polytechnical University used an excimer laser pumped dye laser ($\lambda \sim$ 578.76 nm, $E_p \sim$ 4 mJ) as the source of excitation to observe the super Raman scattering of the excited doublet from 3s through 4D to $^4P_{3/2}$ and $^4P_{1/2}$ in sodium vapor. Their wavelengths were found to be 2.3387 and 2.3356 $\mu$m, respectively. The tunable range is 30 $cm^{-1}$. It may be a new tunable coherent light source.

3.6 Study of Optical Theory With Solitary Wave

Shanghai Institute of Optical Instruments derived a solitary wave equation which describes the interaction between light and atom based on a model which involves the interaction of light with an atom with two energy levels. The precise solution was obtained and it was derived that there are two necessary conditions for the solution to exist. Furthermore, it was extended to situations involving two and three waves. Computer simulation results are in essential agreement with experimental conditions.

IV. Applications of Laser Technology

4.1 Thermal Treatment With 30mm Hardening Width

In laser thermal treatment, the beam is usually focused and the scanning width is generally less than 4mm. Therefore, it is not suitable for treating a wide part which limits its range of applications.

Shanghai Institute of Optical Instruments successfully developed an optical system for laser heat treatment which includes a wide band integral lens assembly and a swaying scanner. It increases the width to 7 - 12mm. With a 1000 W $CO_2$ laser, the hardened depth is greater than 0.4mm.

Tianjin Institute of Textile Engineering studied the scanning pattern of a high-power laser from a rotating polygon of mirrors. They used matrix optics to derive the spatial curve equation of the reflected light beam to provide an expression for the width of laser quenching. Then, they used the rotating mirror in the thermal treatment with a high-power laser to increase the width to 30mm in a continuous adjustable manner. This technique expands the range of applications and improves efficiency and quality as well. It was used in the production of gage blocks for scales and in oil presses with impressive

results. The annual economic benefit has reached 1,500,000 yuan. In addition, it may be used in large area laser melting and laser alloy preparation.

### 4.2 New Progress in Laser Medical Devices

Beijing Institute of Optoelectronics introduced the YJ series of attractive looking, stable and reliable YAG laser medical devices. The device is microprocessor controlled and the power output at the end of the optical fiber is greater than 80 W. It is definitely effective in the treatment of cancer of the mouth, skin, esophagus and rectum. It is also useful in the treatment of vascular blockage and coronary disease.

Zhejiang University and Zhejiang Institute of Medical Instrumentation jointly developed a laser cancer treatment device. It uses a copper vapor laser for diagnosis. Its wavelength is 510 nm and its power is 30 - 200 mW. A copper laser pumped dye laser (longitudinal) is used in treatment. The light conversion efficiency is 40 percent. The center wavelength of the band is 630 nm and the power is 750 mW. Optically coupled fiber is used for output. It can operate continuously for 8 hours. It is already in clinical use with good results.

Shanghai Institute of Optical Instruments successfully developed a Model GZ miniature gallium arsenide semiconductor laser probe. The wavelength ranges from 820 to 870 nm and the maximum power is 1.3 mW. The maximum repetition rate is 3 kHz. The depth of the probe is changed by adjusting the position of the focus. This probe has been used clinically in six medical organizations in Shanghai with satisfactory results.

In cancer diagnosis, Fudan University studied the fluorescence spectrum of early stage cancer with an optical multi-channel analyzer and conducted a comprehensive study on the pictures for diagnosis. A highly sensitive and fast diagnosis method has been provided.

### 4.3 Novel Laser Instrumentation

Hefei University and Anhui Institute of Optical Instruments jointly developed the Model JWG microscopic laser spectrometer. The instrument uses a ruby laser as its light source. The maximum pulse energy is greater than 1.2 J and the energy fluctuation is within 5 percent. The maximum power is over 4.5 MW. The relative sensitivity is $10^{-2}$ - $4 \times 10^{-2}$ percent. The spatial resolution is 10 - 200 $\mu$m. It is also equipped with a device to raise, maintain and lower temperature. The accuracy in thermostating is within 0.2°C. The instrument can analyze a substance in a very small area or with a very minute quantity. It is accurate, fast, sensitive and essentially non-destructive without sample preparation. It can be widely used in mining, metallurgy and public security.

A novel full-featured portable holographic camera and a laser atomization camera were developed by the Beijing Institute of Optoelectronics. These two

cameras use solid state laser as the light source. The latter uses a tunable Q ruby laser and the pulse energy is over 1.5 J. The number of pulses ranges from 1 - 9 and the pulse width 20 - 500 ns. The visual field is 24 x 24mm² or 60 x 60mm² and the resolution is 0.005mm. It can be used to take pictures of fast moving fine particles to record their distribution, velocities and dimensions. The Institute also used a single pulse ruby laser in high speed photography. The visual field is 300 - 500mm in diameter and the capture speed range is 1 - 7 km/s. The probability of capture at a single site is over 90 percent. This can be used in aeronautical, astronautical and ballistic tests.

12553/06662

# Monte-Carlo Solution of Directional Effective Emissivities of Infrared Standard Reference Sources

40100021a Harbin HARBIN GONGYE DAXUE XUEBAO [JOURNAL OF HARBIN INSTITUTE OF TECHNOLOGY] in English, No 1, Feb 88 pp 103-105, 95

[Article by Li Bijuan [2621 4310 1227], and Xu Wenhui [1776 2429 6540], et al., Department of Precise Instruments; received 20 July 1987]

[Excerpts] This work is funded by the National Foundation of Natural Science.

Blackbody cavities are of importance in pyrometry, photometry and radiometry. Methods for calculating both approximately and exactly the local hemispherical effective emissivities within an axisymmetrical cavity with diffusely emitting and reflecting walls have been described previously.[1,2,3] When investigations are extended towards infrared, as in such cases as infrared detector calibration, infrared remote sensing, radiation heat transfer and so on, specular reflection becomes important. Many experiments indicate that the reflection characteristics of a given surface approach a diffuse distribution at short wavelength and a specular distribution at long wavelength. It must be pointed out that the reflection pattern may be described as consisting of a nearly uniform distribution with a diffuse component plus a specular component, that is, uniform specular - diffuse model.[4,5]

In many applications, the directional effective emissivity of a cavity is often required, rather than the hemispherical effective emissivity.[6] The present paper is for cavities whose surfaces are expressed by the uniform specular - diffuse model. The baffled right circular cylinder which has been widely used in the Ministry of Astronautics as a standard reference source is considered and evaluated. Typical results are also given.

We have calculated the directional effective emissivities of the baffled cylindrical cavity which has been used as the standard reference source

in the medium-temperature scale for Institute No. 207 of the Ministry of Astronautics. The total number of incident ray bundles is taken to be $10^5$ in order to assure demanded accuracy. The geometry nomenclatures of the baffled cylindrical cavity are the depth L, the cylinder radius R and the aperture radius $R_0$. The intrinsic wall emissivity is $\varepsilon$.

Typical results of the cavity are listed in Table I. We can now draw a very important conclusion that the specular reflection component must be considered in the infrared region for a standard reference source to assure accuracy of calibration.

Table I. Typical results of directional effective emissivities at the bottom for a baffled cylindrical cavity (L = 160mm, R = 17mm, $R_0$ = 14mm and $\varepsilon$ = 0.88) with different specular reflection components.

| $\rho_s$ | $0.3\rho$ | $0.2\rho$ | $0.1\rho$ | $0.05\rho$ | 0 | Bedford's Precise Solution |
|---|---|---|---|---|---|---|
| $\varepsilon^D_*(x_0)$ | 0.9631 | 0.9755 | 0.9870 | 0.9932 | 0.9992 | 0.9990 |

References


1. R. E. Bedford and C. K. Ma, J. Opt. Soc. Am., 64, 339 (1974).

2. Chu Zaixiang, Chen Shouren, and Chen Hongpan, J. Opt. Soc. Am., 70, 1270 (1980).

3. R. E. Bedford, C. K. Ma, Chu Zaixiang, Sun Yuxing, and Chen Shouren, Appl. Opt., 24, 2971 (1985).

4. R. C. Birkebak and E. R. G. Eckert, J. Heat Transfer 87, 85 (1965).

5. E. Torrance and E. M. Sparrow, J. Heat Transfer 87, 283 (1965).

6. A. Ono, J. Opt. Soc. Am., 70, 547 (1980).


/09599

# A TWO-PHOTON SUPERRADIATION COHERENT BEAT

40090074b Beijing ZHONGGUO KEXUE [SCIENTIA SINICA] in Chinese, Series A No 1, (Jan) 88, pp 46-54

[Article by Sun Taoxiang [1327 7118 (but with horse radical instead) 0078] (Physics Department, Beijing University). Received 24 Oct 86, revised 12 May 87]

[Abstract] The theory of the production--among molecules having hyperfine interactions--of a two-photon superradiation coherent beat having special modulation characteristics is reported. On the basis of semiclassical theory, density matrix equations are used to derive the theoretical formulae for this superradiation coherent beat field. During the experiment, Stark switching technology and a real-time sampling detection system were employed to observe this phenomenon. Experimentally measured results are consistent with theoretical analysis. Since this coherent beat signal contains information on molecular hyperfine splitting, it can have important uses in high-resolution spectroscopy.

\12232

# A CONTOUR-BASED METHOD FOR MAXIMALLY HOMOGENIZED FORM RESTORATION

40090074d Beijing ZHONGGUO KEXUE [SCIENTIA SINICA] in Chinese, Series A No 1, (Jan) 88, pp 74-82

[Article by Li Lingxiao [2621 0407 7197 and Wu Zhongquan [0702 0022 2938] (Department of Radio, Qinghua University, Beijing). Received 18 Sep 86, revised 12 May 87]

[Abstract] The psychological principle that the human eye, when perceiving form, has a tendency to favor homogeneity of form or symmetry of form is used to propose a contour-based, extreme-valued method for restoring the orientation of the visible surfaces of three-dimensional bodies. The existence as well as the uniqueness of solution is discussed and an algorithm for obtaining this solution is given. This method can correctly interpret the form of two kinds of bodies--regularly shaped and irregularly shaped--and therefore has a broad range of applicability. At the same time, it also has the advantage of requiring only a small amount of computation. The experimental results indicate that use of this method for restoring three-dimensional form can yield a satisfactory outcome.

/12232

# EXPERIMENTAL STUDY OF MEDIUM-PRESSURE GAS COOLING SYSTEM FOR LASERS

40090080a Shanghai GUANGXUE XUEBAO [ACTA OPTICA SINICA] in Chinese Vol 8 No 1, Jan 88 pp 28-33

[English abstract of article by Guo Xinsheng [6753 2450 3932], et al., of Xi'an Jiaotong University; Lu Zhonghe [0712 1813 0735], et al., of Xi'an Institute of Applied Physics]

[Text] By using a simulated model, the authors establish the basic heat transfer equations for laser-gas cooling systems. These can be used in the determination of the heat resistance of each part in the system. Analysis indicates that an increase in the circulating gas density can improve the heat transfer effect, decrease the gas flow resistance and reduce power consumption. Based on this, a medium-pressure gas cooling system has been built and used successfully in a YAG laser which has a repetition rate of 10 Hz and heat dissipation power of 200 W.

9717

DEVELOPMENT OF INTERFEROMETRIC OPTICAL FIBER ACOUSTIC SENSORS

40090080b Shanghai GUANGXUE XUEBAO [ACTA OPTICA SINICA] in Chinese Vol 8 No 1, Jan 88 pp 67-74

[English abstract of article by Tang Mingguang [0781 2494 0342], et al., of Chengdu Institute of Radio Engineering]

[Text] In this paper, the pressure sensitivity of an optical fiber acoustic sensor is described theoretically and its sensitivity under inhomogeneous pressure is analyzed and evaluated. An optical fiber interferometric acoustic sensor system with DC phase tracking homedyne detection is established. The threshold of the detectable acoustic pressure is about 200 μPa with an optical fiber 5 m long.

9717

RESEARCH PROPERTIES, STRUCTURES OF BOROSILICATE GLASSES USING PHASE DIAGRAM METHOD. I. NMR STUDIES OF STRUCTURE IN $Na_2O$-$B_2O_3$-$SiO_2$ GLASS

40090080c Shanghai GUANGXUE XUEBAO [ACTA OPTICA SINICA] in Chinese Vol 8 No 1, Jan 88 pp 75-82

[English abstract of article by Jiang Zhonghong [1203 0022 1347], et al., of Shanghai Institute of Optics and Fine Mechanics, Chinese Academy of Sciences]

[Text] NMR spectroscopy has been used for many years to investigate the structures of glasses. NMR spectra have permitted the identification in the glasses of structural groupings from the crystalline compounds, and the relationships of these groupings have also been determined by Krogh-Moe and Bray.

According to computer calculated NMR data based on the experimental results in $Na_2O$-$B_2O_3$-$SiO_2$ system glasses, a new quantitative structural model from the principle of phase diagrams is proposed.

The authors believe that the structure of a simple glass resembles the related congruent melting compound. A multicomponent glass can be regarded as the melting mixture of some of the nearest congruent melting compounds in the phase diagram.

9717

LOCAL, QUASI-LOCAL MODES OF Zn IN CdTe

40090081a Beijing WULI XUEBAO [ACTA PHYSICA SINICA] in Chinese Vol 37 No 2, Feb 88 pp 197-205

[English abstract of article by Lu Wei [7120 5898], et al., of the Laboratory for Infrared Physics, Shanghai Institute of Technical Physics, Chinese Academy of Sciences]

[Text] The authors report the far infrared absorption and reflection spectra of the mixed crystals $Zn_xCd_{1-x}Te$ with small x in the temperature range of 4.2 to 300 K and the frequency region of 20-350 $cm^{-1}$. The local and quasi-local modes induced by Zn and ZnTe in CdTe and the CdTe-like 2TA two-phonon absorption are observed. The frequencies of the modes are estimated using the mass-defect model combined with Green's function method. The random element isodisplacement (REI) model is used to calculate the two-mode behaviors of the mixed crystals and to best fit the reflection spectra. The temperature dependence of the phonon absorption and the relaxation factor of CdTe-like and ZnTe-like modes are calculated and explained.

9717

# INVESTIGATION OF $Cr^{2+}(3d^4)$ IN GaAs UNDER HYDROSTATIC PRESSURE, AlAs ALLOYING

40090081b Beijing WULI XUEBAO [ACTA PHYSICA SINICA] in Chinese Vol 37 No 2, Feb 88 pp 206-213

[English abstract of article by Gu Yiming [7357 0001 7686], et al., of the Department of Physics, University of Science and Technology of China, Hefei]

[Text] A spin-polarized version of the tight-binding Green's function scheme is developed for the GaAs:$Cr^{2+}(3d^4)$ system, which is under hydrostatic pressure and is alloyed with AlAs in different concentrations. Results on the variation trends of $^5E$ excited and $^5T_2$ ground acceptor levels of GaAs:$Cr^{2+}$ with different pressures and aluminum concentrations are reported. The theory shows that under certain pressure and Al concentration, the $^5E$ state will shift into the band gap from the bottom of the conduction band. The $^5E \rightarrow {}^5T_2$ luminescence, not observed in normal conditions, will appear in this case. Good overall agreement between theory and the experiment is found. The theory also predicts that a similar luminescence process will occur if GaAs is alloyed with Gap in certain concentrations, but this still awaits experimental verification.

9717

# STUDY OF ELASTICITY OF ACOUSTICALLY ACTIVE CRYSTALS $NaBrO_3$, $NaClO_3$

40090081c Beijing WULI XUEBAO [ACTA PHYSICA SINICA] in Chinese Vol 37 No 2, Feb 88 pp 214-220

[English abstract of article by Shen Zhigong [3088 1807 1562], et al., of the Department of Physics, Chinese Academy of Sciences]

[Text] The dispersion curves of phonons along three crystallographic axes for isomorphous crystals $NaBrO_3$ and $NaClO_3$ have been measured using coherent inelastic neutron scattering. The velocities of elastic waves along these directions and three independently elastic constants $C_{11}$, $C_{12}$ and $C_{44}$ are deduced from the dispersion curves in the region of small wave vectors. The experimental results directly verified the prediction of Portigal's theory that the velocities of left circularly-polarized phonons and right polarized ones are distributed symmetrically on both sides of a particular average velocity $v_{T_D}$, while the value of $v_{T_D}$ can be uniquely determined by the velocities in other directions or the zero-order approximated elastic constants.

9717

INTERACTION BETWEEN CW PLANE WAVE, TRAVELING PLANE PULSE

40090081d Beijing WULI XUEBAO [ACTA PHYSICA SINICA] in Chinese Vol 37 No 2, Feb 88 pp 221-228

[English abstract of article by Qian Zuwen [6929 4371 2429] of the Institute of Acoustics, Chinese Academy of Sciences]

[Text] From the investigation of sound interaction between two rectangular plane waves, a deduction has been made by Westervelt that there is no sound scattering by sound outside the region of interaction. However, it seems to be of little significance to say "outside the common region," since its volume is practically infinite. In this paper, the interaction between a cw plane wave and a plane pulse traveling with sound speed is taken into consideration. Both satisfy the homogeneous wave equation. Outside the common volume they can be employed to study the sound scattering by sound. It is shown in this paper that there is no scattering which follows the law of causality. It is also shown that it does not appear appropriate to apply Lighthill's far-field integral for calculating sound scattering by sound in this case.

9717

# OBSERVATION OF LASER-INDUCED SELF-DIFFRACTION FROM $LiNbO_3$:Fe CRYSTAL

40090081g Beijing WULI XUEBAO [ACTA PHYSICA SINICA] in Chinese Vol 37 No 2, Feb 88 pp 268-273

[English abstract of article by Liu Simin [0491 1835 2404], et al., of the Department of Physics, Nankai University, Tianjin]

[Text] The authors have observed very regular diffraction patterns on the screen behind the crystal when the focused He-Ne laser beam illuminates the thin sample along the X or Y axis of the $LiNbO_3$:Fe crystal. This is utterly different from the photo-induced light scattering phenomenon which arises from phase-noise-gratings produced by optically-induced refractive index changes in the crystal observed long ago. This self-diffraction pattern can be explained by self-diffraction theory and the complicated lens-like effect formed in the crystal when the focused laser beam illuminates it. These diffraction patterns can show the optically-induced refractive index changes in the crystal clearly, and the maximum number of optically-induced refractive index changes $\Delta n$ can be calculated directly from the number of diffraction rings. The authors have also studied and discussed the conditions of formation of laser-induced self-diffraction and its competitive behavior with photo-induced light scattering.

9717

## Fiber-Optic Polarization -Type Acoustic Transducer

40090088 Beijing YIQI YIBIAO XUEBAO [CHINESE JOURNAL OF SCIENTIFIC INSTRUMENT] in Chinese Vol 9 No 1, Feb 88, pp 3-8.

[Article by Zhang Liming, Xu Qichang, and Wang Dezhao, Institute of Acoustics, Chinese Academy of Sciences]

[Abstract] Two kinds of fiber-optic sound sensors based on photoelastic effect are presented. One is a multi-mode polarization-type fiber-optic sound sensor, and another is a single-mode version. In the first part, the sensitivity and acoustic structure of the multi-mode sensor are analyzed, and the sensitivity is measured. The experimental results are in agreement with the theoretical frequency response. The instability induced by mode noise is reduced by using single-colour incoherent light as a light source.

In the second part, the single-mode polarization-type fiber-optic sound sensor is analyzed, and its sensitivity is measured by substitute method. The theoretical result is consistent with experiment well up to 80 kHz. Polarization retaining single-mode fiber and cladding mode stripper are used to improve the stability of the sensor. (Received Apr 86.)

/9738

## A Compact Atomic Beam Apparatus

40090088 Beijing YIQI YIBIAO XUEBAO [CHINESE JOURNAL OF SCIENTIFIC INSTRUMENT] in Chinese Vol 9 No 1, Feb 88, pp 9-13.

[Article by Zhou Dafan, Liang Xiuqing, Li Yufu, and Li Zhenmei, Changchun Institute of Applied Chemistry, Chinese Academy of Sciences]

[Abstract] This paper describes a compact, low-cost and high-performance atomic beam apparatus. The atomic beam was produced by electrically heating a molybdenum crucible containing metals of interest. A temperature as high as 1600°C could be held. The residual pressure pumped out by a diffusing pump was $3X10^{-6}$ Torr and the collimation ratio was between 5 and 100. Our present design consists of two parts: the laser action room and the evaporation room. Most experiments can be accommodated by rearrangement of only a few parts.

This atomic beam apparatus is suitable for experiments of high-resolution laser spectroscopy, laser isotope separation and laser interaction with atoms and molecules of rare-earth elements. (Received Nov 86.)

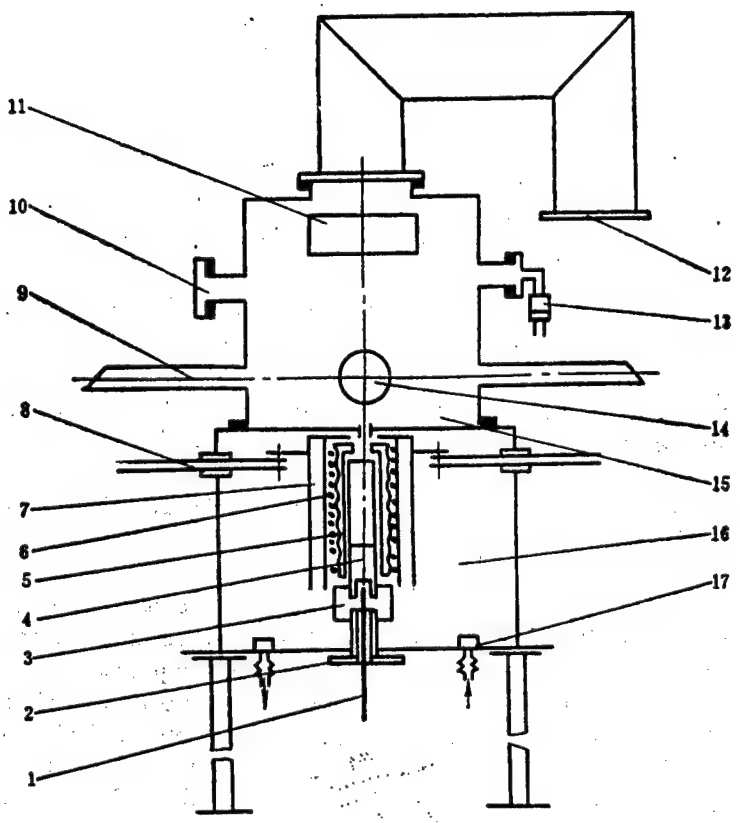


Figure 1: Schematic of the structure of the atomic beam apparatus

Key:
1. Tungsten rhenium thermocouple
2. Crucible bracket
3. Boron nitride heat-proof ring
4. Molybdenum crucible
5. Ceramic tube
6. Molybdenum filament
7. Molybdenum plate heat-shield wall
8. Water-cooled electrode
9. Laser incident conduit
10. Ion-collector electrode lead-wire exit
11. Cold trap
12. Vacuum pipe (and vacuum unit hookup)
13. Vacuum ionization chamber
14. Fluorescence collector window
15. Laser active chamber
16. Evaporation chamber
17. Cooling water entrance

/9738

Approach for Microcomputer- Controlled Laser Microhole-Diameter Measurement Equipment

40090088 Beijing YIQI YIBIAO XUEBAO [CHINESE JOURNAL OF SCIENTIFIC INSTRUMENT] in Chinese Vol 9 No 1, Feb 88, pp 72-76.

[Article by Lü Haibao, Qi Xinmin, and Li Ying, National University of Defense Technology]

[Abstract] Microcomputer-controlled equipment for measuring a microhole diameter using laser diffraction is reported. A measurement principle based on an incremental method is adopted in the equipment; the determination of the Fraunhofer diffracting distance may thus be solved effectively. The increments of the diffracting pattern dimension and the diffracting distance are measured using a laser interferometric system. To move the photoelectric detector in the directions of length and breadth, a cross guide is specially designed. Monitoring for the measuring process, such as distinguishing and locating the orders in the diffracting pattern, choosing and altering the feed direction, and giving on/off gate signals for interferometric counting is assumed by means of a microcomputer. The measured results may be displayed and printed immediately. The precision of the equipment is about 1 percent. If the measuring multipoint method is used, the non-circularity of the microhole may be determined from the equipment. (Received Jan 87.)

/9738

## Large-Signal Self-Consistent Solution for an Orotron

40090084a Beijing DIANZI KEXUE XUEKAN [JOURNAL OF ELECTRONICS] in Chinese Vol 10 No 1, Jan 88 pp 35-41

[English abstract of article by Guo Kaizhou and Song Wenmiao, Institute of Electronics, CAS, Beijing)

[Text] A large-signal self-consistent solution for an orotron in a simplified model is given. In this model the electron beam is modulated by the field and the field is excited by the electron beam inversely. A parameter $Z_c$, which is very important for the efficiency (as well as for getting oscillation), is deduced. By means of this simplified model calculation is carried out for some practical parameters of the orotron. It is shown that for producing a practical orotron in a wide frequency range, it is necessary to design a quasi-optical resonator not only with a high $Q_H$ but also with a wide and long enough mode spot on the grating. And for the electron beam, a very small thickness is needed; it should pass by the grating as closely as possible. A high enough value of current is also very necessary. (Received 19 Jul 85, revised 14 Oct 85).

## Study of a Gyromonotron With a Composite Periodic Magnetic Field and a Coaxial Cyclotron Electron Beam

40090084a Beijing DIANZI KEXUE XUEKAN [JOURNAL OF ELECTRONICS] in Chinese Vol 10 No 1, Jan 88, pp 42-52

[English abstract of article by Wu Jingqiang, Chengdu Institute of Radio Engineering, Chengdu]

[Text] On the basis of the works of the author (1985) and Liu Shenggang (1985), by using the linear kinetic theory, a gyromonotron operating with a composite periodic magnetic field and a coaxial cyclotron electron beam is analysed in detail. The equations for the power interaction between electron beam and wave, the frequency shift and the starting oscillation current are given. (Received 24 Jun 86, revised 30 Dec 86).

## A New Edge Detector With Thinning and Noise Resisting Ability

40090084b Beijing DIANZI KEXUE XUEKAN [JOURNAL OF ELECTRONICS] in Chinese Vol 10 No 2, Mar 88 pp 106-112

[English abstract of article by Chen Genming and Yuan Baozong, Northern Jiaotong University, Beijing]

[Text] A new edge detector using a 5 x 5 window is presented. It can reduce the noise effect efficiently but not increase the width of the detected edge, which has always happened when using the 5 x 5 window edge detector. In addition, in order to handle the problem where the contrast is reduced in the dark region due to underexposure, this detector uses an auto-changeable threshold, so that it can detect the edge in regions of different grey background correctly. (Received 26 Nov 86, revised 29 Aug 87).

## Theory and Numerical Simulation of Beam-Wave Interaction of the Gyro-Peniotron

40090084b Beijing DIANZI KEXUE XUEKAN [JOURNAL OF ELECTRONICS] in Chinese Vol 10 No 2, Mar 88 pp 113-119

[English abstract of article by Chen Zenggui, Institute of Electronics, CAS]

[Text] Starting from the relativistic motion equation and the energy equation of the electron, a large-signal theory which describes the beam-wave interaction of the gyro-peniotron for arbitrary $TE_{mn}$ mode and arbitrary harmonic of the cyclotron frequency is presented. Numerical simulation shows that under defined conditions an electronic efficiency of about 45% for the third cyclotron harmonic at an operating frequency of 35 GHz could be obtained, while the required DC magnetic field is only 4.2 kGs. This fact indicates that this device could be operated with high efficiency and a low magnetic field. Therefore, the practical application of the gyro-device will be greatly extended and the potential for short-millimeter and sub-millimeter wavelengths exists. (Received 1 Aug 86, revised 29 Dec 86).

A New Type of Millimeter-Wave Gunn Oscillator

40090084a Beijing DIANZI KEXUE XUEKAN [JOURNAL OF ELECTRONICS] in Chinese
Vol 10 No 1, Jan 88 pp 89-91

[English abstract of article by Miao Jingfeng and Shen Jinquan, Nanjing Institute of Technology, Nanjing]

[Text] A new type of millimeter-wave Gunn oscillator is proposed. The advantages of NRD (nonradiative dielectric) waveguide and resonant-cap oscillator are employed in the design of the new oscillator. The experimental results show that this kind of oscillator has a good future as a millimeter-wave source. (Received 23 May 86, revised 3 Sep 86).

07310

Electromagnetic Missile Systems

40090084b Beijing DIANZI KEXUE XUEKAN [JOURNAL OF ELECTRONICS] in Chinese Vol 10 No 2, Mar 88 pp 127-136

[English abstract of article by Zhan Jun, Beijing University of Posts and Telecommunications, Beijing]

[Text] The theory of electromagnetic missiles established by T. T. Wu (1985) is developed. The asymptotic condition for the spectrum of the exciting signal of the electromagnetic missile system is derived and several kinds of possible electromagnetic missile systems are given. (Received 22 May 86, revised 3 Sep 87.)

07310

# A STUDY OF THE BaO-$Y_2O_3$ ($La_2O_3$)-CuO TERNARY-SYSTEM PHASE DIAGRAM

40090074c Beijing ZHONGGUO KEXUE [SCIENTIA SINICA] in Chinese, Series A No 1, (Jan) 88, pp 55-67

[Article by Che Guangcan [6508 1639 3503], Liang Jingkui [2733 2417 7608], Chen Wei [7115 4850], Xie Sishen [6043 1835 3234], Yu Yude [0205 5148 1795], Li Hua [2621 5478], Yang Qiansheng [2799 0051 5116], Ni Yongming [0242 0737 2494], Liu Guirong [0491 6311 2837], and Chen Genghua [7115 1649 5478], (Institute of Physics, Chinese Academy of Sciences, Beijing). Received 28 May 87]

[Abstract] Techniques such as X-ray diffraction, thermal analysis, and superconductivity measurements are used to determine the $La_2O_3$-CuO, BaO-CuO, and $Y_2O_3$-CuO binary-system phase diagrams and the BaO-$La_2O_3$-CuO and BaO-$Y_2O_3$-CuO ternary-system room-temperature cross sections. In the rich CuO regions of these two ternary systems, there exist $Ba_xLa_{2-x}CuO_4$ ($x \leq 0.07$), $BaLaCu_2O_{5+\delta}$, $BaLa_4Cu_5O_{14+\delta}$, $BaLa_2Cu_2O_6$, $Ba_2YCu_3O_{9-y}$, and $BaY_2CuO_5$ compounds. $Ba_xLa_{2-x}CuO_4$ ($x \leq 0.07$), $BaLa_4Cu_5O_{14+\delta}$, $BaLaCu_2O_{5+\delta}$, and $BaLa_2Cu_2O_6$ all prove to be tetragonal systems, with respective lattice constants as follows: $a = 5.356$Å, $c = 13.20$Å; $a = 8.660$Å, $c = 3.863$Å; $a = 3.917$Å, $c = 11.75$Å; and $a = 3.992$Å, $c = 19.96$Å. $Ba_2YCu_3O_{9-y}$ has an orthorhombic distorted perovskite structure, with $a = 3.892$Å, $b = 3.824$Å, $c = 11.64$Å; it belongs to the Pmmm space group. $BaY_2CuO_5$ has an orthorhombic structure, with $a = 7.123$Å, $b = 12.163$Å, and $c = 5.649$Å, in the Pbnm space group. The relationship between composition and superconductivity is studied, as is the influence of sintering temperature on the compound structure and superconductivity of $Ba_2YCu_3O_{9-y}$. Finally, the cause of the emergence of superconductivity is discussed.

/12232

## RELATIONSHIP BETWEEN FORM OF NORMALIZED EFFECTIVE PHONON SPECTRUM, SUPERCONDUCTING $T_c$

40090081e Beijing WULI XUEBAO [ACTA PHYSICA SINICA] in Chinese Vol 37 No 2, Feb 88 pp 239-247

[English abstract of article by Weng Zhengyu [5040 1767 1342], et al., of the Department of Physics, University of Science and Technology of China, Hefei]

[Text] The numerical solution of Eliashberg's equation is analyzed by a graphic analytical method, and the following conclusions are drawn. The superconducting $T_c$ of a superconductor can be enhanced through the "hardening" of its normalized effective phonon spectrum $g(\omega)$. The "softening" of $g(\omega)$ can enhance the $T_c$ for a superconducting material with small $\lambda$, but not one for a superconductor whose $\lambda$ is large.

9717

## WEAK LOCALIZATION, INTERACTION EFFECTS IN LOW TEMPERATURE RESISTIVITY, MAGNETORESISTANCE OF DISORDERED $Cu_{33}Y_{67}$

40090081f Beijing WULI XUEBAO [ACTA PHYSICA SINICA] in Chinese Vol 37 No 2, Feb 88 pp 248-253

[English abstract of article by Li Yanfei [2621 3601 7378] of the Department of Technical Physics, Harbin University of Science and Technology]

[Text] The electrical resistivity and magnetoresistance of an amorphous $Cu_{33}Y_{67}$ alloy have been measured. The alloy was prepared by melt-spinning in He gas.

The interaction effect can provide a good quantitative explanation for the temperature dependence of electrical resistivity at low temperatures, with a main contribution in the form of $\sqrt{T}$ below 4.5 K. Its variation at higher temperatures can also be explained by a combination of interaction and weak localization effects.

The magnetoresistance measurements up to 1.8 Tesla reveal predominant localization effects, with the strong influence of spin-orbit scattering. The data are quite larger than those predicted by weak localization. An overall good fit is obtained if one increases the theoretically predicted strength of localization three times. One fitting parameter, the spin-orbit scattering time $\tau_{SO}$, is unchanged, while inelastic scattering time $\tau_i$'s fittings used for two sets of data of resistivity and magnetoresistance are close.

9717

**Design of Digital Filters Used in Compatible HQTV System**

55001031 Beijing DIANZI XUEBAO [ACTA ELECTRONICA SINICA] in Chinese Vol 16 No 1, Jan 88 pp 40-45

[Article by Yu Sile [0205 2448 2867], Chang Lun [1603 0178], and Li Hua [2621 5478] of Tianjin University*]

[Excerpts] **Abstract**

This article discusses High-Quality Television [HQTV] Systems and their significance in the development of a new generation of televisions in China. It describes a simple, reliable, and time-saving method for optimized design of two-dimensional FIR digital filters. It was confirmed through simulation experiments that the designed filters were effective in compatible improvement of picture quality.

**I. Introduction**

Foreign nations began studying a new generation of TV systems in the late 1960's and many new improvement programs have been suggested since then. Examples include the 1,125-line HDTV mode of Japan's NHK (broadcasting association), the EQTV mode from the Federal Republic of Germany's Dortmund University which is compatible with existing TV standards, the MAC system from England's IBA (independent broadcasting company), the two-channel SLSC system from the Illinois College of Engineering in the United States, and others. These programs can be divided into compatible and noncompatible systems. Compatible systems can fully exploit the information-carrying capacity of existing TV channels, and they can use signal-processing techniques to improve signal transmission and displayed signal quality to improve picture quality.

Programs for compatible improvement of TV quality are particularly important in China. China has a huge population and vast territory, and the development of available channel resources has been limited. China has a much broader TV broadcasting audience than other nations but restrictions

---

*This article was a State Natural Science Fund grant project. Received July 1986, revised March 1987.

by real conditions have slowed the pace of TV-set replacement. This makes the compatibility requirements of broadcast TV particularly prominent. Moreover, direct broadcast satellite TV cannot be achieved in China within the foreseeable future, so regardless of the type of TV system adopted for satellite transmission, we eventually will have to replace the existing PAL system used for ground-based broadcasting. From the technical economics and other perspectives, noncompatibility would be irrational.

The main discussion in this article concerns theoretical and experimental research on the use of digital filter processing technologies for compatible improvement of TV picture quality. In dealing with the central question of digital filter design in compatible systems, this article describes a method for optimized design of two-dimensional (or multidimensional) FIR digital filters, and it is used to generate some examples. Finally, it describes experimental results with computer simulation systems.

## II. Principles for the Use of Digital Signal Processing in Improving TV Quality

The basic principles for using digital signal processing to improve TV quality are shown in Figure 1. This system uses a high-resolution signal source (1,250 lines) at the transmitting end which sends a high-quality signal that is completely compatible with existing TV standards (625 lines) after prefiltering and sweep conversion. The reverse process of the receiving end involves post-filtering and line step-up conversion to restore and display a high-line-number (1,250 lines) TV image or a sequential-sweep TV image with a conventional line number (625 lines). In this manner, the reduced resolution created by frequency-spectrum garbling in existing televisions can be eliminated, or interlacing effects can be further eliminated.

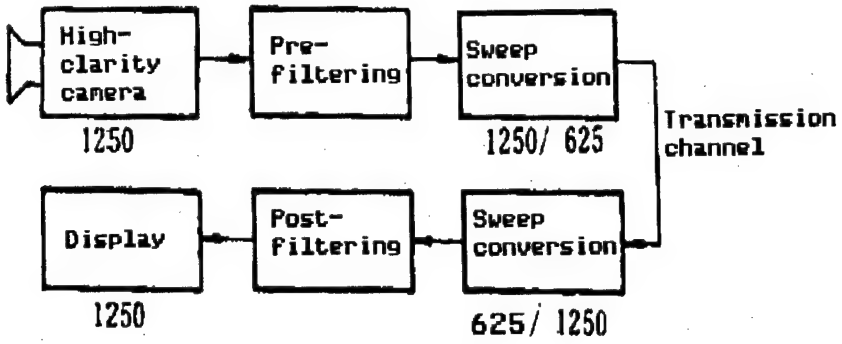


Figure 1. Block Diagram of Principles for Improving TV Quality

Digital signal processing is carried out during prefiltering and post-filtering. Different filters can produce different filtering effects.

## 1. Vertical and horizontal filtering

By taking an orthogonal sample of a picture with a two-dimensional spectrum of $B(f_x, f_y)$, meaning that a sequential sweep at a spacing of $d_y$ is carried out along the y direction and that sequential point sampling at a spacing of $d_x$ is carried out along the x direction, and with cross-registration of the sample points on adjacent lines, one can derive

$$B_s(f_x, f_y) = \frac{1}{d_x d_y} \sum_{i=-\infty}^{\infty} \sum_{j=-\infty}^{\infty} B\left(f_x - \frac{i}{d_x},\ f_y - \frac{j}{d_y}\right) \tag{1}$$

This is a periodic extension of the baseband spectrum along the $f_x$ and $f_y$ directions. In existing TV systems, because the number of sweep lines obviously is insufficient relative to the picture detail that can be handled by camera modulation transfer functions, frequency-spectrum garbling which affects vertical resolution can occur.

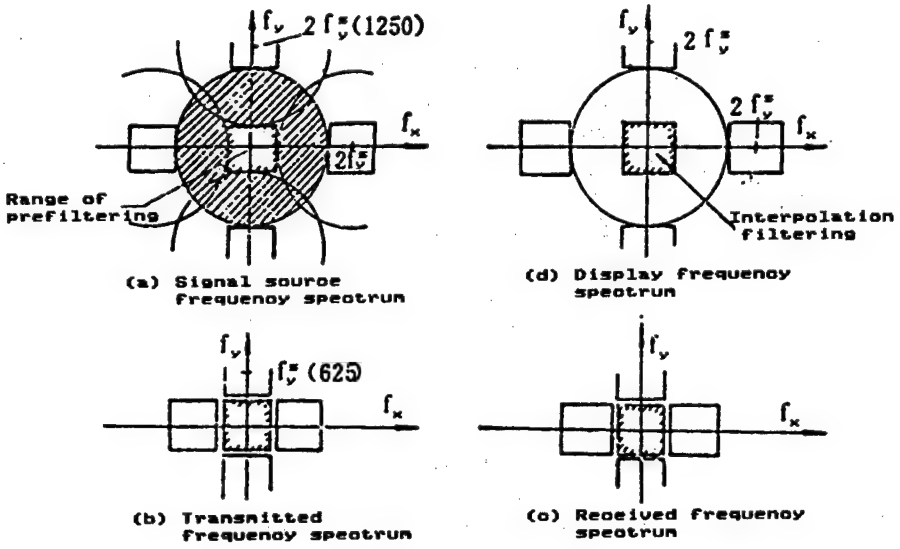


Figure 2. Signal Processing for Vertical and Horizontal Filtering

Figure 2 shows the working frequency-spectrum conversion based on the system in Figure 1 under conditions of orthogonal sampling. Illustration (a) shows the repetitive spectrum and range of prefiltering formed after sampling a multiple-line signal source; (b) shows the frequency spectrum transmitted after vertical and horizontal filtering and line step-down conversion; (c) is the received frequency spectrum; and (d) is the frequency spectrum displayed after interpolation filtering and line step-up conversion. Because only the nongarbled baseband spectrum is displayed, vertical garbling effects can be eliminated and the goals of improved vertical resolution and no-line structure display can be achieved.

## 2. Diagonal line filtering

Further improvement of horizontal resolution can be achieved by adopting a biased sampling format of mutually staggered sampling points on adjacent lines for picture sampling. At this time, the frequency spectrum is:

$$B_s(f_x, f_y) = \frac{1}{2d_x d_y} \sum_{i=-\infty}^{\infty} \sum_{j=-\infty}^{\infty} B\left(f_x - \frac{i}{d_x},\ f_y - \frac{j}{d_y}\right)[1 + (-1)^{i+j}] \qquad (2)$$

It is characterized by a repetitive frequency spectrum oblique extension, which permits diagonal line filtering to make full use of the empty and rather large nongarbled regions in the horizontal direction, as shown in Figure 3. At this time, there is an obvious increase in horizontal resolution, but there also is a loss of diagonal resolution. Given the greater probability that horizontal and vertical structures will appear in the picture compared to the appearance of diagonal structures, and given the fact that the resolution of the human eye is greater in the horizontal and vertical directions than in an oblique direction, the overall result of improved resolution can be obtained.

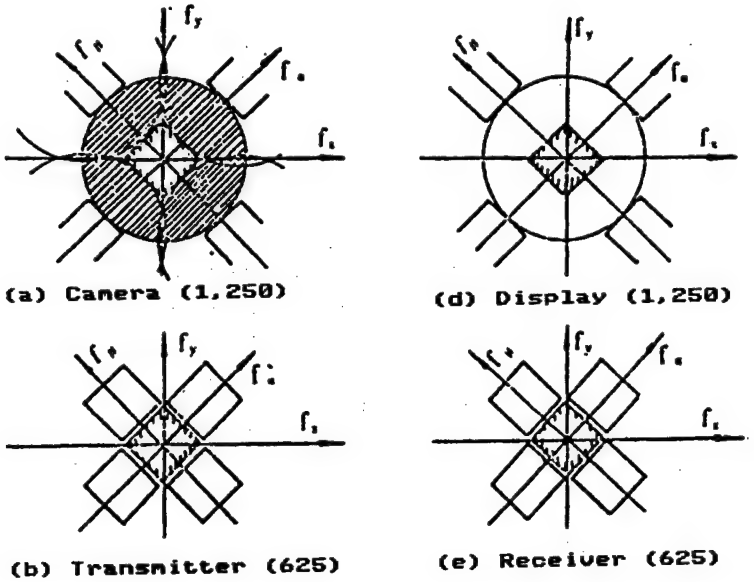


Figure 3. Signal Processing for Diagonal Filtering

## III. A Method for Optimized Design of Two-Dimensional FIR Digital Filters

In consideration of the importance of linear phase in picture processing, this design employs FIR digital filters.

Various two-dimensional digital filters with different frequency responses were designed based on the aforementioned principles of using digital signal processing to improve TV quality. Figure 4 shows three types.

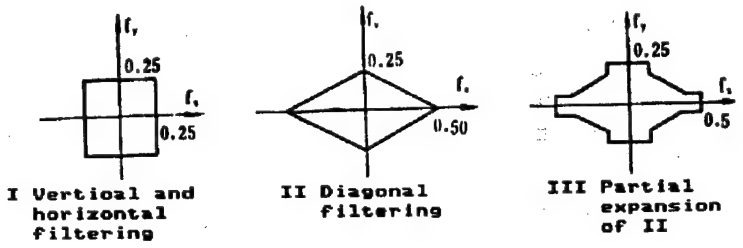


Figure 4. Frequency Response of Three Types of Ideal Two-Dimensional Filters

There are many design methods for two-dimensional linear phase FIR digital filters. They include the window-function method, the frequency-sampling method, the McClellan frequency-conversion method, and others. Each of the computation methods has its own characteristics, but given that a rather small step number more closely approximates ideal characteristics, we studied an optimized design technique for one type of two-dimensional FIR digital filter. This method is based on using an $l_2$ standard to approximate predetermined ideal amplitude-frequency characteristics.

The frequency response and amplitude frequency characteristics of two-dimensional linear phase FIR digital filters can be expressed as:

$$\begin{aligned} \hat{H}(\omega_1, \omega_2) &= \sum_{n1}\sum_{n2} h(n_1, n_2) \exp[-j(\omega_1 n_1 + \omega_2 n_2)] \\ H(\omega_1, \omega_2) &= \sum_{n1}\sum_{n2} b_{n1n2} \cos(\omega_1 n_1 + \omega_2 n_2) \end{aligned} \tag{3}$$

The amplitude-frequency characteristics of two-dimensional FIR digital filters with one-quarter symmetry can be simplified as:

$$H(\omega_1, \omega_2) = \sum_{n1}\sum_{n2} a(n_1, n_2) \cos \omega_1 n_1 \cos \omega_2 n_2 \tag{4}$$

There is a simple relationship of correspondence between $a(n_1, n_2)$ and the filter pulse response coefficient $h(n_1, n_2)$. An even more common form is

$$H(\omega_1, \omega_2) = \sum_{i=1}^{k} a_i f_i(\omega_1, \omega_2) \tag{5}$$

Here, $a_i$ corresponds to $(a(n_1, n_2)$ and $f_i(\omega_1, \omega_2)$ corresponds to $\cos\omega_1 n_1 \cos\omega_2 n_2$.

If we assume that the amplitude-frequency characteristic of an ideal filter is $D(\omega_1, \omega_2)$, it can be defined as being on a discrete-frequency set, i.e., $(\omega_{1m}, \omega_{21})$, $m = 1,2,\cdots\cdots M$, $1 = 1,2,\cdots\cdots L$

If we make $A = [a_1 \cdots\cdots a_k]^T$; $F(\omega_1, \omega_2) = [f_1(\omega_1, \omega_2) \cdots\cdots f_k(\omega_1, \omega_2)]^T$

Then $H(\omega_1, \omega_2) = A^T F(\omega_1, \omega_2)$

If $E_{ml} = [H(\omega_{1m},\omega_{2l}) - D(\omega_{1m},\omega_{2l})]$, the target function is defined as:

$$J(A)=\sum_{m=1}^{M}\sum_{l=1}^{L} W_{ml}E_{ml}^{2}=\sum_{m=1}^{M}\sum_{l=1}^{L}W_{ml}[A^{T}F(\omega_{1m},\omega_{2l})-D(\omega_{1m},\omega_{2l})]^{2} \tag{6}$$

The $W_{ml}$ here is the weighted function, and it can be determined by the designer according to requirements. Thus, the $h(n_1,n_2)$ aspect of the two-dimensional FIR digital filters is solved, and the problem is simplified to solving for the vector A: a minimum target function J(A) will be the optimum situation.

It was discovered through analysis of the target function J(A) that it has first-order and second-order derivatives which also are easy to derive.

$$\nabla J(A)=2\sum_{m=1}^{M}\sum_{l=1}^{L}W_{ml}E_{ml}F(\omega_{1m},\omega_{2l}) \tag{7}$$

$$\nabla^{2}J(A)=2\sum_{m=1}^{M}\sum_{l=1}^{L}W_{ml}F(\omega_{1m},\omega_{2l})F^{T}(\omega_{1m},\omega_{2l}) \tag{8}$$

Thus, it can be solved using the classical Newtonian iteration method. To avoid problems of numerical overflow, normalization of the target function and its derivatives was carried out after each iteration, by setting

$$\overline{J(A)}=\sum_{m}\sum_{l}W_{ml}(E_{ml}/\max_{m,l}\{E_{ml}\})^{2}$$

$$\overline{\nabla J(A)}=2\sum_{m}\sum_{l}W_{ml}(E_{ml}/\max_{m,l}\{E_{ml}\})F(\omega_{1m},\omega_{2l})$$

$$\overline{\nabla^{2}J(A)}=\nabla^{2}J(A)$$

At this time, $\overline{\nabla J(A)}\neq\nabla\overline{J(A)}$, so the Newtonian method is useless. We used the damped Newtonian method as a substitute. One very important aspect of this method is the search for a "Newtonian direction" which involves a one-dimensional search. In the Newtonian method, the "Newtonian direction" is determined by $\nabla J(A)[\nabla^{2}J(A)]^{-1}$. Obviously, as for the target function $\overline{J(A)}$, $P_k = -\overline{\nabla J(A_k)}\cdot[\nabla^{2}J(A_k)]^{-1}$ still cannot be considered a "Newtonian direction." The minimum point derived searching along this direction still is the minimum point of the target function. Thus,

$$A_{k+1}=A_k+\lambda_k P_k$$
$$\overline{J(A_k+\lambda_k P_k)}=\min\{\overline{J(A_k+\lambda P_k)},\ |\ \lambda\geqslant 0\} \tag{9}$$

Much time would be required to do a direct one-dimensional search, which would be very uneconomical. However, the second-order derivative of the target function J(A) here along any direction D is greater than (or equal to) 0. Hence,

$$\left.\frac{d^{2}J(A+\Delta D)}{d\Delta^{2}}\right|_{\Delta\ 0}=2\sum_{m}\sum_{l}W_{ml}[D^{T}F(\omega_{1m},\omega_{2l})]^{2}\geqslant 0 \tag{10}$$

Thus, the target function along any direction is a concave function and has only one minimum point. We can set

$$dJ(A + \Delta D)d\Delta = 0$$

to find that the minimum point along direction D is located at $D_{min} = A + \Delta_{min}D$; here

$$\Delta_{min} = \frac{-\sum_m \sum_l W_{ml}[D^T F(\omega_{1m}, \omega_{2l})]E_{ml}}{\sum_m \sum_l W_{ml}[D^T F(\omega_{1m}, \omega_{2l})]^2} \tag{11}$$

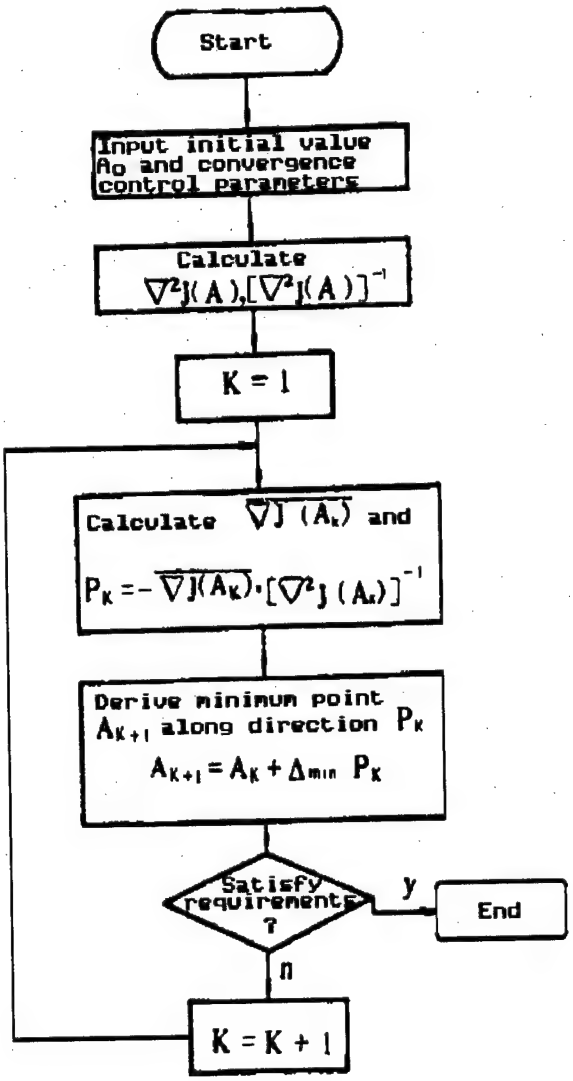


Figure 5. Block Diagram of Two-Dimensional FIR Filter Optimization Calculation Methods

In this manner, one can find the search step length $\Delta_{min}$, along direction D. It is substituted for the one-dimensional search step length $\lambda_k$ along direction $P_k$. From this is derived a block diagram of this computation method as shown in Figure 5.

## IV. Experimental Results

The improvement in picture quality during the experiments was obvious. It also was discovered that signal processing at one end provided rather good results. It is apparent from the experimental results that horizontal resolution is improved substantially by using the orthogonal filter characteristic II in Figure 4, but the diagonal resolution decreases. As for frequency characteristic III relative to II, the resolution can be expanded somewhat. However, there still would be more garbling of picture detail.

## V. Conclusion

This article studied a simple, reliable, and time-saving method for designing and selecting frequency-response characteristics for optimized design of two-dimensional (or multidimensional) FIR digital filters. In compatible HQTV systems, the designed filters also provide obvious benefits in processing stationary pictures. However, additional research is needed on optimization of filter frequency-response characteristics, determination of the dimensions of the filter computer templates, increasing speeds, processing moving pictures, and other areas.

References

1. Wendland, B. and Schnoeder, H., "Signal Processing for new HQTV Systems," SMPTE, Vol 94 No 2, February 1985, pp 182-189.

2. Tonge, G., "Signal Processing for Higher-Definition Television," Experimental & Development Report, 121/83, IBA, UK.

3. Lodge, J.H. and Fahmy, M.M., "An Efficient lp Optimization Technique for the Design of Two-Dimensional Linear-Phase FIR Digital Filters," IEEE TRANS., Vol ASSP-28, No 3, June 1980, pp 308-313.

4. Xu Yuanpei [1776 0337 1014], "Progress in Two-Dimensional Digital Filter Theory," DIANZI XUEBAO [ACTA ELECTRONICA SINICA], Vol 13 No 4, 1985, pp 93-102.

5. Yu Sile [0205 2448 2867], et al., DIANSHI YUANLI [PRINCIPLES OF TELEVISION], National Defense Industry Publishing House, 1984.

12539/9365

# An 8mm-Band Resistive Finline Up-Converter

40100021b Harbin HARBIN GONGYE DAXUE XUEBAO [JOURNAL OF HARBIN INSTITUTE OF TECHNOLOGY] in English, No 1, Feb 88 pp 106-107

[Article by Zhang Qinghui [1728 1987 1798], Department of Electronic Engineering; received 20 September 1986]

[Text] The application of millimeter-wave techniques in the field of radar, guidance and communication has been growing more important since the last decade. The demand for inexpensive millimeter-wave components and reliable subsystems has led to the rapid development of planar millimeter-wave integrated circuits (MIC). As an important option in MIC, finline technique has already been applied successfully to a number of fields, but it is rare so far to find published scientific reports on the resistive finline up-converter either at home or abroad. Therefore, no practical circuit is available or can be used for reference in the study of such a converter.

The resistive balanced up-converter reported in this paper is shown in the sketch. Here we have referred to the general 8mm-band down-converter circuits, and changed its four-port structure into a three-port one. RT-Duroid substrates ($\varepsilon_r = 2.22$) of 0.3mm in thickness are used. The LO port and the output port are of the standard waveguide BJ-320. The combination of a finline and a coplanar line which form a broad-band hybrid of 180 degrees becomes the basis of a finline balanced mixer as described in [1]. The LO power is fed to the diodes via an exponential transition from a standard waveguide to a finline. The signal power is coupled to the diodes via a coaxial line and a low-pass transformation filter. The designs of the transition and the filter are all routine. Another obvious difference between an up-converter and a down-converter is their output port. For a down-converter, the output signal is the IF signal of a lower frequency, but for an up-converter, the output signal is the sum signal of the highest frequency. Because of the high operating frequency, the output-coupled device must be designed carefully, which is the key to a converter of good performance. We have lengthened the coplanar-line center strip to form a loop which serves as a coupled device. But we have never read a report on the

formula for design of a coplanar-line coupled loop. Here we borrow the formula for design of a rectangular waveguide coupled loop to make an initial approximation, and then determine the final size through experiments. The lapping point of the coupled loop and the coaxial probe of the signal input port forms a discontinuous capacitance which will cancel the inductive reactance of the loop to some extent. Therefore adjusting the position of the probe in relation to the loop can improve the match of the coupled loop and so increase the output power of the up-converter remarkably.

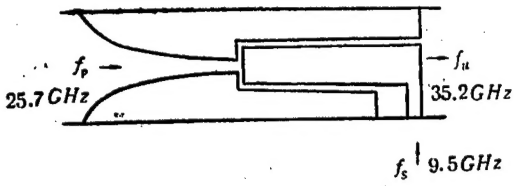


Figure 1. Sketch of the Resistive Balanced Up-Converter

Although the low capacitance and the planar structure of modern beam-lead mixer diodes are suitable for the application of finline circuits, it is difficult for us to find such diodes, and we have to use commercial 8mm GaAs mixer chips instead. Chips used here have some advantages: Besides their low-cost and low capacitance, an important advantage is the very low thermal resistance that is helpful to the large power output of an up-converter.

The measured results of the up-converter circuit are as follows: Conversion loss at the 9.5-GHz center frequency amounts to 6dB. Output power of the 1dB signal compression point is more than 1mw. Bandwidth is greater than 800MHz. The LO-port VSWR is 1.27 to 1.65 in the full band. The inherent frequency-independent decoupling between the LO and the output port makes the isolation greater than 25 dB.

## Reference

[1] U. H. Gysel, A 26.5-to-40-GHz Planar Balanced Mixer, 5th UMC 1975, pp 491-495.

/09599

## SHANGHAI BELL'S S1240 SYSTEM APPLICATIONS EXPANDING

40080091b Beijing JISUANJI SHIJIE [CHINA COMPUTERWORLD] in Chinese 10 Feb 88 p 12

[Article by Wang Xiong [3769 3574]: "Applications Steadily Increase for the S1240 System Offered by the Shanghai Bell Company"]

[Text] The S1240 program-controlled digital exchange system installed by Shanghai Bell Telephone Equipment Manufacturing Company, Ltd., for several entities in China, is a new product being manufactured by this company that represents the telephone exchange technology of the 1980's. It differs from traditional analog exchange equipment in being completely digitized, in using 32-circuit PCM modulation, a sampling frequency of 8 KHz, and an internal rate of transmission of 4 megabits per second. It can conveniently provide the user with reduced digit dialing, hot-wire telephony, call-out limiting, wake-up call services, non-intrusive services, and call transfers. The S1240 has dispensed with the general method whereby the control logic is all concentrated in mainframe CPU's and chooses instead a modular structure, making great use of a common microprocessor (the 8086) and memory (256 KB/512 KB), and sharing the entire system control with modules that can accomplish various functions. At the same time, it uses intelligent digital switching networks (DSN) to connect together all the modules into the famous S1240 spiderweb system structure. The modular structure of hardware and software, the completely dispersed method of control, and the intelligent DSN make it impossible for the S1240 to experience an overall paralyzing failure. As far as hardware is concerned, the S1240 uses special LSI circuitry, bringing safety and reliability to the entire exchange system, as well as a compact structure. Software is structured as finite message machines (FMM) through function modules. FMMs communicate with each other by passing information. Information routing is handled by the operating system resident in each processor. Ninety percent of the software in the S1240 has been written in the high-level language CHILL, as recommended by the CCITT which allows it to provide even more outstanding services to digital telephony, teletyping, facsimile, letterphones, and personnel computers. It is said that worldwide the S1240 now provides 12 million equivalent circuits to exchanges, while in China it is being used in 10 exchanges.

12586/12232

- END -